Legionnaires' Disease – the impact of cigarette smoke and functional lung recovery

Markus Fleischmann

ORCID ID: 0000-0002-8613-9788

from Hirschau, Germany

Submitted in total fulfilment of the requirements of the joint degree of Doctor of Philosophy (PhD) of

The Medical Faculty

The Rheinische Friedrich-Wilhelms-Universität Bonn

and

The Department of Microbiology and Immunology

The University of Melbourne

Bonn/Melbourne, 2023

Performed and approved by the Medical Faculty of The Rheinische Friedrich-Wilhelms-Universität Bonn and The University of Melbourne

1. Supervisor: Prof. Dr. Natalio Garbi

2. Supervisor: Prof. Dr. Ian van Driel

Date of submission: 10th of June, 2022

Date of the oral examination: 7th of February, 2023

Institute of Experimental Immunology, Bonn
Director: Prof. Dr. Christian Kurts

Table of Contents

Abbreviations

ºC	Degrees Celsius
7-AAD	7-Aminoactinomycin D
AEC	Alveolar epithelial cells
AIM2	Absent in melanoma 2
AM	Alveolar macrophage
AnnV	Annexin V
ARDS	Acute respiratory distress syndrome
ASC	Apoptosis-associated speck-like protein containing CARD
BAL	Bronchoalveolar lavage
BCYE	Buffered charcoal yeast extract
CARD	Caspase recruitment domain
CCL	C-C-motif chemokine ligand
CCR	C-C-motif chemokine receptor
CD	Cluster of differentiation
CFU	Colony-forming units
CLR	C-type lectin receptor
cm^2	square centimetre
CO_2	carbon dioxide
COPD	Chronic obstructive pulmonary disease
CXCL	C-X-C-motif chemokine ligand
CXCR	C-X-C-motif chemokine receptor
DAMP	Damage-associated molecular pattern
DNA	Desoxyribonucleic acid
Dot/icm	defect-in-organelle-trafficking/intracellular-multiplication
EGF	Epidermal growth factor
FACS	Fluorescence-activated cell sorting
FGF	Fibroblast growth factor
G	Gauge
g	gravity of earth
G-CSF	Granulocyte-colony stimulating factor

GBP	Guanylate binding protein
GM-CSF	Granulocyte/Macrophage-colony stimulating factor
HGF	Hepatocyte growth factor
i.n.	intranasal
i.p.	intraperitoneal
i.v.	intravenous
IFN	Interferon
Ig	Immunoglobulin
IGF	Insulin-like growth factor
IL	Interleukin
ILC	Innate lymphoid cell
IRF	Interferon-regulatory factor
kg	kilogram
LCV	*Legionella*-containing vacuole
LD	Live/dead
LiSM	Light-sheet microscopy
Llo	Legionella longbeachae
Lpn	Legionella pneumophila
LPS	Lipopolysaccharide
m^2	square meter
MAVS	Mitochondrial antiviral-signalling protein
MC	Monocyte-derived cell
MCP	Monocyte chemoattractant protein
MFI	Median fluorescence intensity
mg	milligram
MHC	Major histocompatibility complex
ml	millilitre
MLKL	Mixed lineage kinase domain-like protein
mM	millimolar
MMP	Matrix metalloproteinase
mRNA	messenger ribonucleic acid
NADPH	Nicotinamide adenine dinucleotide phosphate

NAIP5	NLR family, apoptosis inhibitory protein 5
NET	Neutrophil extracellular trap
NF-κB	Nuclear factor kappa B
ng	nanogram
NLR	NOD-like receptor
NLRC4	NLR family CARD domain-containing protein 4
NLRP3	NLR family pyrin domain containing 3
Nrf2	Nuclear factor erythroid 2-related factor 2
O_2	Oxygen
PAMP	Pathogen-associated molecular pattern
PBS	Phosphate-buffered saline
PFA	Paraformaldehyde
PRR	Pattern recognition receptor
qPCR	quantitative polymerase chain reaction
RLR	RIG-I-like receptor
RNA	Ribonucleic acid
RNS	Reactive nitrogen species
ROS	Reactive oxygen species
SP	Surfactant protein
SpO_2	Blood oxygen saturation
TGFβ	Transforming growth factor β
TLR	Toll-like receptor
TNFα	Tumour necrosis factor α
v/v	volume per volume
VEGF	Vascular endothelial growth factor
w/v	weight per volume
µl	microliter
µm	micrometre

List of Tables

List of Figures

Abstract

Legionnaires' Disease is a severe type of pneumonia most commonly caused by the bacterial species *Legionella pneumophila* and *Legionella longbeachae*. Epidemiological studies show that cigarette smoke is a major risk factor for susceptibility to Legionnaires' Disease, but the underlying mechanisms for this connection are not known. During pneumonia, efficient oxygen uptake in the lung is compromised due to pathogen invasion and the resulting immune response. Some types of immune cells are known to resolve inflammation and promote regeneration of lung structure and function. However, the underlying mechanisms by which immune cells aid in lung recovery from bacterial pneumonia are not well understood.

We used a mouse model of acute cigarette smoke exposure and *Legionella* infection to assess how cigarette smoke could impact the immune response towards *Legionella* and confer more severe disease. This work provides evidence that acute cigarette smoke exposure alone depleted alveolar macrophages (AM) in lungs of wild-type mice, which is contrary to the currently accepted view that smoking causes accumulation of AM within the airways. We investigated the cell death pathways that could be activated by cigarette smoke in AM and found that, in smoke-treated $ASC^{-/-}$ and $NLRP3^{-/-}$ mice, the smoke-induced AM depletion observed in wild-type mice was reversed. These results suggest an important role of NLRP3-dependent pyroptosis, a type of inflammatory cell death, in driving smoke-induced AM death *in vivo*.

Legionella sp. subvert host immunity to establish a protected vacuole for bacterial replication within AM. Concurrent infection of smoke-treated mice with *L. pneumophila* caused more severe disease progression and significantly delayed bacterial clearance. In a model of clodronate-induced AM depletion, *L. pneumophila* clearance was similarly delayed in later stages of infection, despite limited bacterial replication early after infection due to the depletion of the bacteria's replicative niche. In contrast, after concurrently infecting smoke-exposed mice with *L. longbeachae*, bacterial clearance was slightly accelerated. Therefore, smoke-induced AM death may be a risk factor for Legionnaires'

Disease caused by *L. pneumophila*. How AM mediate bacterial clearance under normal circumstances remains subject of future investigation.

Using the mouse model of Legionnaires' Disease, we assessed how immune cells impacted functional lung recovery. Surprisingly, we observed that neutrophils play an important role in the re-establishment of efficient oxygen uptake during the recovery phase from *L. longbeachae* infection. Neutrophils promoted the proliferation of type II alveolar epithelial cells, local progenitor cells that regenerate the alveolar epithelium. Mechanistically, neutrophils contributed to the production of several cytokines and growth factors associated with epithelial cell proliferation after pulmonary infection such as amphiregulin, TNFα, or IL-1β. These results provide novel insights into a regenerative role of neutrophils in the recovery phase of bacterial pneumonia.

Declaration

The work presented in this thesis was conducted at The University of Melbourne and The Rheinische Friedrich-Wilhelms-Universität Bonn in the laboratories of Prof Ian van Driel (Bio21 Molecular Science and Biotechnology Institute, Melbourne) and Prof Natalio Garbi (Institute of Experimental Immunology, Bonn).

This is to certify that

(i) this thesis comprises only my original work towards the PhD except where indicated in the preface,

(ii) due acknowledgement has been made in the text to all other material used,

(iii) the thesis is less than 100,000 words in length, exclusive of tables, graphs, bibliographies and appendices.

Markus Fleischmann

Melbourne/Bonn – June 2022

Preface

My contribution to the experiments within each chapter was as follows:

Chapter 3: 80 %

Chapter 4: 60 %

Chapter 5: 100 %

I acknowledge the important contributions of others to the experiments and figures presented in this thesis:

Chapter 3: Dr Garrett Ng – Figures 3.5, 3.6

Chapter 4: Dr Garrett Ng – Figures 4.1-4.5, 4.12

Chapter 4: Bethany Anderson & Dr Laura Edgington-Mitchell – Figure 4.8

I would also like to acknowledge:
Prof Gary Anderson and Dr Andrew Jarnicki, for their collaboration on the smoking model used in Chapters 3 and 4;
The Biological Optical Microscopy Platform staff for their training and help with light-sheet microscopy imaging and analysis, shown in Chapter 3;
Prof Evdokia Dimitriadis, Dr Ellen Menkhorst, A/Prof Kathryn Lawlor, and Dr Julie McAuley for providing knockout mice used for experiments shown in Chapter 3;
Prof Elizabeth Hartland for providing the *Legionella* strains used in Chapters 4 and 5;
The assistance of the animal facility and flow cytometry core facility staff at both the University of Melbourne and the University of Bonn.
Figures were created using biorender.com.

Funding:
The work in this thesis was supported by awards from the University of Melbourne, the Australian National Health and Medical Research Council (NHMRC), including APP1175976, and the German Research Council (DFG), project number 272482170 – GRK2168. The work was also supported by a Graduate Research Scholarship from the University of Melbourne.

Acknowledgements

There is a long list of people who contributed to the completion of this PhD, and I am very thankful for everyone who supported me on this journey.

First, I would like to thank my main supervisors, Prof Ian van Driel and Prof Natalio Garbi, for giving me the opportunity to work in your labs within the IRTG program.

Ian, thank you for being a fantastic mentor and supervisor, not only during my time in Melbourne. I've learned a great deal over these last 4 years under your guidance, and I'm thankful that you always found time to answer my questions and to discuss my work despite all your other responsibilities. Your continuous encouragement was greatly appreciated, especially during the times when things were not going all too well, and your support certainly helped me to keep going and finish this PhD.

Natalio, you are one of the most enthusiastic scientists and PIs I ever met. Your excitement and energy were a great support and kept encouraging me to move forward. During my time in Bonn, I've learned a lot from you about how to approach and communicate my research, and I'd like to thank you for your positivity during all our meetings, especially when some projects seemed to be stuck. You always came up with a solution that taught me something new and helped me finish this PhD.

Next, I'd like to thank Dr Garrett Ng, who supervised my in the lab during my time in Melbourne and was incredibly helpful throughout the entire PhD. Garrett, it's impossible to list all the things I learned from you. From methods, to approaching and planning experiments, to analysis, etc. – it felt like there was not a single question you didn't have an answer to. I really enjoyed working together with you! Also, thank you very much for the great contribution to a bunch of data and figures presented in this thesis.

I'd also like to thank my co-supervisor Prof Elizabeth Hartland, for all your input and encouragement during our meetings, it has definitely taught me lot on how to approach my research and science in general. Thanks to the other members of my PhD committee, A/Prof Justine Mintern and Dr Laura Edgington-Mitchell, for the discussions, advice and support in our progress meetings, it was always encouraging and much appreciated.

A huge thank you to the IRTG2168 program co-ordinators and administrative staff, Marie Greyer, Lucie Delforge, Annabelle Blum & Sandra Rathmann. Whenever there were issues or questions (and there were quite a lot…), you immediately took care of it, and your help throughout this PhD was simply amazing.

I'd like to thank the collaborators that contributed to the work in this thesis, specifically Prof Gary Anderson and Dr Andrew Jarnicki for the collaboration in the smoking projects, and Dr Laura Edgington-Mitchell and Beth Anderson for performing the neutrophil protease assays. Thanks to all the core facility staff members of the University of Melbourne, from the Biological Optical Microscopy Platform and the Flow Cytometry Core Facility to the animal house staff at Bio21 Institute and at the Medical Building. At the University of Bonn, thanks to the members of the HET, the Flow Cytometry Core Facility and the Spülküche. I'd also like to thank the colleagues who provided mice and reagents, or provided other input throughout this entire PhD.

Next up, the lab members and fellow students in Melbourne and Bonn.
Garrett and Wendy, plus all the members of the Gleeson Lab at Bio21, Andy, Alessa, Xiao Peng, Christian, Fiona, Melinda, Anson, and Lou – it was a lot of fun to work alongside you, thanks for all the support and good times. Massive thanks to my PhD colleagues and the BAMBII members at Bio21, I had the great privilege to meet so many great people and friends in Melbourne. Erin, Kayla, Emily, Emily, Beth, Jasmina, Tom, Alex, Christian and Xiao Peng, I had a truly

special time in Melbourne. Special shoutout once again to Andy, my fellow German beer drinking buddy, for all the good times! I'd also like to thank my friends in Melbourne outside of the lab, especially the volleyball boys and girls, my roomies, and the friends I met the day I arrived in Melbourne.
A huge thank you to Nino and Lari, the most amazing lab partners one could wish for, for all the good times inside and outside of the lab, and for helping me to keep going. Our lunch and coffee breaks, trips and excursions were always a blast, and we certainly created some great album cover shots during our live performances. I'll see you at the BUGA-Marathon 2029, AG Garbi – weeeew!
I'd also like to thank the lab members past and present, Ann-Christine, Christine, Caro, Victoria and David, and my fellow colleagues at the IMMEI and in the IRTG2168 program for creating a great atmosphere to work in. Andrea, Blanca, Daniela, Mary, Mel, Marcel, Natascha, Kostas, Anni, and Helena – you are the best. Thanks also to all my friends here in Germany who I was very happy to be back with after returning from Melbourne, and to the new friends I made in Bonn, the volleyball and DoKo crew, my housemate Sarah, the boys back in Regensburg, and the MolMed elite all over place.

Last, but not least, thanks to my family, including aunts and uncles, cousins and grandparents! Thank you soooo much for the incredible support you gave me these last few years, thanks for encouraging me non-stop, thanks for visiting me for a Christmas at the beach, and thanks for all the happy moments I get to spend with all of you! Mama, Papa, Ute, Anja, Basti, Anton & Paulina, you are the best source of strength ever!

1 Literature review

1.1 Lung structure and function

The lungs are the primary organ of the respiratory system, and their main function is to provide the organism with oxygen to fuel its metabolism while eliminating excess carbon dioxide (Cloutier, 2019). Inhaled air first passes through the upper respiratory tract which includes the nose, pharynx, larynx, trachea, bronchi and conducting bronchioles (Cloutier, 2019). There, it is filtered for environmental particles or microorganisms, warmed and moistened, before it reaches the lower respiratory tract. This distal part of the lungs consists of terminal bronchioles, alveolar ducts, alveolar sacs, and individual alveoli where the oxygen exchange takes place (Cloutier, 2019). The human lung is estimated to contain more than 100 million alveoli, comprising an alveolar surface area of approximately 70 m^2 (Ochs *et al.*, 2004; Vasilescu *et al.*, 2020), whereas in a mouse lung, up to 10 million alveoli and an alveolar surface area of more than 80 cm^2 have been found (Knust *et al.*, 2009; Vasilescu *et al.*, 2013; Schulte *et al.*, 2019).

Alveoli consist of thin, squamous type I alveolar epithelial cells (AEC) representing approximately 95 % of the entire alveolar area, and of cuboidal type II AECs that possess secretory functions (Knudsen and Ochs, 2018). Alveoli are surrounded by an extensive network of fine pulmonary capillaries to form the individual respiratory units. Together, the capillary endothelium, alveolar epithelium and their respective basal membranes constitute the air-blood-barrier across which gases are exchanged between the air space and erythrocytes within the capillaries via diffusion (Knudsen and Ochs, 2018).

Lungs are constantly exposed to potentially harmful microorganisms and environmental particles in the inhaled air. Therefore, lungs also possess important immunological functions and are equipped with a range of defence mechanisms, including physical and chemical barriers, as well as innate and adaptive immune responses in order to prevent disease and to maintain efficient oxygen uptake.

1.2 Pneumonia

1.2.1 Epidemiology and aetiology of pneumonia

Pneumonia can be defined as the invasion and overgrowth of one or more pathogens in the lower respiratory tract and lung parenchyma, causing accumulation of immune cells and fluid within alveoli, as well as compromising respiratory function (Alcón *et al.*, 2005; Quinton *et al.*, 2018). Pneumonia represented a major global health burden even before the COVID-19 pandemic started at the beginning of 2020. Lower respiratory tract infections affected almost 500 million people in 2019, and were responsible for more than 65 million hospitalizations and approximately 2.5 million deaths that year (Troeger *et al.*, 2018; Vos *et al.*, 2020). Depending on the type of pneumonia, numerous risk factors such as sex, young and old age, an immunocompromised state or pulmonary comorbidities, as well as lifestyle factors like smoking are linked to the disease (Torres *et al.*, 2013; Barbagelata *et al.*, 2020; Torres *et al.*, 2021).

Pneumonia can be classified based on the circumstance and location of acquisition, e.g. community- or hospital-acquired, or the causative etiological agent, e.g. bacterial, viral or fungal (Torres *et al.*, 2021). Aside from SARS-CoV2, viral pneumonia is most frequently caused by human rhinovirus, influenza virus and the respiratory syncytial virus, while the main causes of bacterial pneumonia are *Streptococcus pneumoniae* and *Haemophilus influenzae* (Jain *et al.*, 2015; Prina *et al.*, 2015; Troeger *et al.*, 2018; Torres *et al.*, 2021), despite the existence of vaccines against these two bacteria (Kelly *et al.*, 2004; Masomian *et al.*, 2020). Other bacterial species that commonly cause pneumonia are *Staphylococcus aureus*, *Pseudomonas aeruginosa*, *Mycoplasma pneumoniae*, and *Legionella pneumophila* (Prina *et al.*, 2015; Torres *et al.*, 2021). However, the individual contribution of viral and bacterial species towards the overall disease incidence is difficult to assess as in many cases of pneumonia the causative pathogen is not identified (Quinton *et al.*, 2018; Torres *et al.*, 2021).

1.2.2 Pathophysiology of pneumonia

Pathogens that cause pneumonia colonize the airways by adhering to mucosal surfaces and by resisting pulmonary defence mechanisms before they reach the lower respiratory tract via inhalation (Siegel and Weiser, 2015). The lung is not a sterile organ, but harbours a microbiome which, under normal circumstances, does not cause disease (Dickson *et al.*, 2014). Thus, the transition from colonization to active infection and development of subsequent pneumonia depends on additional factors such as virulence and abundance of the causative pathogen, and the host lung's state of health and immune response (Quinton *et al.*, 2018; Torres *et al.*, 2021).

Examples of pathogens that directly contribute to pneumonia development are respiratory viruses like influenza which can infect and thus damage the alveolar epithelium, and bacteria like *S. pneumoniae* or *S. aureus* which secrete toxins that cause AEC death by pore formation in cell membranes (Short *et al.*, 2014; von Hoven *et al.*, 2019; Nishimoto *et al.*, 2020). However, it is the immune resistance directed against invading pathogens which predominantly causes disease (Quinton *et al.*, 2018). Recruitment of immune cells that infiltrate the alveoli in order to eradicate pathogens coincides with a breakdown of epithelial and endothelial barriers, resulting in significant vascular leakage into the airspace (Zemans *et al.*, 2009; Schulte *et al.*, 2011; Broermann *et al.*, 2011; Short *et al.*, 2016). During the acute phase of pulmonary inflammation, enhanced mucus production and dysregulated ion transport compromise the removal of fluid from the airspace (Chen *et al.*, 2004; Lee *et al.*, 2007; Peteranderl *et al.*, 2017). Activated immune cells like neutrophils or mononuclear phagocytes can cause additional tissue injury by releasing agents such as reactive oxygen species (ROS), tissue-degrading proteases or neutrophil extracellular traps (NETs) into the surrounding environment (Saffarzadeh *et al.*, 2012; Bhattacharya and Matthay, 2013; Kruger *et al.*, 2015). Together, these processes heavily compromise pulmonary oxygen uptake and, in severe cases, can lead to acute respiratory distress syndrome (ARDS) or respiratory failure.

1.2.3 Pulmonary repair mechanisms

It is essential that excessive tissue damage is prevented during infection and that the alveolar epithelium recovers to re-establish efficient oxygen uptake. This is achieved by dampening the inflammatory response in the airways and tissue repair, mediated through the induction of epithelial cell proliferation.

A range of anti-inflammatory molecules, including transforming growth factor (TGF)β, interleukin (IL)-10 and IL-1RA are secreted by immune cell populations such as alveolar macrophages (AM) and regulatory T (T_{reg}) cells to control ongoing immune responses and reduce recruitment of immune cells to sites of inflammation (D'Alessio *et al.*, 2009; Wynn and Vannella, 2016; Allard *et al.*, 2018). AM actively phagocytose and remove dying immune cells from the airspace to limit the release of pro-inflammatory intracellular contents into the alveolar environment (Allard *et al.*, 2018). This process, termed efferocytosis, triggers the secretion of growth factors and pro-resolving lipid mediators that display anti-inflammatory and tissue-regenerative features (Serhan and Levy, 2018; Croasdell Lucchini *et al.*, 2021a).

Different populations of epithelial progenitor cells replenish damaged epithelium in different locations within the lung (Hogan *et al.*, 2014). In alveoli, *Sftpc*$^+$ type II AEC serve as local stem cells able to self-renew and differentiate into type I AEC (Barkauskas *et al.*, 2013; Desai *et al.*, 2014). Additional progenitor populations that can give rise to type I AEC after tissue injury are integrin-$\alpha_6\beta_4$-expressing epithelial cells (Chapman *et al.*, 2011), Krt5$^+$Trp63$^+$ basal cells (Zuo *et al.*, 2015), lineage-negative progenitor cells (Vaughan *et al.*, 2015), or stem cells located at the bronchioalveolar duct junction (Liu *et al.*, 2019). The signalling pathways and molecules inducing progenitor cell proliferation and differentiation appear to depend on the type of lung insult, and are subject of intense research since they provide potential therapeutic avenues in acute lung disease (Standiford and Ward, 2016; Zepp and Morrisey, 2019).

A variety of growth factors, cytokines and soluble lipid mediators produced by the damaged epithelium itself or immune cell populations have so far been implicated in driving AEC proliferation (Croasdell Lucchini *et al.*, 2021b). Key growth factors

include epidermal growth factor (EGF) (Mu *et al.*, 2020), vascular endothelial growth factor (VEGF) (Varet *et al.*, 2010), insulin-like growth factor (IGF) (Ghosh *et al.*, 2013), and other molecules that bind to the EGF receptor such as amphiregulin (Monticelli *et al.*, 2011; Zaiss *et al.*, 2015; Lucas *et al.*, 2022). Similarly, soluble lipid mediators like prostaglandin E_2 or lipoxin A_4 can induce epithelial cell proliferation to restore efficient oxygen uptake in the lungs after tissue damage (Savla *et al.*, 2001; Zheng *et al.*, 2016), and cytokines such as IL-22 and IL-33 can influence regeneration of the epithelium in the resolution of infection (Monticelli *et al.*, 2011; Kumar *et al.*, 2013).

Importantly, lung regeneration itself has to be controlled, since dysregulated repair mechanisms and extensive production of anti-inflammatory cytokines like TGFβ can lead to lung pathologies such as fibrosis (Bartram and Speer, 2004; Murray *et al.*, 2011). Thus, pulmonary repair has to be a tightly regulated interplay of several mechanisms that promote tissue regeneration while, at the same time, providing sufficient immune resistance towards invading pathogens.

1.3 Legionnaires' Disease and *Legionella*

1.3.1 Legionnaires' Disease

Members of the bacterial genus *Legionella* sp. cause one type of bacterial pneumonia called Legionnaires' Disease. While most infections with *Legionella* remain asymptomatic, or cause the relatively mild Pontiac fever, it can lead to an acute and potentially fatal pneumonia in susceptible people (Cunha *et al.*, 2016). Legionnaires' Disease was first described after an outbreak in the USA in 1976 (McDade *et al.*, 1977; Fraser *et al.*, 1977) and remains a significant health burden today. It is responsible for an estimated 2 – 9 % of community-acquired pneumonia cases (Cunha *et al.*, 2016). Despite surveillance and prevention measures, epidemiological studies from Europe (Beauté, 2017), USA (Barskey *et al.*, 2022), and Australia (Chambers *et al.*, 2021) demonstrate that the incidence of Legionnaires' Disease is rising globally. Risk factors associated with Legionnaires' Disease are old age, tobacco smoking or chronic lung disease, as

well as immunosuppression. In the case of disease caused by *L. longbeachae*, the use of potting soil is an additional risk factor (Marston *et al.*, 1994; Che *et al.*, 2008; Kenagy *et al.*, 2017; Chambers *et al.*, 2021). The mortality rate of patients ranges between 5 – 10 % (Isenman *et al.*, 2016; Soda *et al.*, 2017) and better survival is dependent on early discovery of disease (Dominguez *et al.*, 2009). Even though initial cases of antibiotic-resistant cases have been reported (Bruin *et al.*, 2014), the disease can usually be treated with antibiotic regimens that include macrolides, quinolones, or tetracyclines (Cunha *et al.*, 2016).

1.3.2 *Legionella*

Legionella sp. are Gram-negative, pleomorphic bacteria that can be classified into more than 60 different species and more than 80 different serogroups (Miyashita *et al.*, 2020). More than half of *Legionella* species have been reported to cause disease in humans (White and Cianciotto, 2019).

L. pneumophila, which was responsible for the first ever outbreak of Legionnaires' Disease, is the predominant causative species worldwide, accounting for 80 – 90 % of all Legionnaires' Disease cases (Yu *et al.*, 2002; Miyashita *et al.*, 2020; Beauté *et al.*, 2020). It comprises 15 individual serogroups of which *L. pneumophila* serogroup 1 is responsible for most cases (Miyashita *et al.*, 2020; Beauté *et al.*, 2020). However, since *L. pneumophila* serogroup 1 is the only species reliably diagnosed by urinary antigen test, which is the most commonly used diagnostic approach, this data may be prone to bias (Mercante and Winchell, 2015). *L. pneumophila* is mainly found in aquatic environments including freshwater lakes or human-made water reservoirs such as air-conditioning cooling towers. There, the bacteria parasitize protozoans such as *Acanthamoeba* and *Naegleria*, but may also survive and replicate in biofilms (Fliermans *et al.*, 1979; Rowbotham, 1980; Rogers *et al.*, 1994; Taylor *et al.*, 2009; Boamah *et al.*, 2017).

L. longbeachae was first isolated in California in 1980 (McKinney *et al.*, 1981) and currently represents the second most frequent species isolated from patients with Legionnaires' Disease. It is particularly prevalent in Australia and New

Zealand, where it accounts for approximately 50 % of cases (Chambers *et al.*, 2021). Clinically, there is no specific variance in progression or outcome of the disease caused by the two different species (Amodeo *et al.*, 2010). In contrast to *L. pneumophila*, *L. longbeachae* is usually found in a soil environment, for example in potting mixes, and isolated strains could efficiently infect and replicate within the ciliate *Tetrahymena pyriformis* (Steele *et al.*, 1990; Steele and McLennan, 1996; Whiley and Bentham, 2011). *L. longbeachae* appears to have adapted to this specific environment, since its genome encodes for enzymes that enable the use of plant cellulose as a source of nutrients (Cazalet *et al.*, 2010). Additional species shown to cause disease in humans are *L. micdadei*, *L. bozemanii*, *L. dumofii*, or *L. sainthelensii*, but together, they combine only for a minor proportion of all reported cases (Beauté, 2017; Miyashita *et al.*, 2020; Chambers *et al.*, 2021).

1.3.3 *Legionella* infection

1.3.3.1 Transmission and uptake of *Legionella*

Legionella are transmitted to humans via inhalation of contaminated aerosols or particles (Cunha *et al.*, 2016). It is believed that human-to-human transmission of *Legionella* does not occur. However, one case of human-to-human transmission of *Legionella* has been reported (Correia *et al.*, 2016). While some *Legionella* species have been found to additionally infect alveolar epithelial cells as well (Mody *et al.*, 1993; Maruta *et al.*, 1998), the bacteria reaching the distal airways are mainly phagocytosed by AM (Mondino *et al.*, 2020). After uptake of pathogens, phagosomes of AM usually mature along the endocytic pathway leading to the formation of phagolysosomes. These vesicles are progressively acidified and contain several degrading enzymes like proteases and hydrolases, resulting in the subsequent degradation of ingested microbes (Uribe-Querol and Rosales, 2017).

1.3.3.2 Intracellular replication of *Legionella*

When *Legionella* are engulfed by AM, the bacteria secrete more than 25 effector proteins via a type II secretion system (White and Cianciotto, 2019), and more than 300 effector proteins via a type IV secretion system, called “defect-in-organelle-trafficking/intracellular-multiplication” (Dot/Icm), into the host cell (So *et al.*, 2015; Mondino *et al.*, 2020). The main purpose of the injected effector proteins is the generation of the so-called *Legionella*-containing vacuole (LCV), a protected intracellular niche allowing for bacterial replication. To achieve LCV formation, translocated effector proteins subvert host cell secretory and trafficking pathways, autophagy and cell death pathways, as well as host transcription and protein ubiquitination (Newton *et al.*, 2010; So *et al.*, 2015; Mondino *et al.*, 2020). The translocation of effector proteins is essential for *Legionella* survival and replication. Strains that lack the *dot* and/or *icm* genes are processed along the regular endocytic pathway, and bacteria are degraded by the host cell (Berger and Isberg, 1993; Andrews *et al.*, 1998).

After initial uptake, *L. pneumophila*-containing phagosomes evade fusion with lysosomes, and phagosome acidification is prevented by an effector called SidK which inhibits the proton pump vacuolar ATPase (Horwitz, 1983; Xu *et al.*, 2010). Additional markers of normal endosomal maturation, for example the small GTPase Rab5 or lysosome-associated membrane glycoproteins, remain absent from the LCV as well (Clemens *et al.*, 2000; Newton *et al.*, 2010; Gaspar and Machner, 2014). Instead, different proteins such as the small GTPases Rab1 and Arf1, or the protein Sec22b, are recruited to the vacuole membrane by effector proteins including SidM and RalF (Nagai *et al.*, 2002; Kagan *et al.*, 2004; Robinson and Roy, 2006; Machner and Isberg, 2006; Murata *et al.*, 2006). These recruited host proteins then mediate the redirection and attachment of endoplasmic reticulum-derived vesicles to the LCV, thus masking it from cellular defence mechanisms. Additional effector proteins mediate the translocation of nutrients for the bacteria into the LCV. Important examples include AnkB, which directs ubiquitinated proteins to the LCV where they are degraded to provide essential amino acids, and MavN, which transports iron across the LCV

membrane (Price *et al.*, 2011; Isaac *et al.*, 2015). Within the protected, pH-neutral and nutrient-rich LCV, *Legionella* can successfully replicate, a process that starts from approximately 4 – 10 hours after initial phagocytosis (Newton *et al.*, 2010; Mondino *et al.*, 2020).

Notably, most of our knowledge on LCV formation results from studies using *L. pneumophila*. Even though some minor differences have been observed, the mechanisms involved in LCV formation and replication of *L. longbeachae* appear to be mostly similar, despite species-specific effector protein repertoires and virulence factors (Asare and Abu Kwaik, 2007; Kozak *et al.*, 2010; Wood *et al.*, 2015).

1.3.3.3 Cell egress of *Legionella*

Although the exact mechanisms by which *Legionella* egress from AM *in vivo* remain to be identified, the bacteria must escape both the LCV and the host cell. Central to *L. pneumophila* egress is the ability to acquire a more virulent and transmissive phenotype which appears to be associated with metabolic changes as a result of exhausted nutrient supply for the bacteria (Bruggemann *et al.*, 2006; Dalebroux *et al.*, 2009; O'Connor *et al.*, 2016; Oliva *et al.*, 2018). In their transmissive state, *L. pneumophila* are able to induce pore formation and exit the LCV into the cytoplasm, where they display cytotoxic traits (Kirby *et al.*, 1998; Alli *et al.*, 2000; Molmeret *et al.*, 2004). Cytotoxicity in these studies was initially attributed to contact-dependent pore formation within the host cell membrane, but more recently has been associated with the activation of the NLRC4-inflammasome (Silveira and Zamboni, 2010). Once liberated from the host cell, the bacteria are distributed throughout the lung, where they are taken up by a range of additional immune cells (Brown *et al.*, 2017).

1.4 The innate immune response in the lung

1.4.1 Pathogen recognition receptors

For an immune response to be generated, pathogens that successfully invade tissues such as the lung must be recognized. This is achieved by different classes of extra- and intracellular pattern recognition receptors (PRR) that sense conserved molecular structures called pathogen-associated molecular patterns (PAMP) or damage-associated molecular patterns (DAMP) in case of cellular stress or damage. PRR include Toll-like receptors (TLR), RIG-I-like receptors (RLR), NOD-like receptors (NLR), C-type lectin receptors (CLR), and cytosolic nucleic acid sensors, all of which are strategically located to rapidly recognize the presence of a pathogen (Takeuchi and Akira, 2010; Cai *et al.*, 2014). In the naïve lung, PRR are expressed by non-immune cells such as bronchial or alveolar epithelial and endothelial cells, as well as by AM and dendritic cells, the two main types of immune cells that probe the airways for inhaled microorganisms and particles (Rohmann *et al.*, 2011; Guilliams *et al.*, 2013; Leiva-Juárez *et al.*, 2018). Ten functional TLRs exist in humans, and 12 in mice, all of which are transmembrane proteins expressed on the cell membrane or in intracellular vesicles (Kawasaki and Kawai, 2014). Each TLR recognizes specific PAMP, ranging from microbial lipoproteins (TLR1/2) to double-stranded RNA (TLR3), lipopolysaccharide (LPS) (TLR4), flagellin (TLR5), and CpG-rich DNA (TLR9) (Takeuchi and Akira, 2010). TLR activation induces the recruitment of the adaptor proteins MyD88 or TRIF, which in turn trigger signalling cascades that activate transcription factors including NF-κB and interferon-regulatory factors (IRF) that translocate to the nucleus (Kawasaki and Kawai, 2014). This leads to the expression of pro-inflammatory cytokines and chemokines, the production of antimicrobial peptides, and the upregulation of major histocompatibility complex (MHC) receptors and other co-stimulatory molecules required for antigen presentation (Gong *et al.*, 2020; Fitzgerald and Kagan, 2020).

RLR are cytosolic sensors of viral nucleic acids, and thus particularly important in antiviral defense. Activated RLR signal through the adaptor protein

mitochondrial antiviral-signalling protein (MAVS), which in turn activates NF-κB and IRFs to induce the production of type I interferons (IFN) and other pro-inflammatory cytokines (Rehwinkel and Gack, 2020).

NLR are a diverse class of cytosolic PRR that includes NOD1 and NOD2, which are able to sense bacterial peptidoglycan derivatives and activate the transcription factor NF-κB (Girardin *et al.*, 2003). It also contains several NLR proteins and the non-NLR proteins AIM2 and Pyrin, all of which are able to form multi-protein complexes called the inflammasomes (Platnich and Muruve, 2019). The inflammasomes consist of its specific receptor, the adaptor protein ASC, and pro-caspase-1, which gets activated and cleaves the effector molecule gasdermin D. Gasdermin D translocates to the cell membrane to form pores and causes pyroptosis, an inflammatory type of cell death associated with the release of the pro-inflammatory cytokines IL-1β and IL-18 (Schroder and Tschopp, 2010). NLR sense a large variety of PAMP and DAMP including microbial DNA or toxins, cellular stress, changes to cellular metabolism, ion or protein composition, or crystalline or particulate matter (Broz and Dixit, 2016; Zheng *et al.*, 2020).

Members of the CLR family, including Dectin-1 and -2, DC-SIGN, or Mincle, mainly sense components of fungal cell walls such as β-glucan or mannan. They are thus particularly important in antifungal immunity but are also able to recognize bacterial or viral PAMP (Hardison and Brown, 2012; Hoving *et al.*, 2014). CLR can be classified into activating or inhibitory receptors based on the intracellular signal transduction pathways which can impact a range of cellular processes like NF-κB-mediated cytokine production, IFN production, inflammasome activation, and antigen presentation (Hoving *et al.*, 2014; Drouin *et al.*, 2020).

Furthermore, cGAS has been identified as an important cytosolic sensor of viral or bacterial DNA (Sun *et al.*, 2013). DNA-sensing by cGAS activates the messenger molecule cGAMP and stimulator of interferon genes (STING), which in turn leads to IRF3-dependent type I IFN production and activation of interferon-stimulated genes (Hopfner and Hornung, 2020).

1.4.2 Pulmonary cytokines and chemokines

Activation of PRR triggers multiple intracellular pathways that lead to the production of signalling molecules required to initiate and orchestrate an immune response. In the lung, the initial cell types to secrete pro-inflammatory molecules are epithelial cells, endothelial cells and AM, and recruited immune cells further contribute the cytokine and chemokine landscape.

Chemokines that are produced upon activation at the site of infections can be bound by their corresponding receptors expressed on immune cells, followed by cell migration along a chemokine concentration gradient and transmigration into infected tissues (Lee *et al.*, 2018; Hughes and Nibbs, 2018). Each immune cell population displays a specific repertoire of chemokine receptors. Neutrophils, for example, express high levels of CCR1 and CXCR2, and are attracted to the lung by several chemokines like CXCL1, CXCL2, and CXCL8 (Rossaint and Zarbock, 2013). Monocyte infiltration to the lung largely depends on the production of the monocyte chemoattractant protein (MCP)-1, also called CCL2, and the binding to its receptor CCR2 (Griffith *et al.*, 2014), whereas NK cells and T lymphocyte recruitment is predominantly mediated by the axis of CXCR3 and its ligands CXCL9, CXCL10 and CXCL11 (Groom and Luster, 2011).

Furthermore, pulmonary epithelium, endothelium and AM also produce a wide range of pro-inflammatory cytokines early after infection, including IL-1α, IL-1β, IL-6, IL-12, GM-CSF, and TNFα (Arango Duque and Descoteaux, 2014; Byrne *et al.*, 2015). These cytokines promote cellular recruitment by inducing or further amplifying chemokine signalling, and can also activate immune cells to execute their microbicidal functions.

IL-1α, which is constitutively expressed by epithelial cells, can increase CXCL8 (IL-8) production by bystander cells in response to an inflammatory stimulus (Dinarello, 2018). IL-1β is a pro-inflammatory molecule that is, together with IL-18, released after inflammasome and caspase-1 activation (Schroder and Tschopp, 2010). Similar to IL-12, IL-18 is an important contributor to cell-mediated immunity by inducing the secretion of IFNγ from NK cells or T cell subsets (Trinchieri, 2003; Kaplanski, 2018). IFNγ in turn activates antimicrobial

effector mechanisms such as ROS production in myeloid cells, upregulates antigen presentation by dendritic cells, and contributes to T cell effector functions (Schroder *et al.*, 2004; Kak *et al.*, 2018). IL-6 and GM-CSF both display a wide range of functions and are involved in cellular recruitment and activation of myeloid and lymphoid immune cell populations (Fleetwood *et al.*, 2005; Scheller *et al.*, 2011). Lastly, TNFα is a rapidly produced cytokine that mediates an acute response towards pathogens, causes vasodilation of blood vessels to support cellular migration and, together with IL-17, triggers the release of CXCL1 and CXCL2 in order to recruit neutrophils to the lung (Griffin *et al.*, 2012; Brenner *et al.*, 2015). AM and epithelial cells also produce type I and type III IFNs, critical groups of cytokines that are particularly produced after recognition of viral pathogens. They aid in preventing spread of infection by promoting antigen presentation and T cell responses, and by maintaining epithelial barrier function (Crotta *et al.*, 2013; Crouse *et al.*, 2015; Stanifer *et al.*, 2020).

While rapid production of these pro-inflammatory cytokines is essential in pathogen clearance, immune responses must be controlled in order to prevent excessive tissue damage. Therefore, anti-inflammatory molecules like TGFβ, IL-10 and IL-1RA, are secreted in the lungs to dampen inflammatory responses and enabling the return to homeostasis (D'Alessio *et al.*, 2009; Wynn and Vannella, 2016).

1.4.3 Innate cellular immune responses in the lung

The innate cellular immune response directed against invading pathogens in the lung is mediated by epithelial cells, AM, dendritic cells, neutrophils, monocytes, and innate lymphoid cells (ILC).

Epithelial cells not only secrete inflammatory mediators to recruit and activate immune cells, but also produce antimicrobial peptides and enzymes when sensing an invading pathogen. These include lysozyme and lactoferrin, defensins such as α- and β-defensin, and cathelicidins like LL-37, all of which predominantly function by targeting and disrupting bacterial membrane components (Bals *et al.*, 1998; Lecaille *et al.*, 2016; Leiva-Juárez *et al.*, 2018). Additionally, the surfactant

proteins SP-A and SP-D secreted by type II AEC promote microbial phagocytosis and clearance by myeloid cells (Wright, 2005).

AM are a lung-specific subtype of macrophages, a highly diverse group of tissue-resident phagocytes with specific functions depending on the tissue they are located in. AM account for more than 90 % of macrophages present in the lung, where they are ideally positioned to sample the alveolar space (Kopf *et al.*, 2015). Macrophages are able to adapt to their environment in that they display distinct phenotypes, leaning either towards a classically activated (M1) macrophage or alternatively activated (M2) macrophage (Hussell and Bell, 2014). In homeostasis, AM tend to resemble M2 macrophages and contribute to maintaining immune homeostasis (Garbi and Lambrecht, 2017). Upon encounter of invading pathogens, they rapidly switch to an M1 phenotype and upregulate antimicrobial mechanisms. In response to microbial uptake, they initiate immune responses through pro-inflammatory cytokine signalling as discussed previously, but also directly mediate bacterial, fungal, and viral clearance (Ibrahim-Granet *et al.*, 2003; Arredouani *et al.*, 2004; Schneider *et al.*, 2014; Kopf *et al.*, 2015). Direct AM effector mechanisms include the production of ROS and reactive nitrogen species (RNS), as well as the activation of enzymes, proteases and peptides able to eliminate pathogens (Uribe-Querol and Rosales, 2017; Szulc-Dąbrowska *et al.*, 2020; Herb and Schramm, 2021).

Dendritic cells are a diverse group of cells that includes two types of conventional dendritic cells and the plasmacytoid dendritic cells (Heath and Carbone, 2009). Each subset secretes a specific range of pro-inflammatory cytokines including type I IFN, TNFα, IL-1 or IL-6. But their main task is to sample the airways for invading pathogens and present pathogen-derived antigens on MHC class I or II molecules to prime or reactivate T cells in the lung during infection (Guilliams *et al.*, 2013).

Neutrophils and monocytes are recruited along chemokine gradients to sites of infection where they transmigrate from the blood vessels into the tissue after attaching to adhesion molecules expressed on the endothelium and specific counterparts on their own cell membrane (Gerhardt and Ley, 2015; Schnoor *et al.*, 2021).

Neutrophils represent the largest proportion of leukocytes in the blood, and are potent phagocytic cells equipped with an array of microbicidal mechanisms. Aside from direct phagocytosis, neutrophils release neutrophil extracellular traps (NETs) in order to engulf pathogens (Brinkmann *et al.*, 2004). One main avenue of neutrophils to degrade phagocytosed pathogens is to generate ROS and RNS via the enzyme complexes NADPH oxidase and nitric oxide synthase (McKenna *et al.*, 2021). Neutrophils also contain different classes of granules and secretory vesicles that harbour specific groups of antimicrobial enzymes and peptides that can directly eliminate pathogens. Well-known examples are myeloperoxidase, neutrophil elastase, cathepsin G or lysozyme, all of which are stored in azurophilic granules, and lactoferrin or neutrophil gelatinase associated lipocalin, which are stored in specific granules (McKenna *et al.*, 2021). However, while degranulation of these contents into the phagolysosome mediates the desired pathogen destruction, their release into the pulmonary environment can cause significant tissue damage and contribute to disease (Grommes and Soehnlein, 2011).

Monocytes are circulating myeloid cells that can be subdivided in classical and non-classical monocytes based on their Ly6C expression in mice, or on their CD14 and CD16 expression in humans (Guilliams *et al.*, 2018). Upon CCR2-dependent infiltration of infected tissues, classical $CD14^{+}CD16^{-}$ and $Ly6C^{hi}$ monocytes display pro-inflammatory properties and functionally resemble macrophages or dendritic cells, which led to their designation as monocyte-derived cells (MC) (Guilliams *et al.*, 2018). MC employ antimicrobial strategies similar to macrophages to eliminate pathogens including phagocytosis, production of ROS and RNS, as well as secretion of pathogen-degrading enzymes (Serbina *et al.*, 2008; Brown *et al.*, 2017; Sampath *et al.*, 2018). They were found to be a major source of TNFα and thus important contributors to bacterial clearance in the lung and other tissues (Serbina *et al.*, 2003; Hackstein *et al.*, 2013; Brown *et al.*, 2016), but are also capable of antigen presentation and modulating T cell responses (Jakubzick *et al.*, 2017).

Lastly, ILC are a diverse group of immune cells that do not express rearranged antigen receptors like classical lymphoid cells, and are divided based on their

functions, which are similar to specific T cell subsets (Spits *et al.*, 2013). Group I ILCs are important producers of IFNγ, and include NK cells which execute direct cytotoxicity against antibody-coated target cells (Vivier *et al.*, 2008). Group II ILCs secrete IL-5, IL-9 and IL-13, cytokines that are characteristic of type II immune responses directed against multicellular parasites, and contribute to tissue homeostasis and the development of allergies (Xiong *et al.*, 2019). Furthermore, the heterogenous group III ILCs share the ability to produce the pro-inflammatory cytokines IL-17 and IL-22 (Melo-Gonzalez and Hepworth, 2017). Even though each ILC subset displays distinct immune functions, all members have been found to contribute to the eradication of specific pulmonary pathogens, including viruses, bacteria, fungi or helminths (Stehle *et al.*, 2018).

Importantly, the pulmonary immune response contains a second major branch, the adaptive immunity. It is mediated by T and B lymphocytes, and is highly specific and able to generate immunological memory. However, it will not be discussed here, since the focus of this thesis is on the function of innate immune cells, and the role of the innate immune response during bacterial pneumonia.

1.5 The pulmonary immune response against *Legionella*

1.5.1 Recognition of *Legionella*

Legionella-associated PAMP are primarily recognized by TLR2, TLR5, and TLR9 (Girard *et al.*, 2003; Hawn *et al.*, 2006; Archer *et al.*, 2009). Interestingly, *Legionella*-derived LPS has been shown to be recognized by TLR2 as well, rather than by TLR4, which was originally identified to sense bacterial LPS (Fuse *et al.*, 2007). TLR2-deficient mice displayed a more severe phenotype after infection with *L. pneumophila*, as it resulted in increased bacterial load and delayed cytokine production as well as reduced neutrophil recruitment (Archer and Roy, 2006; Hawn *et al.*, 2006). TLR5-deficiency has also been implicated in impaired early neutrophil recruitment, but overall bacterial clearance and cytokine production appeared to be unaffected by its absence (Hawn *et al.*, 2007; Archer *et al.*, 2009). Conflicting reports exist on the role in TLR9, but it appears to be

involved in the production of pro-inflammatory cytokines IL-12 and TNFα, both of which contribute to *Legionella* clearance (Bhan *et al.*, 2008; Mascarenhas *et al.*, 2015). A critical role in the defence against *Legionella* infection can be attributed to the shared adaptor protein MyD88. In its absence, reduced cytokine and chemokine production, as well as limited leukocyte infiltration into the lungs was observed, resulting in increased bacterial load and dissemination, as well as higher mortality in mice (Spörri *et al.*, 2006b; Archer *et al.*, 2009; Archer *et al.*, 2010; Mascarenhas *et al.*, 2015). However, when infecting TLR2- and TLR9-double-deficient mice with non-flagellated *L. pneumophila* and thus avoiding the stimulation of TLR2, TLR5, NAIP5/NLRC4, and TLR9, mice were still able to clear the bacteria (Archer *et al.*, 2009). This indicates that additional sensors of microorganisms and other signalling pathways are likely to play a critical role in the immune response towards *Legionella*.

These include, for example, cytosolic nucleic acid sensors such as cGAS, which binds *Legionella*-derived DNA (Stetson and Medzhitov, 2006; Lippmann *et al.*, 2011), and RIG-1 or MDA5, which are able to bind bacterial RNA (Monroe *et al.*, 2009). Their specific downstream signalling pathways lead to the induction of IRF3 and subsequent production of type I IFNs by infected epithelial cells or macrophages, thus contributing to optimal restriction of *Legionella* (Schiavoni *et al.*, 2004; Opitz *et al.*, 2006; Lippmann *et al.*, 2011; Naujoks *et al.*, 2018). *In vivo* studies confirm the importance of nucleic acid sensing after infection, as increased loads of *L. pneumophila* were found in lungs of both cGAS- and STING-deficient mice (Ruiz-Moreno *et al.*, 2018). Furthermore, the NLRs NOD1 and NOD2 were both linked to neutrophil recruitment and *Legionella* clearance, but the exact underlying mechanisms are not yet fully determined (Frutuoso *et al.*, 2010; Berrington *et al.*, 2013). The main NLR involved in the immune response against *L. pneumophila* is NAIP5, which is able to recognize bacterial flagellin expressed by several *Legionella* species including *L. pneumophila* (Ren *et al.*, 2006). Flagellin recognition leads to heterodimerization of NAIP5 with NLRC4, inducing an NLCR4 inflammasome-driven immune response which was able to quickly clear bacteria from the lungs of mice without detectable symptoms of disease (Molofsky *et al.*, 2006; Pereira *et al.*, 2011). However, inflammasome

activity can be initiated in a flagellin-independent manner via caspase-11 activation as well (Case *et al.*, 2013). It was found that the family of guanylate binding proteins (GBPs), which are able to sense cytosolic LPS derived from *L. pneumophila*, are critical mediators of caspase-11 and inflammasome activation (Pilla *et al.*, 2014). Mice deficient in the cluster of GBP encoded on chromosome 3 displayed significantly delayed pro-inflammatory cytokine signalling and impaired restriction of *L. pneumophila* replication (Liu *et al.*, 2018).

In contrast to *L. pneumophila*, the genome of *L. longbeachae* does not encode for flagellin but other potential virulence factors. These differences are one possible explanation for the observation that *L. longbeachae* is more virulent in a number of mouse strains when compared to *L. pneumophila*, and results in significant mortality (Asare *et al.*, 2007; Massis *et al.*, 2017). The specific immune response towards *L. longbeachae* is an ongoing current subject of research.

1.5.2 Cytokines in anti-*Legionella* defence

Early after *Legionella* infection, AM are the main cell type that take up the bacteria, and thus are key to initiate cytokine and chemokine production to attract further innate pulmonary phagocytes like neutrophils, dendritic cells and monocyte-derived cells (MC) (Brown *et al.*, 2017). Similarly, these cells are able to recognize and engulf *Legionella*, and contribute to the secretion of pro-inflammatory mediators.

After phagocytosis, AM produce IL-1α and IL-1β despite translocation of antagonizing effector proteins by *Legionella* (Barry *et al.*, 2013a; Asrat *et al.*, 2014; Copenhaver *et al.*, 2015). IL-1 and IL-1 receptor signalling initiated by AM activates bystander epithelial and immune cells to produce the pro-inflammatory cytokines GM-CSF (Liu *et al.*, 2020), TNFα (Copenhaver *et al.*, 2015; Ziltener *et al.*, 2016), or IL-12 (Copenhaver *et al.*, 2015; Brown *et al.*, 2016). These cytokines attract several innate immune cells to the lung, particularly MC and neutrophils (LeibundGut-Landmann *et al.*, 2011; Ziltener *et al.*, 2016; Brown *et al.*, 2017). Mice deficient in IL-1 receptor signalling displayed reduced neutrophil recruitment and bacterial clearance (Mascarenhas *et al.*, 2015; Copenhaver *et al.*, 2015).

Similarly, mice either depleted in IL-12p40 (Brieland *et al.*, 1998) or deficient in TNFα and TNF-receptor 1 signalling (Fujita *et al.*, 2008; Ziltener *et al.*, 2016) are significantly impaired in their capability to eradicate the bacteria.
Further cytokines associated with either driving lung infiltration of inflammatory cells or triggering release of IFNγ are IL-17 (Cai *et al.*, 2016), IL-18 (Brieland *et al.*, 2000), and IL-23p19 (Fontana *et al.*, 2011). Although *Legionella*-infected AM produce type I IFN, its exact contribution during infection *in vivo* remains unclear, since IFNα receptor-deficient mice are readily able to clear bacteria (Ang *et al.*, 2010; Lippmann *et al.*, 2011; Naujoks *et al.*, 2016).
IFNγ is of major importance in eradicating *L. pneumophila*. Mice lacking IFNγ or the IFNγ-receptor are unable to restrict bacterial replication, leading to systemic dissemination and increased mortality (Shinozawa *et al.*, 2002; Spörri *et al.*, 2006a; Lippmann *et al.*, 2011). Previous work by our group demonstrated that IL-12 stimulates IFNγ-production by NK cells and a variety of T cell subsets, which in turn induced IFNγ-dependent bacterial killing specifically by MC (Brown *et al.*, 2016). Human patients with acute Legionnaires' Disease showed elevated serum levels of IFNγ and IL-12, suggesting that these cytokines are of relevance in human disease as well (Tateda *et al.*, 1998).
Since *L. longbeachae* is morphologically different and encodes species-specific virulence factors, other cytokines and chemokines may play a critical role during the immune response as well. While it has been demonstrated that TNFα, IFNγ and IL-12 are required for efficient clearance of *L. longbeachae* as well (Massis *et al.*, 2017), IL-18 appears to be of special relevance in the elimination of *L. longbeachae* from the lung (Oberkircher *et al.*, 2022, in preparation).

1.5.3 Cellular immune responses towards *Legionella*

Programmed cell death is an effective way of the host immune response to eliminate infected cells. AM, the first cells to encounter *Legionella*, can sense *L. pneumophila*-derived flagellin and, in response, undergo NAIP5/NLRC4-dependent pyroptosis (Zamboni *et al.*, 2006; Molofsky *et al.*, 2006; Case *et al.*,

2009). Accordingly, NLRC4-deficient mice have been shown to clear infection less efficiently (Zamboni *et al.*, 2006; Case *et al.*, 2009). Interestingly, infection with non-flagellated *L. pneumophila*, which are not sensed by NAIP5, still induces transient AM depletion (Brown *et al.*, 2016), which may be attributed to caspase-1-independent pyroptosis (Case *et al.*, 2013). Additionally, AM were reported to display direct bactericidal activity mediated by TNFα (Ziltener *et al.*, 2016).

Aside from this, the clearance of *Legionella* from the lung highly depends on a quickly mounted innate immune response. Infiltrating neutrophils phagocytose *Legionella* and generate ROS via NADPH oxidase activity in response to bacterial effector translocation, and display antimicrobial protease activity (Ziltener *et al.*, 2016; Anderson *et al.*, 2019). Thus, they are one key cell type in clearing *Legionella*, and neutrophil-deficient mice are highly susceptible to infection (Tateda, *et al.*, 2001; LeibundGut-Landmann *et al.*, 2011). Neutrophils also dominate the immune response against *L. longbeachae* (Massis *et al.*, 2017). A second major cell population required for resolving infection and degrading *Legionella* are MC. During *L. pneumophila* infection, they engulf bacteria and contribute to their clearance by killing them in an IFNγ-dependent manner. CCR2-deficient mice are unable to efficiently recruit these cells to the lung, and are significantly impaired in their ability to clear *L. pneumophila* (Brown *et al.*, 2016).

While dendritic cells have been found to engulf *L. pneumophila* as well (Brown *et al.*, 2016), their contribution to bacterial clearance is not clear. An adaptive immune response, and thus antigen presentation by dendritic cells, appear to be of lesser importance, since mice lacking T and B lymphocytes readily eliminate *L. pneumophila* (Cai *et al.*, 2016). Nevertheless, T cell subsets, along with NK cells, represent an important source of IFNγ to induce bactericidal activity in myeloid cells such as MC (Brown *et al.*, 2016). The presence of *Legionella*-specific IgG and IgA antibodies identified in later stages of infection suggests at least some B cell activity (Joller *et al.*, 2007). One recently identified type of innate-like lymphocytes, namely mucosal associated invariant T (MAIT) cells, was shown to be enriched and activated in the lungs of mice infected with *L. longbeachae*, where they mediated IFNγ-dependent protection and reduction of

bacterial load (Wang *et al.*, 2018). This study also reported that in Rag2$^{-/-}\gamma C^{-/-}$ mice, which lack conventional T cells, B cells, and NK cells, were highly susceptible to *L. longbeachae* infection and were unable to clear the bacteria.

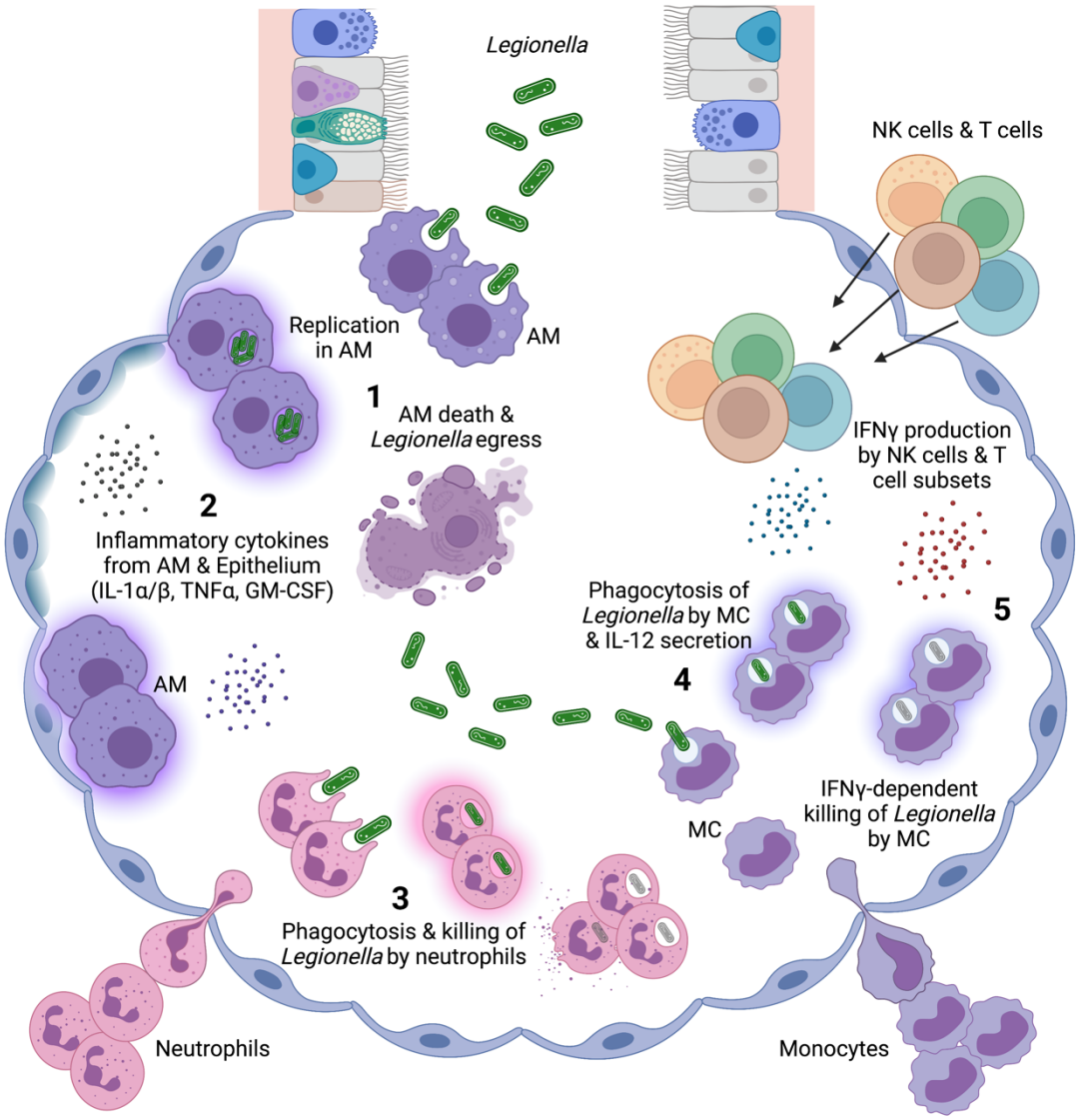

Figure 1.1: The pulmonary immune response against *L. pneumophila*.
(1) Upon inhalation, *Legionella* are engulfed by AM, in which they replicate by establishing a *Legionella*-containing vacuole.
(2) AM initiate an immune response, inducing the production of pro-inflammatory cytokines such as IL-1α, IL-1β, TNFα, or GM-CSF by epithelial cells and bystander AM. Inflammatory AM death enhances the pro-inflammatory cytokine production.
(3) Neutrophils are recruited and infiltrate the lung, phagocytosing and killing *Legionella* in an NADPH-oxidase-dependent manner.
(4) Monocyte-derived cells (MC) are recruited and infiltrate the lung. They phagocytose *Legionella* and secrete IL-12.
(5) IL-12 in turn activates recruited NK cells and T cell subsets to secrete IFNγ, which feeds back to MC and induces IFNγ-dependent bactericidal activity of MC.
Figure adapted from (Brown *et al.*, 2017), created with biorender.com.
AM = alveolar macrophage, MC = monocyte-derived cell.

1.6 Impact of cigarette smoke on pulmonary immune responses

1.6.1 Cigarette smoking

1.6.1.1 Cigarette smoking as a global health burden

Cigarette smoking is one of the most relevant environmental risk factors associated with morbidity and mortality in humans. According to recent estimations, cigarette, i.e., tobacco smoking accounts for more than 8.5 million deaths each year (Murray *et al.*, 2020; Reitsma *et al.*, 2021). This includes approximately 1 million deaths of non-smokers that are only indirectly exposed to cigarette smoke. Smoking-related deaths are distributed between a wide variety of conditions like malignant neoplasms (cancer), lower respiratory tract infections, cardiovascular diseases and chronic respiratory diseases (Murray *et al.*, 2020). Despite considerable efforts to reduce the size of the smoking population, more than one billion people worldwide are estimated to be current smokers, thus making smoking a major global health burden (Jha and Peto, 2014; Reitsma *et al.*, 2021).

1.6.1.2 Cigarette smoke components

Cigarette smoke itself is a highly variable and complex mixture consisting of a particulate phase and a gaseous phase generated via combustion, pyrolysis, sublimation and condensation processes (Borgerding and Klus, 2005). In total, cigarette smoke contains more than 7,000 components, many of which have been classified as toxic, carcinogenic or otherwise harmful substances. These substances include toxic gases like carbon monoxide or hydrogen cyanide, ROS and free radicals, aldehydes and ketones like formaldehyde, aromatic amines and nitrosamines such as aminobiphenyl, polycyclic aromatic hydrocarbons, trace metals like mercury or lead, addictive substances such as nicotine, and tar (Talhout *et al.*, 2011; Soleimani *et al.*, 2022). These components are not only present in the so-called mainstream smoke which is directly inhaled into the

lungs, but also in the sidestream smoke that forms at the tip of the cigarette and is released into the environment (Borgerding and Klus, 2005). Sidestream smoke and exhaled mainstream smoke can distribute through the air and persist for hours in closed areas, thus exposing non-smokers to cigarette smoke as well (Van Deusen *et al.*, 2009; Kraev *et al.*, 2009; Soleimani *et al.*, 2022).

1.6.2 Impact of cigarette smoke on pulmonary immune responses

Cigarette smoke and its individual components strongly contribute to the development, progress and outcome of a wide range of disease (Reitsma *et al.*, 2021). This is particularly the case in the lung which is directly exposed to inhaled smoke. Here, smoking is associated with the development of chronic obstructive pulmonary disease (COPD) (Kirkham and Barnes, 2013), lung cancer (de Groot *et al.*, 2018) or asthma (Polosa and Thomson, 2013). Additionally, cigarette smoke increases the susceptibility to microbial infections due to its major effects on pulmonary immune functions (Arcavi and Benowitz, 2004; Bagaitkar *et al.*, 2008). Importantly, the impact of cigarette smoke on the pulmonary immune response is of dual nature. While smoking can act as a pro-inflammatory stimulus, it is mostly associated with a suppressed innate immune response towards invading pathogens (Stämpfli and Anderson, 2009; Strzelak *et al.*, 2018).

1.6.2.1 Pulmonary epithelium

Cigarette smoke can cause a sustained persistence of invading pathogens within the airways by impairing the mucociliary transport machinery. Smoke dysregulates the ion transport across the pulmonary epithelium and causes mucus overproduction that is driven by excessive epithelial secretion of the mucin MUC5AC (Innes *et al.*, 2006; Cohen *et al.*, 2009; Xavier *et al.*, 2013). Smoke exposure also reduces the number and function of cilia, small protrusions on epithelial cells that constantly beat to transport mucus from distal parts of the airways to the pharynx (Cohen *et al.*, 2009; Tamashiro *et al.*, 2009; Leopold *et al.*, 2009). Furthermore, the integrity of the epithelial barrier is disrupted due to a

smoke-induced downregulation of cell-cell interactions and the development of paracellular gaps (Gangl *et al.*, 2009; Shaykhiev *et al.*, 2011; Heijink *et al.*, 2012; Moazed *et al.*, 2016).

Smoking also leads to defects in the secretory functions of AEC, resulting in decreased production of surfactant proteins (Honda *et al.*, 1996) or antimicrobial peptides like β-defensin (Herr *et al.*, 2009; Zhang *et al.*, 2011). Similarly, the production of chemokines and cytokines by the epithelium are affected by smoke. Bronchial and alveolar epithelial cells were, on the one hand, reported to strongly produce pro-inflammatory cytokines such as IL-6, IL-8, or TNFα in response to smoke exposure (Mio *et al.*, 1997; Vlahos *et al.*, 2006; Gao *et al.*, 2015). On the other hand, in presence of bacterial or viral pathogens, the initiation of an immune response by the epithelium was diminished. Lower cytokine production of type I and type II IFNs (Bauer *et al.*, 2008; Modestou *et al.*, 2010), or IL-6 and IL-8, as well as delayed cellular recruitment (Kulkarni *et al.*, 2010; Manzel *et al.*, 2011) were observed as a result of decreased nuclear presence of IRF3 and NF-κB due to smoke.

In summary, pulmonary epithelium tends to display functional deficiencies in the context of a pulmonary infection, even though it is capable of mediating pro-inflammatory processes.

1.6.2.2 Alveolar macrophages

AM are the major phagocyte within the airways, yet their ability to phagocytose invading microorganisms appears to be reduced due to cigarette smoke. This was shown for a number of bacterial pathogens including *S. pneumoniae*, *H. influenzae*, or *L. monocytogenes* (King *et al.*, 1988; Berenson *et al.*, 2006; Martí-Lliteras *et al.*, 2009; Phipps *et al.*, 2010). Mechanistically, limitations in bacterial uptake was attributed to disrupted cytoskeletal function and the accumulation of oxidised phospholipids in the cell membrane due to smoke exposure (Kimura *et al.*, 2012; Thimmulappa *et al.*, 2012). Cigarette smoke also decreases macrophage efferocytosis capability due to a down-regulation of surface recognition molecules, and these defects remained present for months after

cessation of smoke exposure (Hodge *et al.*, 2007; Richens *et al.*, 2009; Noda *et al.*, 2013). Notably, pharmacologic activation of nuclear erythroid-related factor (Nrf) 2 signaling was able to restore phagocytic capacity of *H. influenzae* and *P. aeruginosa* by AM from COPD patients and smoke-exposed mice, thus presenting an avenue for pharmacological intervention in infected smokers (Harvey *et al.*, 2011).

Furthermore, pathogen recognition and subsequent pro-inflammatory signalling cascades can be impaired in AM due to smoke exposure. For example, TLR2 and TLR4 signalling after LPS stimulation, and TLR3 signalling after polyI:C stimulation was shown to be decreased in AM from smokers (Droemann *et al.*, 2005; Chen *et al.*, 2007; Todt *et al.*, 2013). In mouse models, presence of cigarette smoke diminished production of TNF-α, IL-6 and the T cell attracting chemokine CCL5 in response to TLR stimuli due to reduced nuclear NF-κB translocation (Gaschler *et al.*, 2008). In models of *P. aeruginosa* or *M. tuberculosis* infection, a similar inhibition of cytokine secretion could be observed, coinciding with delayed bacterial clearance that further underscores the immunosuppressive role of cigarette smoke during infection (Drannik *et al.*, 2004; O'Leary *et al.*, 2014).

1.6.2.3 Neutrophils

Neutrophils are actively recruited to the lung during smoke exposure by inflammatory mediators and via increased expression of adhesion molecules required for transmigration across the epithelium (Mio *et al.*, 1997; Overbeek *et al.*, 2011; Pouwels *et al.*, 2016). Within the airways, neutrophils are a major driver of the tissue damage and chronic inflammation associated with COPD, for example by secreting serin proteases and matrix metalloproteinases (MMP). Despite this increased activity, neutrophils were reportedly unable to improve bacterial clearance in the context of infection. This has mainly been attributed to limited phagocytosis of pathogens including *E. coli*, *S. aureus* or *Candida* species (Prieto *et al.*, 2001; Stringer *et al.*, 2007; Guzik *et al.*, 2011), and to reduced microbial killing capacity (Pabst *et al.*, 1995; Dunn *et al.*, 2005). Cigarette smoke

was also shown to influence the formation and function of NET by neutrophils, but how this may impact specific immune responses has yet to be examined in more detail (Qiu *et al.*, 2017; White *et al.*, 2018).

1.6.2.4 Dendritic cells, NK cells and monocytes

The main function of dendritic cells, which is the presentation of pathogen-derived antigens to prime T cell responses can be significantly impacted by cigarette smoke. Reduced surface expression of MHC class II, as well as downregulation of co-stimulatory molecules and the maturation markers CD80 and CD86 were observed *in vitro*, and in a murine model of smoke exposure (Robbins *et al.*, 2008; Givi *et al.*, 2015). Additionally, a range of cytokines normally secreted by dendritic cells in response to pathogen sensing were produced less efficiently because of smoke. These include IL-12 and IL-23 (Kroening *et al.*, 2008), as well as IL-1β and type I IFN due to reduced IRF7 activation (Castro *et al.*, 2011).

The impact of cigarette smoke on NK cells is currently still in debate since some studies reported an increased activity (Motz *et al.*, 2010; Bozinovski *et al.*, 2015), while others observed a reduction in NK cell cytotoxicity and pro-inflammatory TNFα and IFNγ production, mechanisms that usually contribute to pathogen clearance (Mian *et al.*, 2008; Mian *et al.*, 2009). However, decreased NK cell function and immunosurveillance was also associated with pulmonary tumour development (Lu *et al.*, 2007).

The impact of cigarette smoke on monocyte activity in the lung is more difficult to assess due to the different phenotypes they obtain upon infiltration of tissues. Like other immune cells, however, the pro-inflammatory effect of cigarette smoke causes their enhanced recruitment to the lung (Barnes, 2009; Barnes, 2016). Cigarette smoke also changes the proportion of different monocytes subsets in the lung and skews their cytokine profile to resemble that of pulmonary macrophages (Pérez-Rial *et al.*, 2013; Oliveira da Silva *et al.*, 2017; da Silva *et al.*, 2020). It is thus likely that the smoke causes the same functional differences in monocytes and monocyte-derived macrophages infiltrating the lung as AM.

Additional to the innate immune response, cigarette smoke also modulates adaptive immunity in the lung (Stämpfli and Anderson, 2009; Strzelak *et al.*, 2018). But similar to the effects on innate immune mechanisms, the complexity of cigarette smoke induces both pro- and anti-inflammatory effects in T and B lymphocytes. Further investigations are therefore essential to increase our understanding on how smoking renders the individual components of the immune system less capable of fighting invading pathogens.

1.7 Thesis aims

Cigarette smoke has diverse effects on the pulmonary microenvironment and on the components of pulmonary immune responses. Cigarette smoke is capable of inducing cell death, but *in vivo*, this has never been demonstrated for AM. Cigarette smoke is a major risk factor associated with the bacterial pneumonia Legionnaires' Disease, but it is not known how smoke mechanistically renders individuals more susceptible to disease.

Therefore, the aims of the first two parts of this thesis were

(i) to investigate if cigarette smoke caused AM depletion *in vivo*, and to identify the cell death pathways that mediated a potential cigarette smoke-induced AM death,

(ii) to assess how smoke exposure impacted disease progression and the immune response after infection with two *Legionella* species, *L. pneumophila* and *L. longbeachae*.

Recently emerging evidence suggested that several immune cell populations are able to promote tissue regeneration after infection or injury. However, little is known about the mechanisms by which immune cells contribute to lung recovery from bacterial pneumonia.

Therefore, the aim of the third part of this thesis was

(iii) to investigate the contribution of different immune cells to the functional recovery of lungs from Legionnaires' Disease.

2 Materials and Methods

2.1 Material

2.1.1 Mouse strains

Mice were bred and maintained under specific pathogen-free conditions and in accordance with institutional animal guidelines in the animal facilities House of Experimental Therapy (HET) of the University of Bonn, Biological Research Facility at Bio21 Molecular Science and Biotechnology Institute, and Biomedical Science Animal Facility (BSAF) of the University of Melbourne. Mice bred in other animal facilities indicated below were imported to the BSAF of the University of Melbourne and maintained there for at least one week prior to the start of experiments. All animal experiments were performed at these facilities under approval of the ethics committees of the associated universities.
C57BL/6J mice were used as wild-type strain, and either bred as described above or purchased from Charles River Laboratories (Sulzfeld, Germany). Knock-out strains were either created on a C57BL/6 background or were backcrossed to a C57BL/6 background for at least 10 generations. Experiments were performed with mice 7 – 14 weeks of age.

Table 2.1: Mouse strains

Strain	Source and description
C57BL/6J	C57BL/6J non-transgenic wild-type (WT) mice.
$ASC^{-/-}$	B6.129S5-$Pycard^{tm1Flv}$ mice (Sutterwala *et al.*, 2006) were bred as homozygotes in the BSAF, and were a kind gift from Eva Dimitriadis. Mice of this strain are deficient in the adaptor protein ASC which is required for inflammasome formation and activation of Caspases and Gasdermin D. These mice are deficient in all forms of Caspase-1-dependent pyroptosis.

NLRP3$^{-/-}$	B6.129S5-Nlrp3^{tm1Flv} mice (Sutterwala *et al.*, 2006) were bred as homozygotes in the Peter-Doherty-Institute animal facility, and were a kind gift from Julie McAuley. Mice of this strain are deficient in the intracellular sensor NLRP3 which is specifically required for NLRP3 inflammasome formation. These mice are deficient in NLRP3-dependent pyroptosis.
MLKL$^{-/-}$	B6-Mlkl$^{tm1.2wsa}$ mice (Murphy *et al.*, 2013) were bred as homozygotes in the Walter and Eliza Hall Institute animal facility in Parkville, and were a kind gift from Kathryn Lawlor. Mice of this strain are deficient in the pseudokinase MLKL. These mice are deficient in necroptosis.

2.1.2 Pathogens

Legionella strains used in this study were kindly provided by Elizabeth Hartland, Hudson Institute of Medical Research.
The vector pON.mCherry was a gift from Howard Shuman (Addgene plasmid #84821; RRID:Addgene_84821) (Gebhardt *et al.*, 2017).

Table 2.2: *Legionella* strains

Species	Description
L. pneumophila	Strain 130b ΔflaA; containing a deletion of the flaA gene, resulting in non-flagellated *L. pneumophila*
Heat-inactivated *L. pneumophila*	See above; inactivated by incubation at 95 ºC for 60 minutes
L. longbeachae	Strain NSW150; clinical isolate
L. longbeachae-mCherry	Genetically modified *L. longbeachae* NSW150; transformed with pON.mCherry to constitutively express the fluorescent protein mCherry (Oberkircher *et al.*, 2022, in preparation).

2.1.3 Equipment

Table 2.3: Equipment

Device	Manufacturer
Amnis® ImageStream® Mk II	Luminex, Seattle, WA, USA
Anaesthetic machines	Harvard Apparatus, Holliston, MA, USA DarvallVet, Gladesville, Australia
Neubauer cell chamber	BRAND, Wertheim, Germany
Centrifuges	Eppendorf, Hamburg, Germany
ChemiDoc XRS+	BioRad, Hercules, CA, USA
Dissection equipment	Fine Science Tools, Foster City, CA, USA
FACSCanto™ II, LSRFortessa™ flow cytometer	Becton-Dickinson, Franklin Lakes, NJ, USA
FlexMap 3D System	Luminex, Seattle, WA, USA
Gel electrophoresis equipment	BioRad, Hercules, CA, USA
Gyratory rocker	Stuart Equipment, Stone, UK
Heat block	HTA-Biotec, Bovenden, Germany
HERAsafe workbench	Heraeus, Braunschweig, Germany
Incubators	Heraeus, Braunschweig, Germany Thermo Fisher Scientific, Waltham, MA, USA
IVC mouse cages	Tecniplast Smartflow, Hohenpleißenberg, Germany
MoFlo Astrios EQ Cell Sorter	Beckman Coulter, Brea, CA, USA
QuantStudio 6 RT-PCR system	Thermo Fisher Scientific, Waltham, MA, USA
Spectrophotometers (NanoDrop™, OD600 nm)	Thermo Fisher Scientific, Waltham, MA, USA BioRad, Hercules, CA, USA Implen, Munich, Germany

Thermocycler (Mastercycler Nexus)	Eppendorf, Hamburg, Germany
Tissue Lyser LT	Qiagen, Hilden, Germany
Tissue Homogenizer	IKA, Staufen, Germany
Typhoon 5	GE Healthcare
UltraMicroscope II	LaVision Biotec, Bielefeld, Germany

2.1.4 Consumables and reagents

Table 2.4: Consumables

Consumable	Manufacturer
BCYE Agar plates	Media Preparation Unit, Peter Doherty Institute, Melbourne, Australia, ThermoFisher Scientific, Waltham, MA, USA
Cannulas & Catheters	Braun, Melsungen, Germany, Terumo, Somerset, NJ, USA
Cell strainers (40 µm & 70 µm)	Corning, Corning, NY, USA, Miltenyi, Bergisch-Gladbach, Germany
FACS tubes polystyrene, 5 ml	Corning, Corning, NY, USA Sarstedt, Nümbrecht, Germany
FACS tubes polypropylene, 5 ml	Corning, Corning, NY, USA Sarstedt, Nümbrecht, Germany BD Biosciences, Franklin Lakes, NJ, USA
Injection needles (23 G, 25 G, 27 G)	Becton-Dickinson, Franklin Lakes, NJ, USA Braun, Melsungen, Germany
Microcentrifuge cups	Eppendorf, Hamburg, Germany
Microtiter plates (6-well, 96-well)	TPP, Transadingen, Switzerland Greiner bio-one, Solingen Germany

Petri dishes	Greiner bio-one, Solingen, Germany
Polypropylene tubes (15 ml, 50 ml)	Greiner bio-one, Solingen, Germany Corning, Corning, NY, USA
Surgical thread	Fine Science Tools, Foster City, CA, USA
Syringes	Becton-Dickinson, Franklin Lakes, NJ, USA Terumo, Somerset, NJ, USA
Three-way taps	Terumo, Somerset, NJ, USA

Table 2.5: Chemicals and reagents

Chemical/Reagent	**Manufacturer**
1-propanol	Sigma-Aldrich, St. Louis, MO, USA
1-propanol (anhydrous)	Sigma-Aldrich, St. Louis, MO, USA
7-AAD	BioLegend, San Diego, CA, USA
ACK buffer	Lonza, Cologne, Germany
Ammonium chloride (NH_4Cl)	Sigma-Aldrich, St. Louis, MO, USA
Bovine serum albumin (BSA)	Sigma-Aldrich, St. Louis, MO, USA
Calcium chloride ($CaCl_2$)	Sigma-Aldrich, St. Louis, MO, USA
CaliBRITE™ beads	BD Biosciences, Franklin Lakes, NJ, USA
Collagenase III & IV	Worthington Biochemical Corporation, Lakewood, NJ, USA
Dimethylsulfoxide (DMSO)	Roth, Karlsruhe, Germany
DNase I	Sigma-Aldrich, St. Louis, MO, USA
Ethanol	Roth, Karlsruhe, Germany
Ethlylene diamine tetra acetic acid (EDTA)	Merck, Darmstadt, Germany

Ethyl cinnamate	Sigma-Aldrich, St. Louis, MO, USA
FACSLysing solution	BD Biosciences, Franklin Lakes, NJ, USA
Foetal calf serum (FCS)	Life Technologies, Carlsbad, CA, USA
Fixable Viability Dye eFluor® 506	eBioscience, San Diego, CA, USA
Fixable Viability Dye eFluor® 780	eBioscience, San Diego, CA, USA
HEPES	Merck, Kenilworth, NJ, USA
Isoflurane	AbbVie, North Chicago, IL, USA
Paraformaldehyde (PFA) 16 %, methanol-free	ThermoFisher Scientific, Waltham, MA, USA
Pentobarbital (Narcoren)	Covetrus, Portland, ME, USA
Phosphate-buffered saline (PBS)	Life Technologies, Carlsbad, CA, USA
Potassium hydrochloride ($KHCO_3$)	Merck, Kenilworth, NJ, USA
RPMI 1640 medium	Invitrogen, Darmstadt, Germany
Saponin	Sigma-Aldrich, St. Louis, MO, USA
Sodium azide (NaN_3)	Roth, Karlsruhe, Germany
Sodium chloride (NaCl)	Sigma-Aldrich, St. Louis, MO, USA
Triton X-100	Sigma-Aldrich, St. Louis, MO, USA
Trypan Blue (0.4 %)	Lonza, Cologne, Germany
Xylazine	Bayer, Leverkusen, Germany

2.1.5 Buffers and media

Table 2.6: Buffers and media

Buffer	Composition
Annexin V Binding Buffer	10 mM HEPES (pH7.4), 140 mM NaCl, 2.5 mM $CaCl_2$ in double distilled water
Digestion Buffers	1 mg/ml Collagenase IV, 1 mg/ml DNase I in PBS; 1 mg/ml Collagenase III, 1 mg/ml DNase I, 3 % (v/v) FCS in RPMI-1640
Erythrocyte lysis buffer (ACK buffer)	150 mM NH_4Cl, 10mM $KHCO_3$, 1 mM EDTA in double distilled water
FACS Buffer	3 % (v/v) FCS, 0.1 % (v/v) NaN_3 in PBS
PBS	137 mM NaCl, 2.7 mM KCl, 10 mM Na_2HPO_4, 1.8 mM KH_2PO_4 in double distilled water (pH 7.4)
Perm/Block buffer	5 % (w/v) BSA, 10 % (v/v) DMSO, 2 % (v/v) TritonX-100, 0.05 % (v/v) NaN_3 in PBS

2.2 Methods

2.2.1 Treatment of mice

2.2.1.1 Cigarette smoke exposure

Cigarette smoke exposure was conducted in class II biosafety hoods as described previously by the group of Gary Anderson, University of Melbourne (Bozinovski *et al.*, 2015). Mice were exposed to cigarette smoke from commercially available cigarettes containing 1.2 mg nicotine and 16 mg tar per cigarette (Winfield Red, British American Tobacco Australia, Woolomooloo, Australia). For each smoking treatment, a maximum of 20 mice were transferred

into an 18-liter plastic container connected to a 50 ml syringe and one lit cigarette via a three-way tap. The lit cigarette's smoke was repeatedly drawn into the syringe at a rate of 8 seconds per draw and pushed into the container until the cigarette was used up. Mice were exposed to the smoke of one cigarette within the container for a total of 15 minutes before the lid was removed for 5 minutes of fresh air. This procedure was repeated three times for each treatment, and mice received three such treatments per day, equalling 9 cigarettes per day. Mice were returned to their housing cages for at least 2 hours between treatments. Control animals were likewise transferred between housing cages and identical plastic containers but not exposed to cigarette smoke.

2.2.1.2 Intranasal delivery of *Legionella* and liposomes

Legionella strains were grown on selective buffered charcoal yeast extract (BCYE) agar plates for 72 hours at 37 ºC. For intranasal infections, between 10 and 20 *Legionella* colonies were collected from BCYE agar plates, pooled and resuspended in sterile PBS. The absorbance of the bacterial suspension at an optical density of 600 nm was adjusted to 1, corresponding to $1x10^9$ CFU/ml *Legionella*. The infectious dose was then adjusted by dilution in sterile PBS. For infections with *L. pneumophila*, mice received $2.5x10^6$ CFU. For infections with *L. longbeachae*, mice received $2.5x10^5$ CFU in experiments performed in Melbourne, or $2.5x10^4$ CFU in experiments performed in Bonn. The infectious dose used in each experiment was confirmed by retrospective CFU quantitation. *Legionella* was delivered to mice under controlled isoflurane-induced anaesthesia (2 % isoflurane/O_2 (v/v)) by intranasal administration of 50 µl PBS containing the infectious dose. Control mice received 50 µl PBS only.
Likewise, mice were administered 50 µl sterile PBS, PBS liposomes, or Clodronate liposomes (Liposoma B.V., Amsterdam, Netherlands) under controlled isoflurane-induced anaesthesia.

2.2.1.3 *In vivo* cell depletion

In vivo depletion antibodies were diluted in sterile PBS prior to injection. For the depletion of neutrophils, mice received one i.p. injection of 200 µg anti-Ly6G antibody (clone 1A8) and 50 µg of anti-rat Kappa Immunoglobulin light chain antibody (clone MAR18.5) in 150 µl PBS on day 5 after infection (Boivin *et al.*, 2020). Control mice were treated with an equivalent amount of irrelevant, isotype-matched antibody (rat IgG2a, clone 2A3). For the depletion of specific T cell populations, mice received either one i.p. injection of 300 µg anti-CD4 antibody (clone GK1.5) in 150 µl PBS, or one i.p. injection of 300 µg anti-CD8 antibody (clone YTS169.4) in 150 µl PBS, on day 5 after infection. Control mice were treated with an equivalent amount of irrelevant, isotype-matched antibody (rat IgG2b, clone LTF-2).

Table 2.7: Antibodies for *in vivo* cell depletion

Antibody	Clone	Isotype	Company
Anti-CD4	GK1.5	Rat IgG2b	BioXCell, Lebanon, NH, USA
Anti-CD8	YTS169.4	Rat IgG2b	BioXCell, Lebanon, NH, USA
Anti-Ly6G	1A8	Rat IgG2a	BioXCell, Lebanon, NH, USA
Anti-rat Kappa Immunoglobulin Light Chain	MAR18.5	Mouse IgG2a, κ	BioXCell, Lebanon, NH, USA
Phycoerythrin (isotype control)	2A3	Rat IgG2a	BioXCell, Lebanon, NH, USA
KLH (isotype control)	LTF-2	Rat IgG2b	BioXCell, Lebanon, NH, USA

2.2.1.4 Respiratory mechanics

Respiratory mechanics in mice were measured using a FlexiVent™ system and *flexiware* v8.2.0 software (SciReq, Montreal, Canada) according to manufacturer's instructions. Mice were anesthetized by i.p. injection of 8 mg/kg Xylazine diluted in 100 µl sterile PBS and 90 mg/kg Pentobarbital diluted in 100 µl sterile PBS. Mice were tracheotomised by exposing the trachea and inserting an 18 G catheter, fixed with a surgical thread. Mice were then attached to the FlexiVent™ system via the catheter and a sequence of protocols as indicated in table 2.8 was initiated. After the completed measurement, the catheter was removed from the trachea, mice were killed by i.p. injection with an overdose of Pentobarbital, and lungs were retrieved for subsequent processing.

Table 2.8: FlexiVent™ protocol

Order	Name	Description	Measured Parameters
1	Baseline Breathing	Ventilation at frequency of 150 breaths per minute	
2	Recruitment Manoeuvre	Deep inflation of the lung to recruit all areas for measuring	
3	Baseline Breathing	Ventilation at frequency of 150 breaths per minute	
4	Lung Mechanics	Three subsequent rounds of below respiratory manoeuvres	
4.1	Baseline Breathing	Ventilation at frequency of 150 breaths per minute	Tidal volume
4.2	Deep Inflation	Inflation of lungs to reach total lung capacity	Inspiratory capacity

4.3	Single-Frequency Forced Oscillation	Perturbations to evaluate the lung as whole compartment	Resistance; Elastance; Compliance
4.4	Broadband Forced Oscillation	Perturbations to separate central airways from alveolar tissues	Newtonian resistance; Tissue damping; Tissue elastance
4.5	Pressure-Volume Loop	Slow, stepwise inflation to total lung capacity and deflation to functional residual capacity	Inspiratory capacity; Quasi-static compliance

2.2.1.5 Blood oxygen saturation

Blood oxygen saturation (%SpO_2) in arterial blood of mice was determined via pulse oximetry using a MouseOx® Plus Pulse Oximeter system and MouseOx® Plus software (Starr Life Sciences, Oakmont, PA, USA).

Mice were anesthetized as previously described and attached to the system by clipping the infrared sensor that communicated with the software to the left thigh of mice. After a calibration period to ensure stable signal recording, %SpO_2 was continuously monitored for a period between 3 – 5 minutes. At regular intervals within this timeframe, five-second-long measurements were initiated at least four times per mouse. From each measurement, the five-second average %SpO_2 value was calculated and recorded by the software. For data visualisation, the %SpO_2 level for each mouse was calculated by averaging all individual %SpO_2 values recorded for that mouse.

2.2.2 Isolation of cells and organs

Prior to isolation of cells or organs, mice were humanely killed by CO_2 asphyxiation or by i.p. injection with an overdose of Pentobarbital.

2.2.2.1 Lung isolation for wet/dry ratio

As an indicator of pulmonary edema, lungs were isolated to determine the ratio of wet weight and dry weight. Right lungs were dissected from the mice, briefly rinsed in PBS to remove residual blood and dried on paper towels to remove excess PBS. Lungs were weighed to determine the wet weight and subsequently dried for 48 hours at 95 ºC on a heat block before determining the dry weight.

2.2.2.2 Bronchoalveolar lavage

To isolate cells specifically from the bronchoalveolar space, mice were tracheotomised by exposing the trachea and inserting a 20 G catheter, fixed with a surgical thread. Bronchoalveolar lavages (BAL) were performed by instilling and retrieving 3 x 1 ml PBS using a 1 ml syringe attached to the catheter. The collected samples were pooled, centrifuged for 5 minutes at 500 g and 4 ºC, washed with ice-cold PBS, and resuspended in 1 ml ice-cold PBS for further processing.

2.2.2.3 Lung digest

Left lung lobes or whole lungs were dissected from the mice and collected in 3.5 ml or 4 ml digestion buffer, respectively. Lungs were manually disrupted using dissection tools and incubated in digestion buffer for 30 minutes at 37 ºC. Samples were regularly mixed by pipetting, resulting in complete digestion. Cell suspensions were filtered through 70 µm cell strainers, centrifuged for 5 minutes at 500 g and 4 ºC, washed with ice-cold PBS, and resuspended in 1 ml ice-cold PBS for further processing.

2.2.3 Flow cytometry

Unless specified otherwise, all washing and centrifugation steps were carried out for 5 minutes at 500 g and 4 ºC. All incubations were carried out in the dark.
Single cell suspensions generated from BAL or enzymatic lung digests were distributed to 96-well U-bottom plates and centrifuged. For lung digestion samples, erythrocyte lysis was performed by resuspending cells in FACSlysing solution or ACK buffer for up to 10 minutes at room temperature. Cells were washed with 200 µl ice-cold PBS and pelleted by centrifugation. Cells were then incubated with Fixable Viability Dye eFluor506 or eFluor780 diluted 1:1000 in 50 µl PBS for 30 minutes at 4 ºC to distinguish viable and dead cells. After washing with ice-cold PBS, surface staining of cells was performed in a 50 µl monoclonal antibody cocktail in FACS buffer for 30 minutes at 4 ºC. After washing with ice-cold FACS buffer, cells were fixed in 200 µl PBS containing 2 % PFA for 30 minutes at room temperature. Cells were washed in ice-cold FACS buffer and resuspended in 200 µl FACS buffer containing a pre-determined amount of fluorochrome-labelled BD CaliBRITE™ Beads for quantification of cell numbers by flow cytometry.
Where indicated, *L. pneumophila* or *L. longbeachae* bacteria were intracellularly stained using a Foxp3/Transcription Factor Staining Kit (eBioscience, San Diego, CA, USA). Following viability staining and staining of surface antigens as described above, cells were incubated in Fixation/Permeabilization Buffer for 30 minutes at 4 ºC. Cells were washed with Permeabilization Buffer and incubated in 50 µl Permeabilization Buffer, containing either FITC-conjugated anti-*L. pneumophila* antibody or rabbit anti-*L. longbeachae* polyclonal serum, for 30 minutes at room temperature. In case of *L. longbeachae*, cells were washed with Permeabilization Buffer and incubated in 50 µl Permeabilization Buffer containing AlexaFluor488-conjugated anti-rabbit antibody for 30 minutes at room temperature. *Legionella*-stained cells were washed once with Permeabilization Buffer, once more with FACS buffer, and resuspended in 200 µl FACS buffer containing CaliBRITE™ Beads for quantification of cell numbers by flow cytometry.

Where indicated, cell proliferation of alveolar epithelial cells was determined by intracellular staining with Ki67 (Gerdes *et al.*, 1983) using a Foxp3/Transcription Factor Staining Buffer Set (eBioscience, San Diego, CA, USA). Following viability staining and staining of surface antigens as described above, cells were incubated in Fixation/Permeabilization Buffer for 30 minutes at 4 ºC. Cells were washed with Permeabilization Buffer and incubated in 50 µl Permeabilization Buffer containing anti-Ki67 antibody for 60 minutes at room temperature. Cells were washed once with Permeabilization Buffer, once more with FACS buffer, and resuspended in 200 µl of FACS buffer.

All samples were acquired on an LSRFortessa™ using FACSDiva v.8.0.1 software (BD Biosciences, Franklin Lakes, NJ, USA) for data acquisition and FlowJo v10.8 software (Tree Star, Ashland, OR, USA) was used for data analysis.

Table 2.9: Antibodies for flow cytometry

Antigen	Clone	Conjugates	Company
CD11b	M1/70	BUV395, BV711	BioLegend, San Diego, CA, USA
CD11c	N418	FITC, PB, PE-CF594	BD Biosciences, Franklin Lakes, NJ, USA, BioLegend, San Diego, CA, USA
CD16/32 (FcγII/III)	93 2.4G2		BioLegend, San Diego, CA, USA WEHI monoclonal facility
CD169	3D6.112	AF647	BioLegend, San Diego, CA, USA
CD19	6D5	BV786, PE	BioLegend, San Diego, CA, USA
CD24	M1/69	BV510	BioLegend, San Diego, CA, USA
CD31	390	BV605	BioLegend, San Diego, CA, USA
CD326	G8.8	BV421	BioLegend, San Diego, CA, USA
CD3e	17A2 145-2C11	BV650 PerCP-Cy5.5	BioLegend, San Diego, CA, USA

CD4	GK1.5	BUV737, eFluor450	BD Biosciences, Franklin Lakes, NJ, USA
	RM4-4	FITC	BioLegend, San Diego, CA, USA
CD45	30-F11	AF700, V500, PE-Cy7, PO	BD Biosciences, Franklin Lakes, NJ, USA, BioLegend, San Diego, CA, USA
CD49f	GoH3	PE-Cy7	BioLegend, San Diego, CA, USA
CD64	X54-5/71	AF647 BV421, BV605	BD Biosciences, Franklin Lakes, NJ, USA, BioLegend, San Diego, CA, USA
CD8a	53-6.7	BV711 BUV805	BD Biosciences, Franklin Lakes, NJ, USA, BioLegend, San Diego, CA, USA
CD8b	YTS156.7.7	PerCP-Cy5.5	BioLegend, San Diego, CA, USA
FcεRIα	MAR-1	PE-Cy7	eBioscience, San Diego, CA, USA
I-A/I-E	M5/114.15.2	AF700, APC eFluor 450	BioLegend, San Diego, CA, USA eBioscience, San Diego, CA, USA
Ki67	16A8	PE	BioLegend, San Diego, CA, USA
Legionella longbeachae	Rabbit polyclonal serum		Kind gift from Prof. Hartland, Hudson Institute of Medical Research
Legionella pneumophila	polyclonal	FITC	ViroStat, Westbrook, ME, USA
Ly6C	AL21	BV605	BioLegend, San Diego, CA, USA
	HK1.4	PE-Cy7	BioLegend, San Diego, CA, USA
Ly6G	1A8	APC, BV711, PB,	BD Biosciences, Franklin Lakes, NJ, USA,

		PerCP-Cy5.5	BioLegend, San Diego, CA, USA
NK1.1	PK136	APC, FITC	BioLegend, San Diego, CA, USA
Rabbit IgG	polyclonal	AF488	Invitrogen, Waltham, MA, USA
Siglec-F	E-50-2440	AF647, PE, BV421	BD Biosciences, Franklin Lakes, NJ, USA
TCRβ	H57-597	AF700	BioLegend, San Diego, CA, USA
TCRγ/δ	GL3	PE-Cy7, PE	BD Biosciences, Franklin Lakes, NJ, USA

2.2.4 Fluorescence-activated cell sorting (FACS)

Whole lungs were enzymatically digested as described in section 2.2.2.3. Single cell suspensions of 2 or 3 mice were pooled in 5 ml polystyrene tubes to ensure sufficient yield of cells. Erythrocyte lysis was performed using 1 ml of ACK buffer, and surface antigen staining was carried out by resuspending cells in 300 µl of antibody cocktail diluted in FACS buffer as described in section 2.2.3. Cells were washed twice in 1 ml FACS buffer and resuspended in 500 µl PBS. Shortly before sorting, 7-AAD was added to samples to a final concentration of 0.5 µg/ml to distinguish viable and dead cells. Samples were filtered through 35 µm nylon mesh cell strainer caps into 5 ml polystyrene tubes prior to acquisition and sorted using a MoFlo Astrios EQ Cell Sorter at the Flow Cytometry Core Facility of the Peter-Doherty-Institute, Melbourne.

AM were sorted as 7-AAD$^-$ CD11c$^+$ Siglec-F$^+$ cells, neutrophils were sorted as 7-AAD$^-$ Siglec-F$^-$ Ly6G$^+$ CD64$^-$ cells, and MC were sorted as 7-AAD$^-$ Siglec-F$^-$ Ly6G$^-$ CD64$^+$ cells. Gating strategies are shown in the relevant results section. Specific cell purities were after sorting were assessed using the same gating strategy. Sorted cell fractions were recovered in 5 ml polypropylene tubes containing 50 µl FCS and kept on ice until further use.

2.2.5 Imaging flow cytometry

Single cell suspensions from digested lungs were generated as described in section 2.2.2.3. Red blood cell lysis was performed by resuspension in water for 10 seconds, immediately followed by addition of 10X PBS buffer to restore isotonicity. Cells were washed in PBS and incubated with FITC-conjugated Annexin V and Fixable Viability Dye eFluor506 diluted in 1X Annexin V Binding Buffer (AVBB) for 15 minutes at room temperature. Cells were then surface stained with lineage-specific antibodies diluted in AVBB for 30 minutes at 4 ºC. Fixation of cells was performed in a 1:1 mixture of 4 % PFA in PBS:AVBB for 30 minutes at room temperature. To reduce autofluorescence, cells were treated with 1X Fixation/Permeabilization buffer (BD Cytofix/Cytoperm™ Fixation/ Permeabilization Kit, BD Biosciences, Franklin Lakes, NJ, USA) for 30 minutes at room temperature and subsequently washed and resuspended in AVBB for acquisition. Data was acquired using an Amnis ImageStream®^{X} MkII (Luminex, Seattle, WA, USA) at low speed and 40X magnification for imaging, and analysed using IDEAS Image Analysis v.6.2 software (Luminex, Seattle, WA, USA).

2.2.6 Quantitation of *Legionella* CFU

Legionella CFU were quantified from homogenized lungs or FACS-purified cells. Right lungs or whole lungs were dissected from mice and collected in ice-cold PBS. Lungs were homogenized using either a T10 Basic Ultra Turrax Homogenizer (IKA) or a TissueLyser LT (Qiagen) with spheric stainless steel beads at 50 oscillations/s. 1 ml of lung homogenate was incubated with 0.1 % saponin (w/v) for 30 minutes at 37 ºC, and lysed lung homogenates were serially diluted in sterile PBS in 1:10 steps.

Individual cell populations were FACS-sorted as described in section 2.2.4. Recovered cells were diluted 1:2 in Trypan Blue and counted using a Neubauer cell counting chamber. From each cell fraction, $2x10^4$ viable cells were incubated in 200 µl sterile PBS containing 0.1 % saponin (w/v) for 30 minutes at 37 ºC. Lysed cell fractions were serially diluted in sterile PBS in 1:10 steps.

From a range of relevant dilutions, 25 µl of homogenate were plated in quadruplicates, or 50 µl of homogenate were plated in duplicates on selective BCYE agar plates using the spot plating method. *Legionella* were grown for 72 hours at 37 ºC after which colonies were counted manually. CFU/lung was calculated based on the average number of counted colonies, multiplied by the specific factors from sample dilution.

2.2.7 Cytokine profiling

Cytokine levels were determined from lung homogenates prepared as described in section 2.2.6. Prior to saponin lysis, an aliquot of lung homogenate was collected and stored at -20 ºC or -80 ºC until further use. Cytokine levels in lungs were measured using either custom Cytometric Bead Array Mouse Flex Kits (BD Biosciences, Franklin Lakes, NJ USA), custom ProcartaPlex™ Mouse Mix & Match Panel Kits (ThermoFisher Scientific, Waltham, MA, USA), or a ProteomeProfiler™ Mouse XL Cytokine Array Kit (R&D Systems, Minneapolis, MN, USA). For each method, samples were processed as per manufacturer's instructions.

In case of cytometric bead arrays, prepared samples were resuspended in a total volume of 100 µl FACS buffer and acquired on an LSRFortessa™ using FACSDiva v8.0.1 software. Data was analysed using FlowJo v10.6 and GraphPad Prism v9.1.2 software. For each cytokine in the assay, a standard curve was calculated based on known standard concentrations and the corresponding MFI recorded by flow cytometry using a nonlinear, sigmoidal regression model. For each cytokine, concentrations in individual samples were back calculated from the recorded MFI based on the fitted standard curves.

In case of ProcartaPlex™ assays, prepared samples were resuspended in 120 µl Reading Buffer and acquired using a FlexMap3D system (Luminex). The acquired data was exported and analysed based on the same principles described above, using the online tool provided by the manufacturer.

The ProteomeProfiler™ assay was used to screen a larger panel of cytokines, chemokines and growth factors. For this, 25 µl lung homogenate from five mice

per experimental group were pooled, choosing those mice closest to the group average. Following manufacturer's instructions, the pooled samples were incubated on nitrocellulose membranes overnight at 4 ºC while shaking on a gyratory rocker, binding to specific capture antibodies spotted in duplicates on the membrane. After several washing steps, relative quantification of each analyte was performed using the chemiluminescence signal detected with a ChemiDoc XRS+ system (BioRad, Hercules, CA, USA). Data was analysed using Image Lab v6.0.1 software (BioRad, Hercules, CA, USA). The average pixel density of the duplicate spots for each analyte of the array was determined and background signal was subtracted. Relative changes in the analyte levels were calculated by comparing the average pixel intensity values from the array for neutrophil-depleted samples with those from the array of undepleted samples.

2.2.8 Light-sheet microscopy

2.2.8.1 Preparation of lungs

The protocol for preparation and staining of lungs for light-sheet microscopy was modified and optimized from previously published studies (Masselink *et al.*, 2019; Salwig *et al.*, 2021).

Lungs of mice were perfused with 10 ml of PBS and 10 ml of 4% PFA diluted in PBS through the right heart chamber. An incision was made into the upper part of the trachea, and a 20 G catheter was inserted and fixed with a surgical thread. Lungs were filled with 1 ml of 4 % PFA, removed entirely and kept in 4 % PFA for further fixation at 4 ºC overnight. Lungs were briefly washed in PBS and permeabilized in Perm/Block solution containing 2 % TritonX-100, 10 % DMSO, 5 % BSA, and 0.05 % NaN_3 diluted in PBS for 2 days (Masselink *et al.*, 2019).

Lungs were separated into individual lobes and incubated in Perm/Block solution containing 4 µg/ml APC-conjugated rat anti-CD169 antibody for 5 days at room temperature while shaking on a gyratory rocker. After 2 days of washing in Perm/Block solution, lung lobes were incubated in Perm/Block solution containing

4 µg/ml of a goat-anti-rat-AlexaFluor790 antibody for 5 days at room temperature while shaking on a gyratory rocker.
After washing with Perm/Block for 2 days, lung lobes were stepwise dehydrated in 30 %, 50 %, 70 %, 99 % 1-propanol diluted in PBS, and in anhydrous 1-propanol (99.7 %) at 4°C. Each dehydration step took 4 hours, except for 50 % 1-propanol in PBS, which was carried out overnight. Optical clearing was achieved by overnight incubation in ethyl cinnamate at room temperature.

Table 2.10: Antibodies for light-sheet microscopy

Antigen	Clone	Conjugate	Company
CD169	3D6.112	AF647	BioLegend, San Diego, CA, USA
Rat IgG	polyclonal	AF790	Jackson ImmunoResearch, Westgrove, PA, USA

2.2.8.2 Recording of lung lobes

Optically cleared lung lobes were imaged in ethyl cinnamate using an UltraMicroscopeII and Biotec Inspector software (LaVision Biotec, Bielefeld, Germany) at the Biological Optical Microscopy Platform (BOMP) of the University of Melbourne. The microscope was equipped with an Olympus MVX-10 Zoom body, a bi-directional triple light sheet module, a LaVision LVMI-Fluor dipping objective, and an Andor Neo sCMOS camera. Sample were excited with LASOS Diode Lasers at 488 nm, 639 nm, and 785 nm, and fluorescence was spectrally filtered using classical emission filters at 525/50 nm (autofluorescence), 680/30 nm (AF647) and 845/55 nm (AlexaFluor790). Multicolour stacks of samples were acquired in increments of 8 µm or 10 µm by sequentially recording each colour channel. Images were saved as .tiff files and analysed as described below.

2.2.8.3 Software-based AM quantitation

Imaris Software v8.4.1 (Bitplane, Zurich, Switzerland) was used to analyse the images recorded by light-sheet microscopy. Individual .tiff files were

reconstructed into 3D images of lung lobes and AM were quantitated from the AlexaFluor790 channel using the software's "Spot" tool. All acquired lung lobes were treated in an identical and blinded manner to prevent bias during analysis. AM spots were defined within three 3D regions of interest using the regional contrast of the fluorescent signal in the AlexaFluor790 channel (CD169 staining) and applying an estimated XY diameter of 15 µm. AM diameters of 15 µm have been reported in the literature (Haley *et al.*, 1991) and were confirmed in our group during imaging flow cytometry experiments. Selected regions of interest were distributed across the lobes to include areas both in the centre and on the edge of the lobes. Based on events identified in the regions of interest, the software detected AM throughout the entire lobe. AM spots were further filtered for their size, excluding events with a diameter larger than 30 µm. Absolute AM numbers from each lung lobe were then exported and displayed for each mouse.

2.2.9 qPCR

2.2.9.1 RNA isolation and cDNA synthesis

RNA was extracted from $1x10^6$ neutrophils that were FACS-sorted on day 3 after infection with *L. pneumophila* using a RNeasy© Mini Kit (Qiagen, Hilden, Germany) and spin technology according to the manufacturer's instructions. RNA was eluted from the columns in 30 µl RNase-free water and the concentration of RNA was determined using a NanoDrop™ spectrophotometer.
cDNA was generated from 150 ng isolated RNA using a Reverse Transcription System (Promega, Madison, WI, USA) according to manufacturer's instructions. The reaction mix contained 4 µl GoScript™ Reaction Buffer, 2 µl GoScript™ Reverse Transcriptase Enzyme Mix, 0.5 µl Oligo(dT) Primer (0.25 µg), the required volume for 150 ng of isolated RNA per sample and was filled to a total volume of 20 µl with nuclease-free water. Reverse transcription was performed on a Mastercycler Nexus thermocycler (Eppendorf) for 60 minutes at 42 ºC, and enzyme was inactivated at 95 ºC for 5 minutes. Samples were kept on ice and were directly processed for qPCR.

2.2.9.2 qPCR and data analysis

The subsequent qPCR reaction contained 5 µl 2x GoTaq® qPCR Master Mix (Promega, Madison, WI, USA), 0.8 µl of cDNA generated as described above, 0.8 µl of specific forward and reverse primers (0.2 µM), and was filled to a total volume of 10 µl with nuclease-free water. Negative controls contained nuclease-free water instead of cDNA. Primers were designed to amplify the genes *Spi1*, *Tlr2*, *CybA*, and the reference gene *Rpl32*, with their sequences indicated in below table 2.11 (Integrated DNA Technologies, Coralville, Iowa, USA).

The qPCR reaction was run using a QuantStudio 6 Real-Time PCR system (ThermoFisher Scientific, Waltham, MA, USA). After hot-start activation of polymerase enzyme at 95 ºC for 2 minutes, 40 amplification cycles were run including a denaturation step at 95 ºC for 15 seconds and an annealing/extension step at 60 ºC for 60 seconds. Fluorescence of the DNA-binding dye was measured after the extension step at the end of each cycle. After amplification, a gradual melting curve with temperature increments from 60 ºC – 95 ºC was performed as quality control for the reaction.

For each sample, Ct values for each gene of interest and the reference gene *Rpl32* were determined by the software based on the fluorescence signal. The relative expression of the genes of interest was then calculated using the delta-delta Ct method.

Table 2.11: qPCR Primers

Primer (Gene) name	Sequence
Cyba_forward	ACTTCCTGTTGTCGGTGCC
Cyba_reverse	CCTCACTCGGCTTCTTTCGG
Rpl32_forward	GAGGTGCTGCTGATGTGC
Rpl32_reverse	GGCGTTGGGATTGGTGACT
Spi1_forward	CTCGATACTCCCATGGTGCC

Spi1_reverse	CTCCCCGTGCAGAAGACC
Tlr2_forward	ACCGAAACCTCAGACAAAGC
Tlr2_reverse	TTCATGGCTGCTGTGAGTCC

2.2.10 Neutrophil elastase activity

The activity of neutrophil elastase in neutrophils was assessed using the specific chemical probe PK105b as previously described (Anderson *et al.*, 2019). PK105b was a kind gift from Laura Edgington-Mitchell, University of Melbourne.
Briefly, $1x10^6$ neutrophils from air- and smoke-exposed, *L. pneumophila*-infected mice purified by FACS as described in section 2.2.5 were lysed on ice in PBS containing 0.1 % Triton X-100. Lysates were cleared by centrifugation at 21,000 g at 4 ºC for 10 minutes and total protein was labelled with 1 µM PK105b at 37 ºC for 30 minutes. Proteins were then solubilized, boiled and run on a 15 % SDS-PAGE under reducing conditions, and the amount of probe-labelling was detected by scanning the gel for Cy5 fluorescence using a Typhoon 5 laser scanner (GE Healthcare). Gel images were analysed by determining the intensity of the Neutrophil Elastase-specific band for each sample using densitometry.

2.2.11 Data processing and statistics

Raw data was analysed using Microsoft Office 365, v16 (Microsoft, Remond, WA, USA), FlowJo v10.8, or Imaris v8.4.1 software. Statistical significance was determined using GraphPad Prism v9.1 software (GraphPad Software, La Jolla, CA, USA). Mann-Whitney test was used for the statistical analysis of differences between two groups, and repeated-measurements one-way ANOVA with Dunnett post-test was used for the statistical analysis of differences between more than two groups. Stars indicate statistical significance (* $p \leq 0.05$; ** $p \leq 0.01$; *** $p \leq 0.001$).

3 Cigarette smoke exposure depletes alveolar macrophages *in vivo* with the contribution of NLRP3-dependent pyroptosis

3.1 Introduction

AM are lung tissue-resident cells located in the alveolar space where they are critical for maintaining tissue homeostasis, initiating and resolving pulmonary immune responses, and repairing damaged tissue (Hussell and Bell, 2014; Garbi and Lambrecht, 2017). Cigarette smoke is one of the main environmental risk factors associated with disease worldwide (Murray *et al.*, 2020) and most of its components have been classified as toxic, carcinogenic, or otherwise harmful substances (Talhout *et al.*, 2011). As AM are located in the airways alongside bronchial and pulmonary epithelial cells, they are directly exposed to inhaled cigarette smoke which can have profound effects on the function and viability of these cells. In particular, high levels of cigarette smoke-derived ROS, which are often further amplified by ROS from lung-infiltrating immune cells, were shown to induce significant oxidative stress in cells. This in turn can change cellular metabolism, cause DNA damage, and ultimately induce a variety of cell death pathways in smoke-exposed cells (Nakayama *et al.*, 1985; Kirkham and Barnes, 2013; Zuo *et al.*, 2014; Sauler *et al.*, 2019). Accordingly, *in vitro* studies provide evidence that cigarette smoke-induced cellular damage initiates AM death pathways (Aoshiba *et al.*, 2001; Park *et al.*, 2018; Wang *et al.*, 2020).

In contrast, others consistently reported higher yields of AM in BAL from human smokers and animal models of cigarette smoke exposure (Harris *et al.*, 1975; Jimenez Ruiz *et al.*, 1998; D'hulst, 2005; Morris *et al.*, 2008; Karimi *et al.*, 2012; Strzelak *et al.*, 2018). This observation has been attributed to the pro-inflammatory properties of cigarette smoke, causing the release of DAMP or chemokines that attract immune cells, including macrophages, to the lung (Barnes, 2016). While differences in duration and intensity of smoking in humans and animal models may introduce some variance between studies (Morris *et al.*,

2008; Karimi *et al.*, 2012), such directly contradicting results between *in vitro* and *in vivo* studies are unexpected.

Since AM are the pulmonary immune system's front line to eliminate invading pathogens, their cellular function and abundance can have significant impact on the development of disease and the outcome of pulmonary infection. We therefore investigated if acute cigarette smoke exposure indeed causes an accumulation of AM in the lung, or if cigarette smoke induces AM death *in vivo*.

3.2 Results

3.2.1 Acute cigarette smoke depletes alveolar macrophages *in vivo*

We assessed the impact of cigarette smoke on the abundance of AM in the lung by using an established mouse model of acute, daily cigarette smoke exposure (Bozinovski *et al.*, 2015) (Figure 3.1A). Daily exposure to cigarette smoke caused slight weight loss in mice (Figure 3.1B) which may be attributed to the well-documented, appetite-suppressing effects of certain components in cigarette smoke (Audrain-McGovern and Benowitz, 2011). After 10 days of smoke exposure, AM were quantified in BAL and enzymatically digested lungs by flow cytometry (Figure 3.1C-E). AM were identified using common lineage markers CD11c and Siglec-F, and gated as single live $CD45^+CD11c^+Siglec\text{-}F^+$ cells (Misharin *et al.*, 2013).

Surprisingly, when we quantified AM in digested whole lungs, we detected substantially decreased numbers of AM in smoke-treated mice (Figure 3.1F), as well as a lower percentage of AM in total $CD45^+$ leukocytes (Figure 3.1G). This finding directly contradicted previous reports from the literature that investigated AM in the bronchoalveolar compartment of smoke-exposed mice (D'hulst, 2005; Vlahos *et al.*, 2006).

We specifically quantified AM in the BAL of air- and smoke-exposed mice as well. We observed an almost 5-fold increase in the number of AM in the BAL of smoke-exposed mice when compared to control mice (Figure 3.1H), consistent with previous studies in literature. As expected, the $CD45^+$ leukocytes retrieved by BAL were almost exclusively AM in control mice. This percentage of AM in total immune cells was reduced in smoke-exposed mice due to airway infiltration of additional immune cells such as neutrophils or dendritic cells (Figure 3.1I). Notably, we yield much higher overall amounts of AM from lung digests, suggesting that this method represents the actual number of AM in the entire lung more accurately than BAL (Figure 3.1F/H).

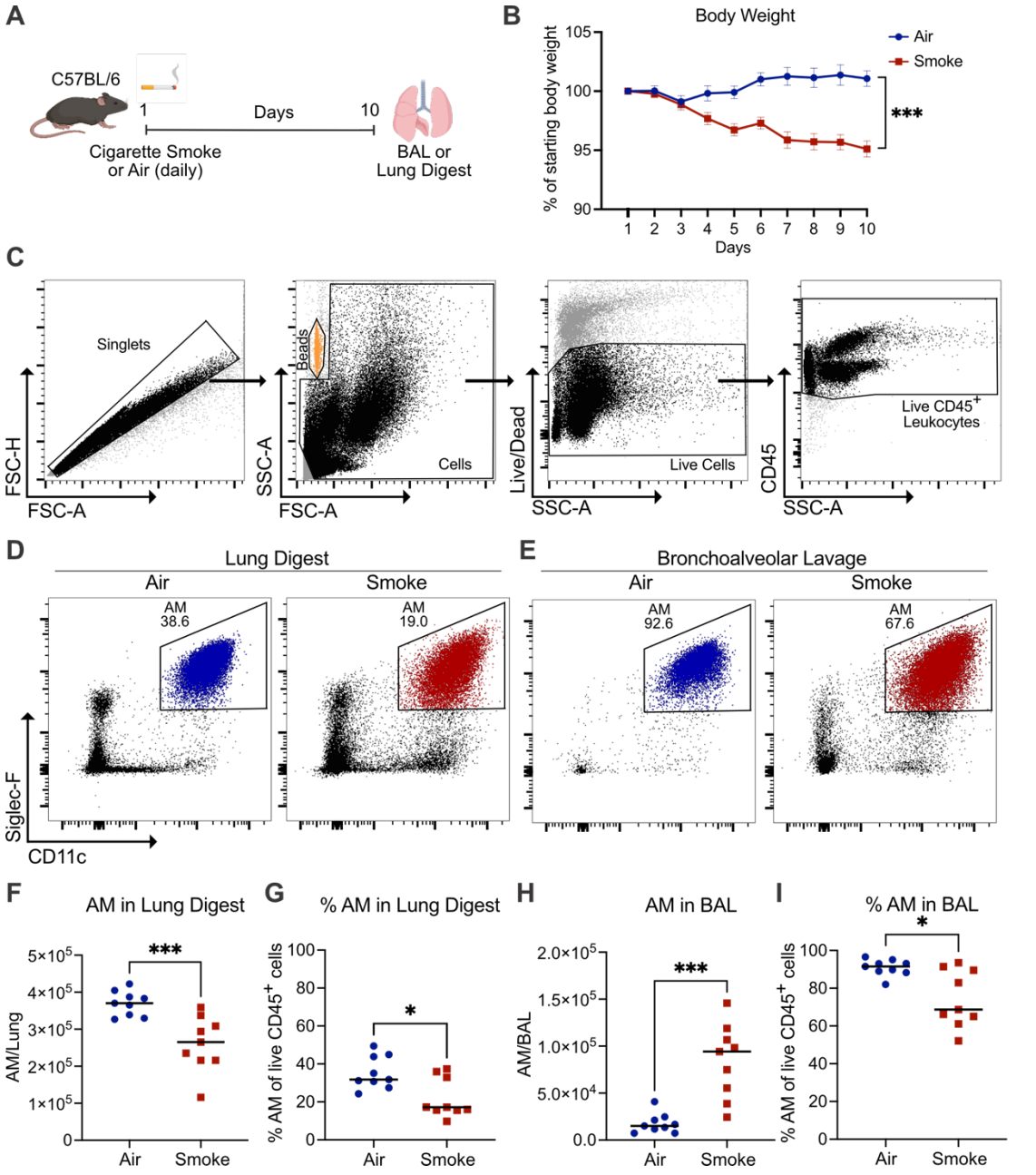

Figure 3.1: Reduced number of AM in whole lung digests of cigarette smoke-exposed mice.

(A) Scheme of cigarette smoke exposure. Mice were exposed to cigarette smoke or room air daily for 10 days. **(B)** Relative body weight of air- and smoke-exposed mice. Statistical significance compares the area under the curve. **(C)** Representative flow cytometry gating strategy to identify single live CD45$^+$ leukocytes, **(D)** AM in enzymatic lung digests, and **(E)** AM in BAL. **(F/H)** AM were quantified from lung digests and BAL from air- and smoke-exposed mice. **(G/I)** Percentage of AM of total CD45$^+$ leukocytes from lung digests and BAL from air- and smoke-exposed mice. (B) Curves are shown as mean ± SEM. (F-I) Graphs show medians, with each dot representing an individual mouse. Data is pooled from two independent experiments (n ≥ 8 mice per group). *p<0.05, ***p<0.001, Mann-Whitney-U test.

We next used quantitative light-sheet microscopy (LiSM) as an independent method to enumerate AM in lungs of air- and smoke-exposed mice since it does not suffer from the potential artifacts associated with cell extraction procedures (Steinert *et al.*, 2015; Amich *et al.*, 2020). We first assessed the utility of CD169 as a single, definitive marker for AM in the smoking model. CD169 is a transmembrane protein involved in cell-cell interactions and has previously been reported to distinguish AM from other pulmonary macrophage populations (Bharat *et al.*, 2016). Using flow cytometry, we confirmed that CD169 was not expressed by pulmonary $CD45^+$ leukocytes other than AM, and AM-specific expression of CD169 was maintained in smoke-treated mice (Figure 3.2A-C). We next isolated entire lungs from air- and smoke-exposed mice and stained individual lung lobes with an CD169-specific antibody before imaging the optically cleared lobes by LiSM (Figure 3.2D). $CD169^+$ AM (green) could be readily identified above background autofluorescence used to visualize lung structure (red) in 3D-reconstructed lung lobes (Figure 3.2E).

To quantitate $CD169^+$ AM in whole lung lobes, z-stacks were recorded at a magnification able to visualize the entire lobe (Figure 3.3). Z-stacks were then reconstructed into 3D models (Figure 3.4A/B) and $CD169^+$ AM were identified by automated digital analysis of images. Signal intensity was measured based on local contrast in individual segments across the lung lobe to account for variation of staining efficiency in different depths and areas of the tissue. Additionally, AM were identified based on an estimated diameter of 15 µm (Haley *et al.*, 1991), and a size filter was applied to exclude AM spots smaller than 8 µm and larger than 30 µm, removing potential staining artifacts. Quantitation revealed that AM numbers in lungs were significantly reduced when mice were exposed to cigarette smoke (Figure 3.4C). The relative extent of this reduction closely reflected our findings from enzymatically digested, whole lungs (Figure 3.4D). Taking into account the estimated distribution of volume and alveoli within the mouse lung (Knust *et al.*, 2009; Hoang *et al.*, 2018), our results suggest that approximately 8 – $9x10^5$ AM could be detected in an entire lung from an air-exposed mouse using LiSM-based quantitation, more than twice the average number of AM found in lung digests from air-exposed controls.

In summary, these results provide convincing evidence that acute cigarette smoke exposure causes a depletion of AM and not an accumulation as others have previously observed by exclusively analysing BAL.

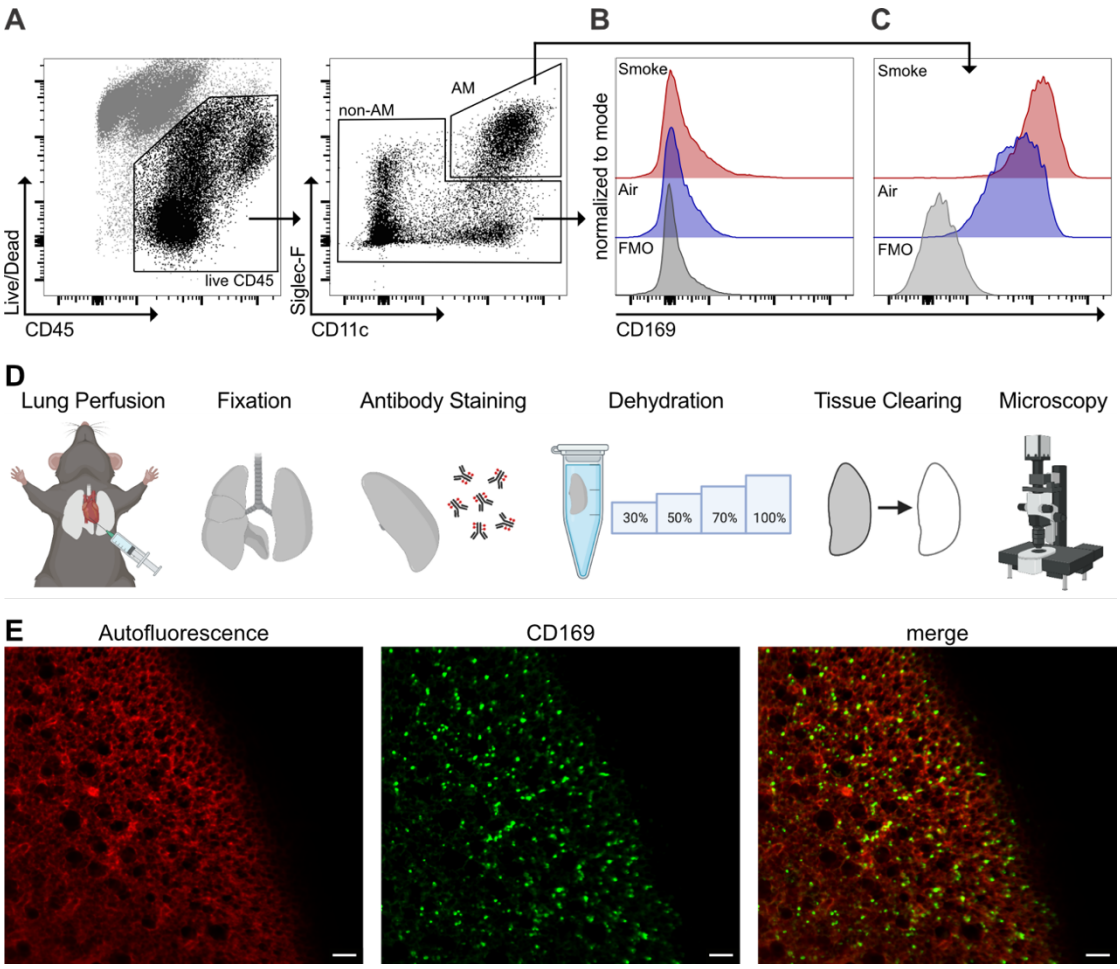

Figure 3.2: CD169 is an AM-specific marker suitable for detection of AM using light-sheet microscopy.
Mice were exposed to cigarette smoke or room air daily for 10 days. **(A)** Single cell suspensions were generated by enzymatic lung digest. Representative flow cytometry gating strategy for AM and non-AM. **(B/C)** CD169 expression in non-AM and AM of air- and smoke-exposed mice, compared to unstained fluorescence-minus-one control (FMO). **(D)** Scheme of workflow to prepare lung tissue samples for light-sheet microscopy. **(E)** Representative z-stack of a partial right superior lung lobe, stained for CD169, and recorded by light-sheet microscopy. Green dots represent individual AM and autofluorescence is shown in red. Scale bar, 100 µm.

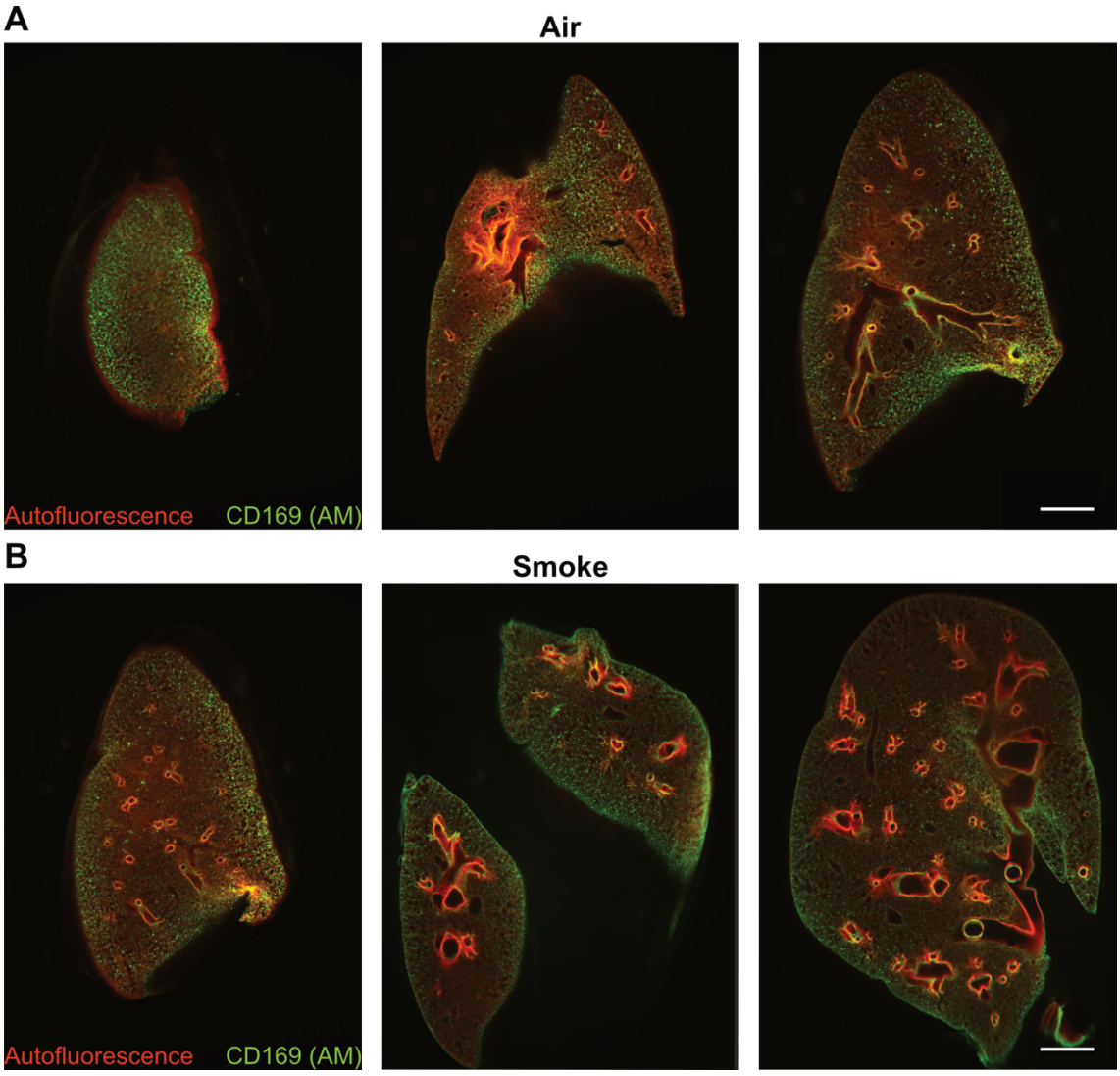

Figure 3.3: Representative sections from CD169-stained lungs acquired by light-sheet microscopy.
Mice were exposed to cigarette smoke or room air daily for 10 days and lungs were prepared for imaging by light-sheet microscopy. **(A/B)** Representative, individual sections taken across a lung lobe from an air- or smoke-exposed mouse, stained for CD169 and recorded by light-sheet microscopy. Green dots represent individual AM and autofluorescence is shown in red. Scale bar, 1000 µm.

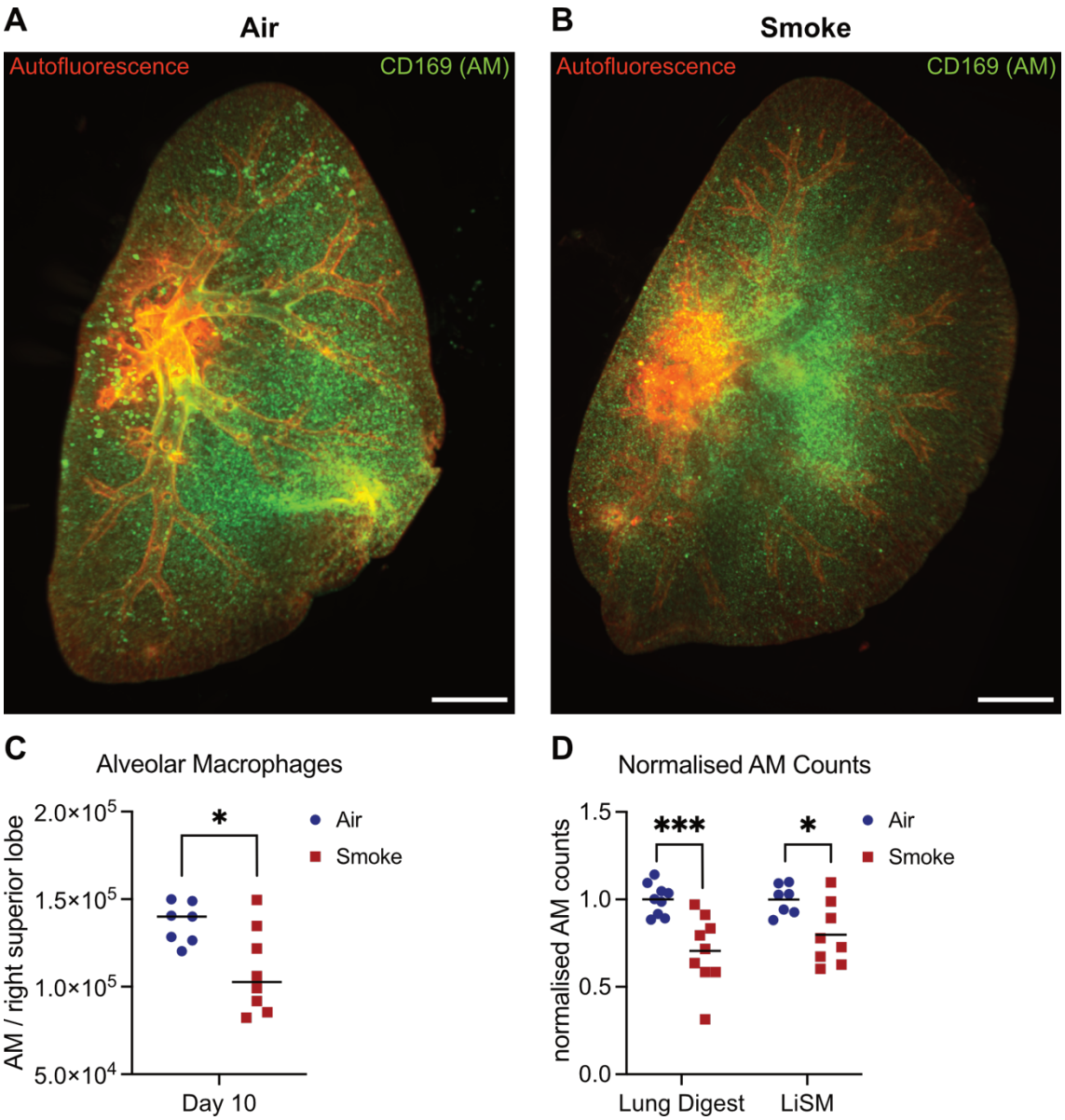

Figure 3.4: Light-sheet microscopy-based quantitation confirms cigarette smoke-induced depletion of AM *in vivo*.
Mice were exposed to cigarette smoke or room air daily for 10 days and lungs were prepared for imaging by light-sheet microscopy. **(A/B)** Representative, software-based 3-D reconstruction of entire right superior lung lobes. Green dots represent individual AM and autofluorescence is shown in red. Scale bar, 1000 µm. **(C)** Software-based enumeration of AM from 3D-reconstructed right superior lung lobes from air- and smoke-exposed mice. **(D)** Comparison of methods used to quantitate AM. Results were normalised to the air-exposed control group for each method. (C/D) Data is pooled from two independent experiments (n ≥ 7 mice per group). Graphs show median (C) and average (D), respectively, with each dot representing an individual mouse. *p<0.05, ***p<0.001, Mann-Whitney-U test.

3.2.2 Alveolar macrophage morphology suggests an inflammatory type of cigarette smoke-induced death

We next investigated which cell death pathways could be involved in AM depletion following acute cigarette smoke exposure. To assess induction of AM death *in vivo*, we used imaging flow cytometry (George *et al.*, 2004) and stained lung single cell suspensions from air- or smoke-exposed mice with fluorescently labelled annexin V (AnnV) and a live/dead dye (LD) that binds to proteins (Figure 3.5A/B). Annexin V was restricted to cell membranes in $AnnV^{+}LD^{-}$ AM (Figure 3.5B, middle panel), whereas it was distributed throughout the entire cell in most $AnnV^{+}LD^{+}$ double-positive AM, together with the intracellular LD dye (Figure 3.5B, lower panel).

We also quantified the size of each AM subset based on the cell area from the recorded brightfield images (Figure 3.5C/D). The size of $AnnV^{+}LD^{-}$ AM was increased in smoke-exposed mice compared to viable $AnnV^{-}LD^{-}$ AM in these mice, and $AnnV^{+}LD^{+}$ AM were significantly larger than both of these AM subsets in smoke-exposed mice (Figure 3.5D). Additionally, $AnnV^{+}LD^{-}$ and $AnnV^{+}LD^{+}$ AM in smoke-treated mice were found to be significantly enlarged compared to their specific counterparts from air-exposed controls (Figure 3.5D). This size increase suggested the involvement of an inflammatory type of cell death in smoke-treated AM (Galluzzi *et al.*, 2018).

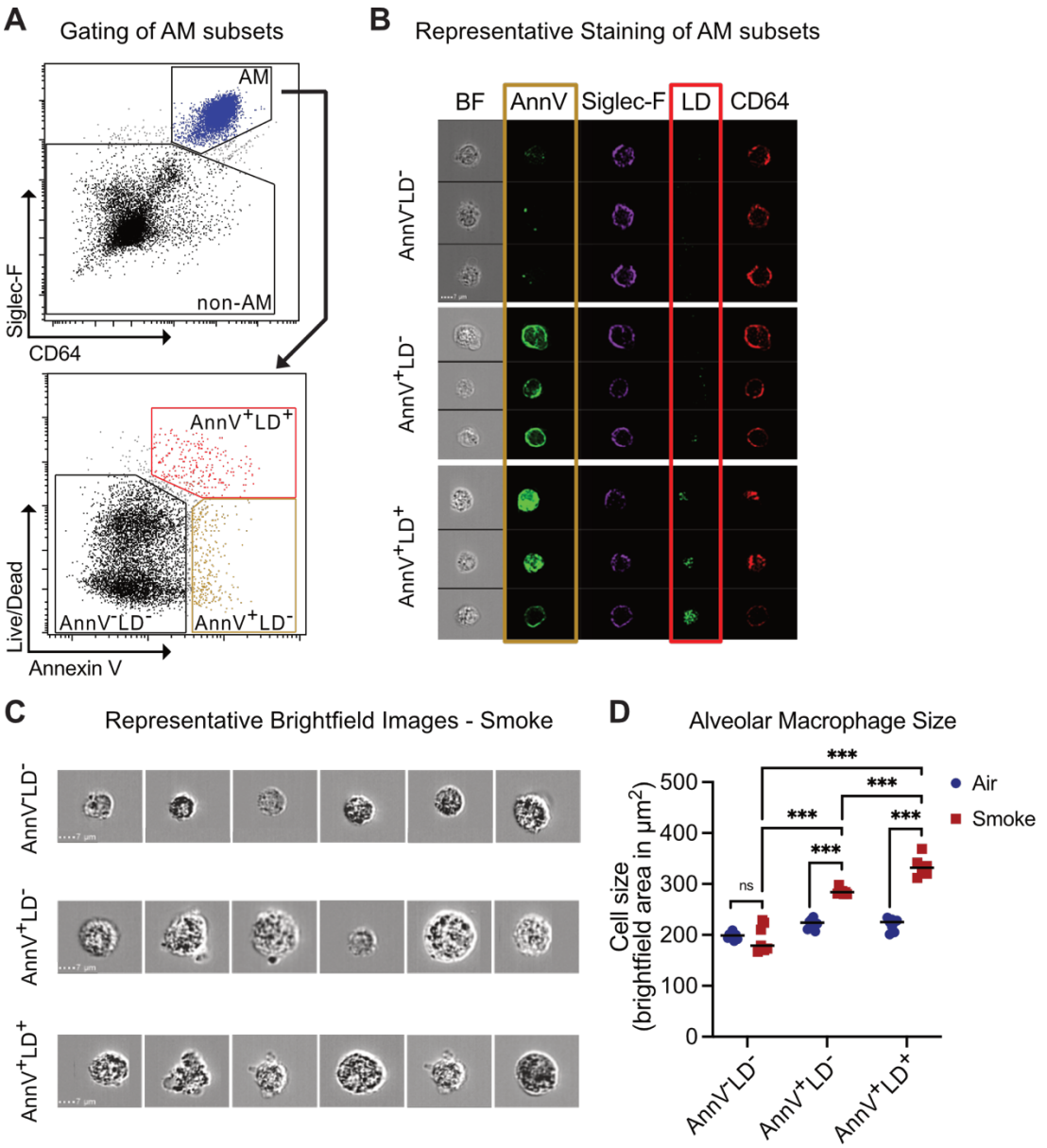

Figure 3.5: Cell morphology suggests an inflammatory type of cigarette smoke-induced AM death.
Mice were exposed to cigarette smoke or room air daily for 10 days. Lung single cell suspensions were generated for imaging flow cytometry analysis. **(A)** Gating strategy to classify viable and dead AM by imaging flow cytometry based on staining with annexin V (AnnV) and intracellular live/dead (LD) dye. **(B)** Representative events for each AM subset, recorded by imaging flow cytometry, including brightfield (BF) and fluorescent channels. **(C)** Representative brightfield images for each AM subset from smoke-exposed mice. **(D)** Average cell size (area) of each AM subset from air- and smoke-exposed wild-type mice, quantified based on recorded brightfield images. Data is pooled from two independent experiments (n ≥ 6 mice per group). Graph shows median, with each dot representing an individual mouse. ***p<0.001, Mann-Whitney-U test.

3.2.3 NLRP3-dependent pyroptosis contributes to cigarette smoke-induced alveolar macrophage death *in vivo*

Previous *in vitro* studies have linked the inflammatory cell death pathways pyroptosis and necroptosis to cigarette smoke-induced cell death (Wang *et al.*, 2020; Zhang *et al.*, 2021; Ma *et al.*, 2021). We therefore repeated flow cytometry-based quantitation of AM in lungs of air- and smoke-exposed mice, using necroptosis-deficient $MLKL^{-/-}$ mice, pyroptosis-deficient $ASC^{-/-}$ mice, and NLRP3-dependent pyroptosis-deficient $NLRP3^{-/-}$ mice. Moreover, we used the viability staining approach and imaging flow cytometry analysis to assess if the proportions of $AnnV^{+}LD^{-}$ and $AnnV^{+}LD^{+}$ AM in these knockout mice were changed in comparison to wild-type mice after cigarette smoke exposure.

Once again, we observed a substantial and significant reduction of the number of AM in lungs of smoke-exposed, wild-type mice (Figure 3.6A/D), and the percentage of dead $AnnV^{+}LD^{+}$ AM was on average twice as high in smoke-exposed mice (Figure 3.6C/F), providing further evidence of smoke-induced death of AM *in vivo*.

In smoke-exposed $MLKL^{-/-}$ mice, the percentages of $AnnV^{+}LD^{-}$ AM and $AnnV^{+}LD^{+}$ AM were significantly increased, as was the percentage of $AnnV^{+}LD^{-}$ AM (Figure 3.6B/C). Although not statistically significant, a trend towards reduced AM numbers in smoke-exposed $MLKL^{-/-}$ mice was present (Figure 3.6A). These results suggested that necroptosis does not contribute greatly to the increased rate of AM cell death induced by cigarette smoke exposure.

In contrast, AM death was clearly decreased in smoke-treated, pyroptosis-deficient mice. Unlike wild-type mice, we did not observe a depletion of AM after smoke exposure in $ASC^{-/-}$ and $NLRP3^{-/-}$ mice (Figure 3.6D). A small increase in $AnnV^{+}LD^{-}$ AM was detected in $ASC^{-/-}$ mice, but not in $NLRP3^{-/-}$ mice (Figure 3.6E). Additionally, the percentages of $AnnV^{+}LD^{+}$ AM in both $ASC^{-/-}$ and $NLRP3^{-/-}$ mice were similar between air- and smoke-treated mice (Figure 3.6F).

In summary, these findings indicate that NLRP3-dependent pyroptosis is a pathway involved in driving cigarette smoke-induced AM death *in vivo*.

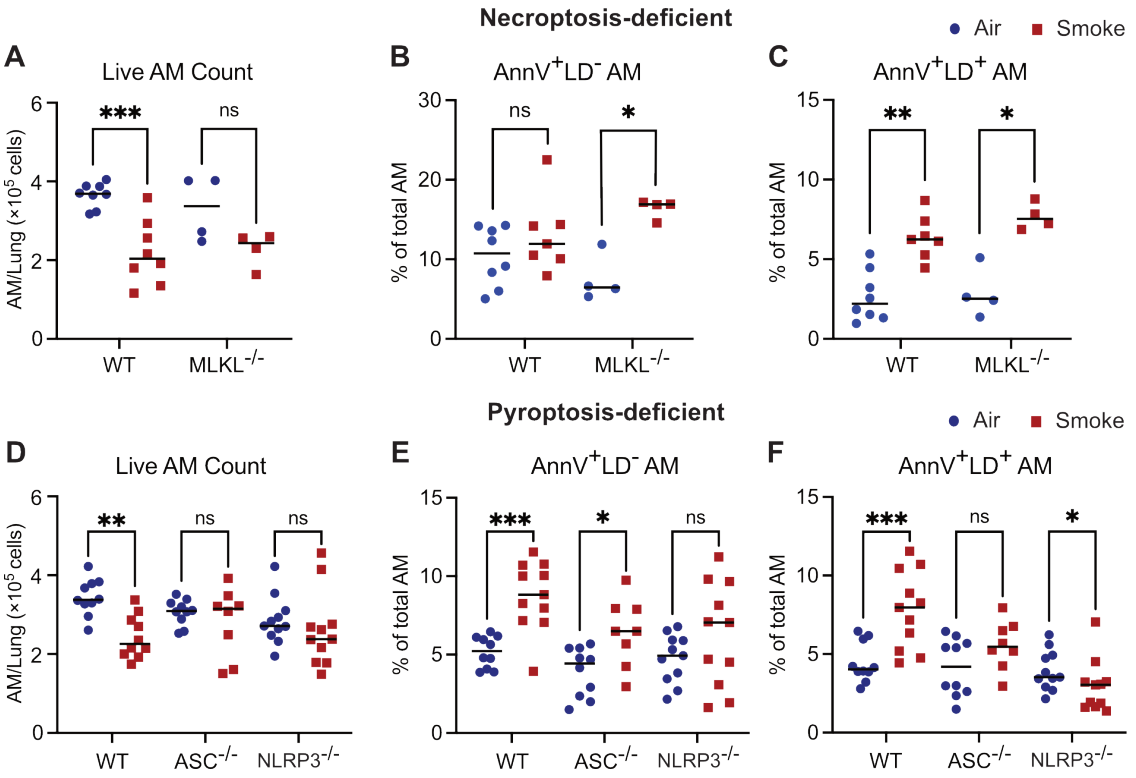

Figure 3.6: Pyroptosis contributes to cigarette smoke-induced AM depletion *in vivo*.

Mice were exposed to cigarette smoke or room air daily for 10 days. Lung single cell suspensions were generated for flow cytometry or imaging flow cytometry analysis. **(A/D)** AM counts in lungs from air- and smoke-exposed, wild-type and indicated knock-out mice were quantified by flow cytometry. **(B/E)** Percentages of AnnV$^+$LD$^-$ AM and **(C/F)** percentages of AnnV$^+$LD$^+$ AM from air- and smoke-exposed, wild-type and indicated knock-out mice were determined by imaging flow cytometry. (A-C) Data is from one experiment (n ≥ 4 mice per group). (D-F) Data is pooled from two independent experiments (n ≥ 9 mice per group). Graphs show median, with each dot representing an individual mouse. *p<0.05, **p<0.01, ***p<0.001, Mann-Whitney-U test.

3.3 Discussion

The work in this chapter demonstrates that acute cigarette smoke induces death of AM *in vivo*, and suggests that smoke-induced AM death is, at least in part, driven by NLRP3-dependent pyroptosis.

These findings are in contrast to the generally accepted view that cigarette smoke causes an accumulation of AM in the airways of mice and humans. Previous studies, which to our knowledge all analysed cells in BAL, consistently suggest that smoke exposure results in an expansion of AM (Harris *et al.*, 1975; D'hulst, 2005; Vlahos *et al.*, 2006; Morris *et al.*, 2008; Karimi *et al.*, 2012). While we were able to replicate this in our model, retrieving approximately 5-fold higher AM numbers from BAL after smoke exposure, we found that this increase was not representative of the actual number of AM in the whole lung. Assessment of immune cells in whole lung digests by flow cytometry and *in situ* by LiSM revealed a depletion of AM in smoke-exposed mice. Imaging-based techniques such as LiSM have been shown to obviate potential artifacts caused by cell extraction from tissues, including the lung, to quantify immune cells (Steinert *et al.*, 2015; Amich *et al.*, 2020).

The fact that analysis of cells in BAL underestimates total AM counts in lungs of mice has been reported previously (Bhattacharya and Westphalen, 2016), and efforts have been made to significantly improve the yield of AM extracted from murine lungs by BAL (Busch *et al.*, 2019). With regard to cigarette smoke-exposed AM, it is conceivable that smoke-induced changes to mucus composition (Innes *et al.*, 2006; Kanai *et al.*, 2015), the alveolar epithelium (Jones *et al.*, 1980), or surface expression of cellular adhesion molecules increases the number of AM found in BAL, despite lower overall numbers in the lung. Several studies reported reduced expression of AM surface markers mediating cell-cell interactions such as CD11a or ICAM-1 in smokers compared to non-smokers (Sköld *et al.*, 2003; Löfdahl *et al.*, 2006). Additionally, macrophages obtained from the airways of smokers, or smoke-treated mice, displayed increased expression of surface markers like CD11b or CD14, which are highly expressed by monocytes (Hodge *et al.*, 2007; Cass *et al.*, 2021; Lugg *et al.*, 2022). In response

to inflammatory stimuli such as cigarette smoke, monocytes are attracted to the airways where they can assume a macrophage-like phenotype (Barnes, 2016; Kapellos *et al.*, 2018). Since tissue-resident AM express low levels of CD11b or CD14 (Misharin *et al.*, 2013; Bharat *et al.*, 2016), this suggests that the lung harbours a heterogenous pool of AM due to cigarette smoke, comprising a large proportion of monocyte-derived AM. These cells may be easier to retrieve by BAL even though the total number of AM is reduced due to cigarette smoke.

Our data indicate that the lower overall numbers of AM in smoke-treated mice are a result of cigarette smoke-induced inflammatory cell death. Imaging flow cytometry revealed a substantial size increase of dead $AnnV^{+}LD^{+}$ AM from smoke-treated mice, a key morphological characteristic of inflammatory cell death (Galluzzi *et al.*, 2018). Necroptosis and pyroptosis, two types of inflammatory cell death, have recently been linked with cigarette smoke-induced death of pulmonary epithelial cells (Pouwels *et al.*, 2016; Sauler *et al.*, 2019; Zhang *et al.*, 2021). Furthermore, increased levels of IL-1β and IL-18 found in smoke-exposed mice and human smokers indicate inflammasome activity (Barnes, 2009; Botelho *et al.*, 2011; Dima *et al.*, 2015). However, there are as yet no *in vivo* reports on inflammatory death pathways being induced by smoke in AM.

In this study, we provide evidence that NLRP3-dependent pyroptosis is a major driver of the smoke-induced, pro-inflammatory death of AM *in vivo*. Specifically, we observed partial reversal of AM death in smoke-treated $NLRP3^{-/-}$ and $ASC^{-/-}$ mice, suggesting involvement of pyroptosis, whereas AM from smoke-exposed $MLKL^{-/-}$ mice still underwent cell death. However, further experiments are required to dissect the potential involvement of other cell death pathways in smoke-induced AM death. These could include apoptosis, which has previously been observed in smoke-treated AM *in vitro* (Aoshiba *et al.*, 2001; Park *et al.*, 2018), or ferroptosis which has recently been linked to smoke-induced death of pulmonary epithelial cells (Yoshida *et al.*, 2019).

It is not clear how cigarette smoke could activate NLRP3 inflammasome formation in this system. However, there are several plausible possibilities. NLRP3 has been reported to sense DAMP that are commonly associated with

cigarette smoke exposure, such as cellular oxidative stress and changes to cellular metabolism, ion, lipid or protein composition (Schroder and Tschopp, 2010; Yang *et al.*, 2019; Swanson *et al.*, 2019). Potassium efflux from cells which can be induced by uptake of particulate matter has also been identified as an upstream trigger of the NLRP3 inflammasome and caspase-1 activation (Pétrilli *et al.*, 2007; Muñoz-Planillo *et al.*, 2013). In isolated murine alveolar macrophages, cigarette smoke exposure has been demonstrated to induce such potassium efflux. This in turn caused NLRP3 inflammasome assembly and caspase-1 activation mediated by ATP release and signalling through the purinergic P2RX7 receptor (L. Zhang *et al.*, 2018). Moreover, increased levels of oxidized low density lipoprotein have been found in cigarette smokers (Linna *et al.*, 2008), and oxidized low density lipoproteins in turn activated the NLRP3 inflammasome in human monocyte-derived macrophage cultures (Lin *et al.*, 2013). Additionally, NLRP3 activation induced by ROS has been described in epithelial and endothelial cells *in vitro* (Wang *et al.*, 2019; Zhang *et al.*, 2021), and continuous oxidative stress in the lungs induced by cigarette smoke is known to contribute to cell death and chronic disease (Rahman and Kinnula, 2012).

AM are the frontline immune cell in the defense against pathogens invading the airways, and are essential in initiating immune responses and mediating microbial clearance (Kopf *et al.*, 2015). Functional deficiency and eventual cell death due to smoke-induced oxidative stress is therefore likely to contribute to the increased susceptibility of cigarette smokers towards pulmonary infection (Bagaitkar *et al.*, 2008; Bauer *et al.*, 2013). Further investigations to identify how cigarette smoke causes NLRP3-dependent pyroptosis in AM may provide insights towards a new therapeutic avenue to prevent smoke-induced AM loss. For example, in case of an oxidative stress-related NLRP3 activation induced by cigarette smoke, intervention strategies using antioxidants or small molecules targeting the antioxidative Nrf2 signalling pathway could be explored to retain AM function and prevent smoke-induced AM death (Rangasamy *et al.*, 2004; Harvey *et al.*, 2011). Eventually, these strategies may be able to reverse the increased susceptibility of cigarette smokers to lung disease and infection.

4 Cigarette smoke-induced depletion of alveolar macrophages delays clearance of *L. pneumophila* but not *L. longbeachae*

4.1 Introduction

As with many other pulmonary bacterial infections (Arcavi and Benowitz, 2004; Bagaitkar *et al.*, 2008), cigarette smoking is one of the main risk factors linked to Legionnaires' Disease (Straus *et al.*, 1996; Den Boer *et al.*, 2006; Che *et al.*, 2008; Kenagy *et al.*, 2017). The detrimental effects of cigarette smoke on numerous components of local immune responses in the lung are well established (Stämpfli and Anderson, 2009; Strzelak *et al.*, 2018), but it remains unclear, how cigarette smoke mechanistically renders individuals more susceptible to Legionnaires' Disease.

One possible explanation is that cigarette smoke delays the immune response towards *Legionella*. Smoke can cause a downregulation of extra- and intracellular pattern recognition receptors in AM as well as impair cytokine secretion (Droemann *et al.*, 2005; Chen *et al.*, 2007; Gaschler *et al.*, 2008). Additionally, reduced phagocytosis by AM has been described in human cigarette smokers and in mouse models of cigarette smoke exposure (Martí-Lliteras *et al.*, 2009; Phipps *et al.*, 2010; Taylor *et al.*, 2010; Berenson *et al.*, 2013). This observation has been suggested to play a central role in the delayed clearance of extracellular bacteria such as *S. pneumoniae*, non-typeable *H. influenzae*, or *P. aeruginosa* (Drannik *et al.*, 2004; Martí-Lliteras *et al.*, 2009; Phipps *et al.*, 2010). However, there is little evidence to show which of these deficiencies caused by cigarette smoke exposure actually contributes to impaired clearance of infection.

The increased susceptibility towards Legionnaires' Disease and *Legionella* infection in smokers could also be due to enhanced intracellular bacterial replication resulting from smoke-induced defects in cell intrinsic immunity. Insufficient control of *L. pneumophila* replication has been reported *in vitro*, using a smoke-treated and infected AM cell line (Matsunaga *et al.*, 2001; Matsunaga *et al.*, 2002). *Legionella* have also been shown to translocate effector proteins into neutrophils (Copenhaver *et al.*, 2014), which during cigarette smoke exposure,

could potentially provide an expanded niche for bacterial replication. It is also conceivable that, due to cigarette smoke, *Legionella* persist in other pulmonary phagocytes that usually take up the bacteria, for example dendritic cells or monocyte-derived cells (Brown *et al.*, 2016).

While cigarette smoke clearly suppresses some aspects of host immunity, it paradoxically induces secretion of pro-inflammatory cytokines and chemokines. *In vivo*, smoke-induced activation of the respiratory epithelium increases levels of cytokines such as TNFα, IL-6, IL-8 or MCP-1, causing the accumulation of immune cells such as neutrophils in the lungs of smokers (Mio *et al.*, 1997; de Boer *et al.*, 2000; D'hulst, 2005; Barnes, 2009).

In this study, we investigated how cigarette smoke affected disease progression and the pulmonary immune response towards *Legionella* after concurrently infecting cigarette smoke-exposed mice. From these studies, we aimed to gain mechanistic insights into how cigarette smoke increases susceptibility to Legionnaires' Disease.

4.2 Results

4.2.1 Cigarette smoke exposure causes more severe disease after infection with *L. pneumophila*

We used a mouse model of acute cigarette smoke exposure to examine the effects of cigarette smoke on *Legionella* pathogenesis. Mice were exposed to cigarette smoke for 10 days as described in the previous chapter, and subsequently infected with *L. pneumophila* (Figure 4.1A). Smoke exposure was continued throughout the infection period to reflect the habits of human smokers. *L. pneumophila* was chosen as it is the most frequently diagnosed causative species of Legionnaires' Disease worldwide (Yu *et al.*, 2002; Cunha *et al.*, 2016; Chambers *et al.*, 2021).

As observed in the previous chapter, smoke-exposed mice displayed slightly lower body weight than air-exposed controls (Figure 4.1B), which is likely due to the appetite-suppressing effect of cigarette smoke (Audrain-McGovern and Benowitz, 2011). After infection with *L. pneumophila*, the relative body weight in air-exposed controls was reduced to approximately 90 % on day 3, but mice recovered quickly to an average of 95 % of relative body weight by day 5 after infection (Figure 4.1C). In contrast to this, cigarette smoke-exposed mice lost significantly more body weight, reaching a minimum of 84 % of starting body weight on day 4 after infection. Additionally, these mice barely recovered any body weight between days 4 and 5 after infection (Figure 4.1C).

Pulmonary bacterial load was determined at indicated time points after infection (Figure 4.1D). *L. pneumophila* CFU in lungs of smoke-treated mice was drastically increased compared to controls, with approximately 25-fold higher pulmonary bacterial burden on day 3, and almost 40-fold higher pulmonary bacterial burden on day 5 after infection (Figure 4.1D). Compared to the initially administered dose of 2.5×10^6 CFU *L. pneumophila*, most control mice had already cleared more than 99 % of bacteria by day 5 after infection, whereas approximately 25 % of the initial bacterial load was still detectable in smoke-exposed mice.

In summary, cigarette smoke exposure caused more severe disease and delayed bacterial clearance after *L. pneumophila* infection.

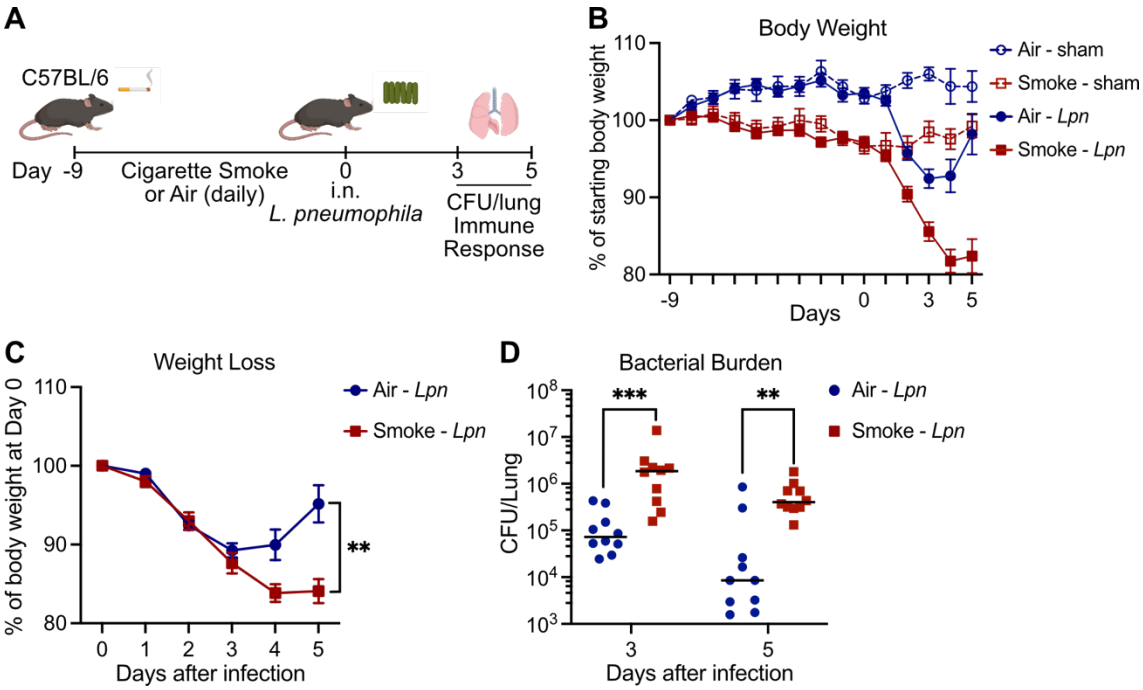

Figure 4.1: Cigarette smoke delays body weight recovery and bacterial clearance after *L. pneumophila* infection.
(A) Scheme of cigarette smoke exposure. Mice were exposed to cigarette smoke or room air daily. Mice were intranasally (i.n.) infected with 2.5 x 10^6 CFU *L. pneumophila* 130b ΔflaA (*Lpn*) on day 0. Body weight was monitored daily and at indicated time points after infection, pulmonary bacterial load was assessed. **(B)** Relative body weight of mice normalised to starting body weight on day -9. **(C)** Relative body weight of mice normalised to body weight on day 0, the day of infection. **(D)** Quantitation of *L. pneumophila* colony-forming units (CFU) in lungs of air- and smoke-exposed mice. (B/C) Graphs show mean ± SEM. (D) Graph shows median, with each dot representing an individual mouse. (B/C/D) Data is pooled from two independent experiments (n = 10 mice per group and time point). **p<0.01, ***p<0.001, Mann-Whitney-U test.

4.2.2 Cigarette smoke depletes alveolar macrophages and causes a neutrophil-dominated immune response towards *L. pneumophila*

We also profiled pulmonary immune cells in the same mice as above in an attempt to uncover why cigarette smoke significantly worsened the course of disease after *L. pneumophila* infection. Representative flow cytometry gating strategies are shown from an uninfected air-exposed mouse (Figure 4.2A) and an air-exposed mouse infected with *L. pneumophila* for 3 days (Figure 4.2B).

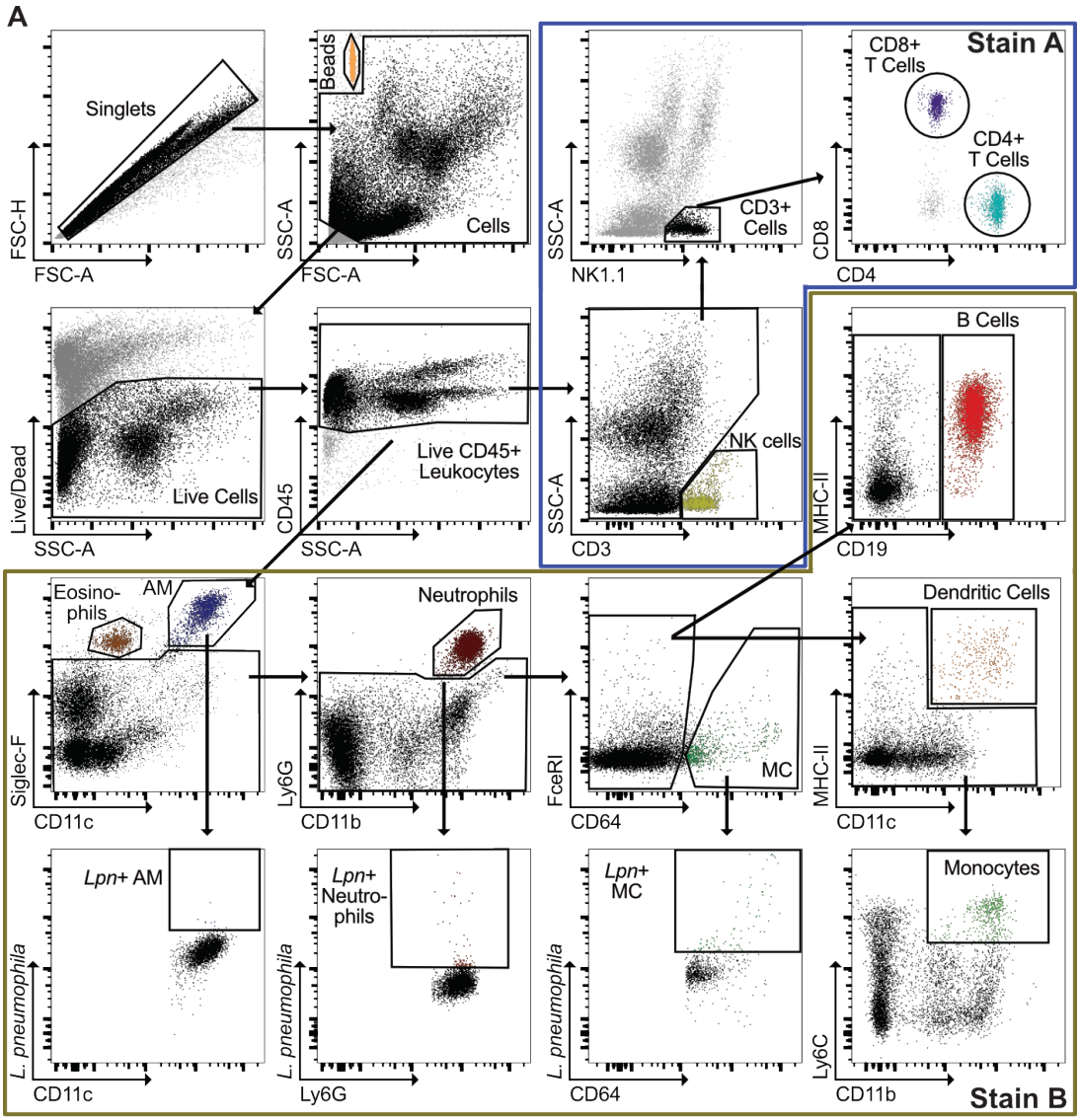

(Figure continued on next page.)

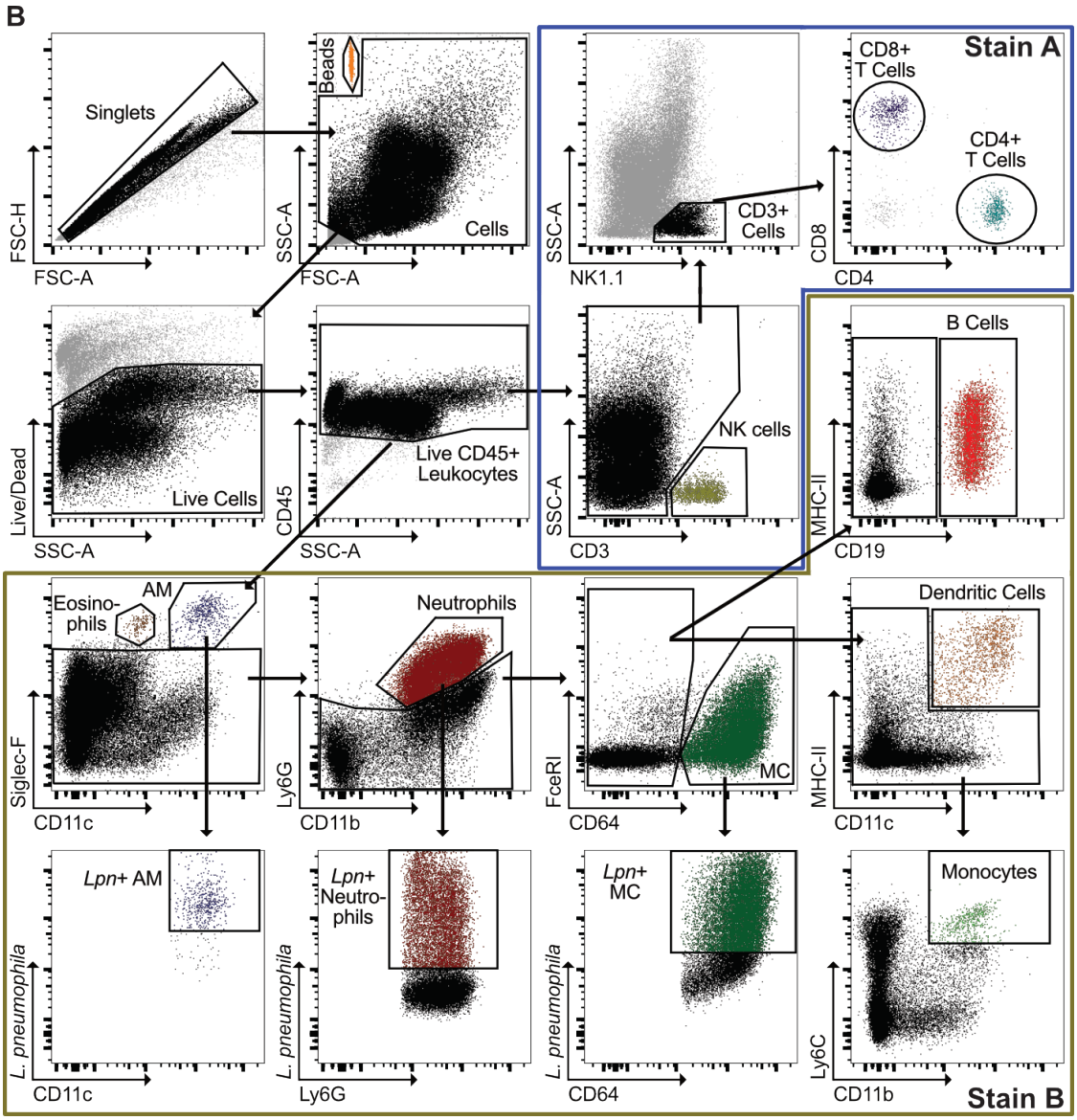

Figure 4.2: Representative flow cytometry gating strategy for identification of immune cells in the naive and infected lung.
Single-cell suspensions of enzymatically digested lungs from **(A)** an uninfected and **(B)** a *L. pneumophila*-infected mouse were stained and analysed by flow cytometry. Immune cell populations were identified from single live CD45$^+$ cells as follows: alveolar macrophages (AM) as Siglec-F$^+$CD11c$^+$ events, eosinophils as Siglec-F$^+$CD11c$^-$ events, neutrophils as Siglec-F$^-$CD11b$^+$Ly6G$^+$ events, monocyte-derived cells (MC) as Siglec-F$^-$Ly6G$^-$CD64$^+$FcεRI$^+$ events, B cells as Siglec-F$^-$Ly6G$^-$CD64$^-$CD19$^+$ events, dendritic cells as Siglec-F$^-$Ly6G$^-$CD64$^-$CD19$^-$ CD11c$^+$MHC-II$^+$ events, monocytes as Siglec-F$^-$Ly6G$^-$CD64$^-$CD19$^-$CD11b$^+$Ly6C$^+$ events, NK cells as NK1.1$^+$ events, CD4+ T cells as NK1.1$^-$CD3$^+$CD4$^+$ events, and CD8+ T cells as NK1.1$^-$CD3$^+$CD8$^+$ events. *L. pneumophila* (*Lpn*)-positive cells were identified by intracellular staining for the bacteria as described in the methods section.

Infection with *L. pneumophila* caused an accumulation of both myeloid and, to lesser extent, lymphoid cell populations in the lung. However, there were no statistically significant differences in the total number of $CD45^+$ leukocytes between air- and smoke- exposed mice (Figure 4.3A).

As observed previously, AM were depleted as a result of cigarette smoke exposure alone, and this difference was maintained throughout the course of infection (Figure 4.3B). On average, more than 1.5-fold more AM were identified in lungs from air-exposed control mice at each analysed time point. In contrast to this, cigarette smoke treatment resulted in significantly more neutrophils in the lungs of both uninfected mice and *L. pneumophila*-infected mice. On both days after infection, neutrophils were almost 5-fold more abundant in smoke-exposed mice compared to air-exposed controls (Figure 4.3C). Overall, neutrophils were by far the largest proportion of total immune cells in smoke-exposed mice, constituting approximately 60 % of $CD45^+$ leukocytes on day 3, and about 40 % of $CD45^+$ leukocytes on day 5 after infection.

The other common immune cells present in the lung were less consistently affected by cigarette smoke. The numbers of MC, which are the second-most common recruited phagocyte and known to be essential in anti-*L. pneumophila* defence (Brown *et al.*, 2016), was not affected by cigarette smoke (Figure 4.3D). Dendritic cells were increased due to cigarette smoke exposure alone but not after infection (Figure 4.3E). Significantly higher numbers of monocytes (Figure 4.3F), eosinophils (Figure 4.3G), and NK cells (Figure 4.3H) were found in lungs of smoke-treated mice after infection with *L. pneumophila*. However, cigarette smoke appeared to have no significant impact on the numbers of pulmonary B and T lymphocytes, before or after infection (Figure 4.3I-K).

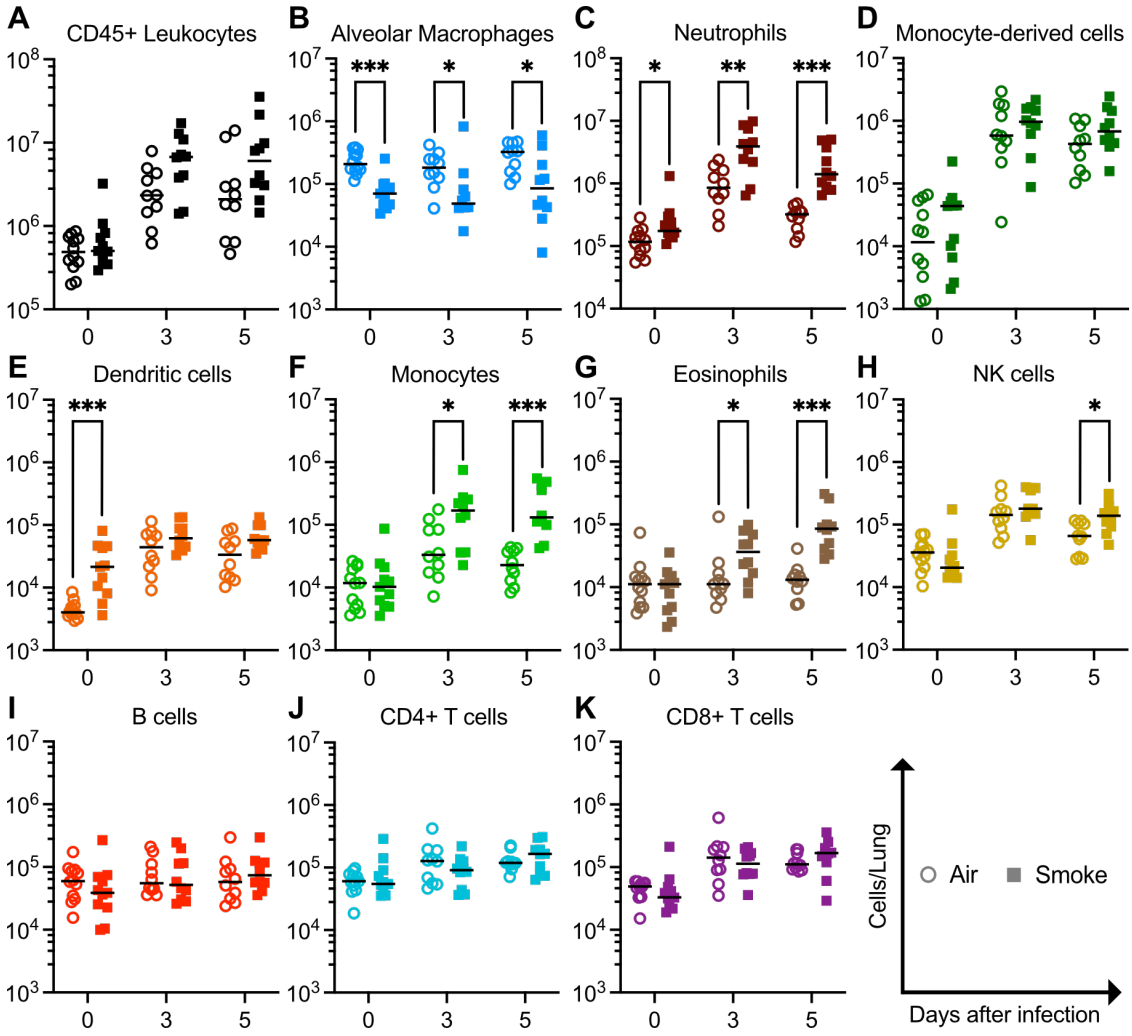

Figure 4.3: Cigarette smoke exposure depletes AM and causes a strong inflammatory innate immune response towards *L. pneumophila*.
Lungs were harvested from air- and smoke exposed mice at indicated time points and single cell suspensions were generated by enzymatic digest. **(A)** Total CD45$^+$ leukocytes and **(B-K)** indicated individual immune cell populations were quantified by flow cytometry. (A-K) Graphs show medians, with each dot representing an individual mouse. Data is pooled from two independent experiments (n ≥ 10 mice per group and time point). *p<0.05, **p<0.01, ***p<0.001, Mann-Whitney-U test.

Next, we assessed if cigarette smoke changed the bacterial uptake within AM, neutrophils and MC after infection by intracellular *L. pneumophila* staining (Figure 4.4). These three cell types are known to be the major cells which phagocytose *L. pneumophila* (Brown *et al.*, 2016), and represented more than 90 % of total *L. pneumophila*-positive cells after infection in both air- and smoke-exposed mice in this assay.

On day 3 after infection, the percentage of *L. pneumophila*-positive AM remained similar between air- and smoke-treated mice, although the total number of *L. pneumophila*-positive AM was reduced in smoke-exposed mice, probably due to the smoke-induced depletion of AM (Figure 4.4A/D). The most striking differences induced by cigarette smoke were once again observed in neutrophils. There was an approximately 1.5-fold increase in the percentage of neutrophils straining positive for the bacteria after smoke exposure and almost 10-fold more *L. pneumophila*-positive neutrophils overall in smoke-treated mice (Figure 4.4B/E). Neutrophils also accounted for most *L. pneumophila*-positive cells in smoke-exposed mice on day 3 after infection (Figure 4.4A-C). MC displayed very high proportions of cells that were *L. pneumophila*-positive. However, the number and proportion of *L. pneumophila*-positive MC were only affected to a minor extent by cigarette smoke (Figure 4.4C/F).

In summary, cigarette smoke induced a strong pulmonary accumulation of most innate immune cells after infection with *L. pneumophila*, with the exception of AM, which were depleted. The pulmonary cellular immune response in smoke-treated mice was heavily skewed towards neutrophils, which represented both the most abundant cell type overall as well as the cell type containing most intracellular *L. pneumophila*.

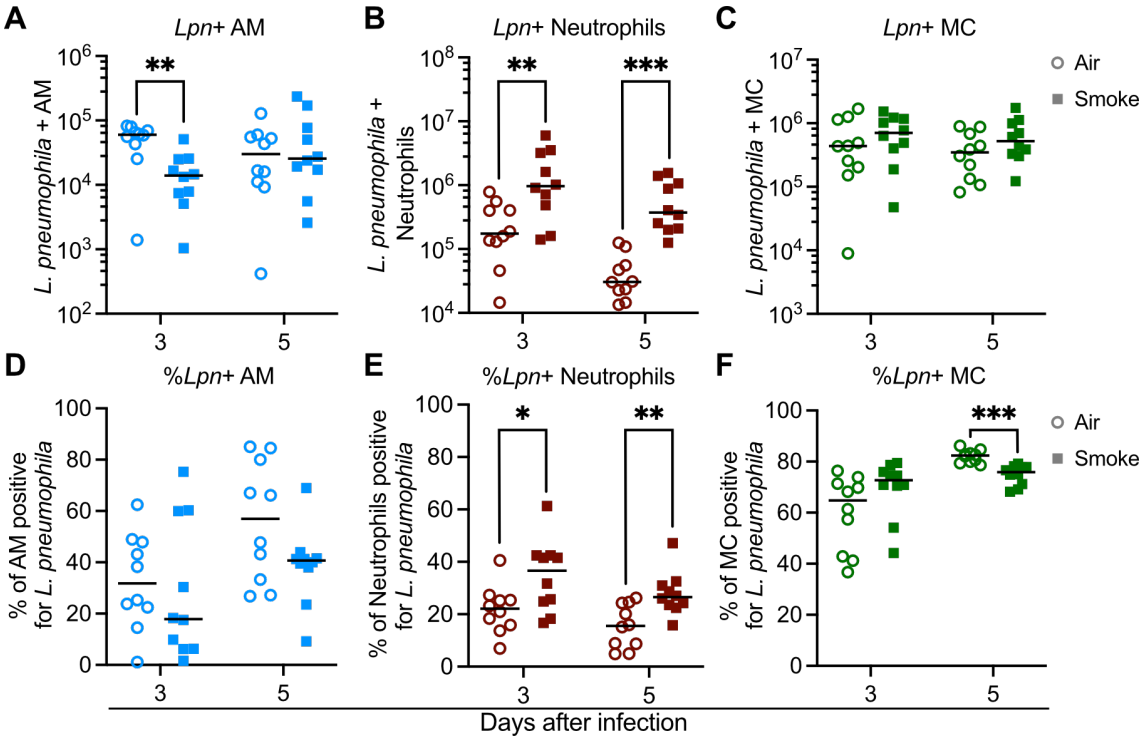

Figure 4.4: Increased *L. pneumophila*-positive neutrophils in smoke-exposed mice.
Lungs were harvested from air- and smoke exposed mice at indicated time points after infection and single cell suspensions were generated by enzymatic digest. **(A-C)** Total amounts of *L. pneumophila*-positive cells, and **(D-F)** the percentages of *L. pneumophila*-positive cells within the indicated cell population were identified by intracellular flow cytometry staining. (A-F) Graphs show group medians, with each dot representing an individual mouse. Data is pooled from two independent experiments (n = 10 mice per group and time point). *p<0.05, **p<0.01, ***p<0.001, Mann-Whitney-U test.

4.2.3 Cigarette smoke causes strong pro-inflammatory pulmonary cytokine response after *L. pneumophila* infection

Cytokine signalling to initiate the immune response and trigger bactericidal activity in myeloid cells is critical in anti-*L. pneumophila* defense (Brown *et al.*, 2017). We therefore investigated how cigarette smoke impacted the pulmonary production of chemokines and cytokines before and after infection with *L. pneumophila*.

We observed significantly increased levels of pro-inflammatory mediators such as IL-1α (Figure 4.5A), GM-CSF (Figure 4.5B), and MCP-1 (Figure 4.5C) in uninfected, smoke-exposed mice. This provides one possible explanation for the enhanced pulmonary infiltration of neutrophils (Figure 4.3C) and dendritic cells (Figure 4.3E), even though other chemoattractants such as CXCL1, CXCL8, or CCL20 are most likely to play a role in this context as well (Bracke *et al.*, 2006; Demedts *et al.*, 2007; Botelho *et al.*, 2010; Barnes, 2016).

Infection with *L. pneumophila* induced the production of all assessed cytokines in both air- and smoke-treated mice. In air-exposed control mice, the highest cytokine levels were detected on day 3 after infection, yet at that time point, no significant differences were found relative to smoke-exposed mice for any cytokine or chemokine (Figure 4.5). On day 5 after infection, cigarette smoke-treated mice still displayed strongly elevated levels of IL-1α, GM-CSF, MCP-1, IL-6, TNFα, and IFNγ (Figure 4.5A-F), consistent with and most likely caused by the substantially higher pulmonary loads of *L. pneumophila* (Figure 4.1D). This also correlated with the increased presence of several immune cell populations such as neutrophils, monocytes, eosinophils, and NK cells (Figure 4.3). IL-17A and IL-12 are known to induce bactericidal activity in neutrophils and MC (Brown *et al.*, 2016; Cai *et al.*, 2016). However, we did not identify any major differences in these cytokines between air- and smoke-treated mice (Figure 4.5G/H).

In summary, cigarette smoke caused a strong pro-inflammatory cytokine response in the lung, before and after infection with *L. pneumophila*.

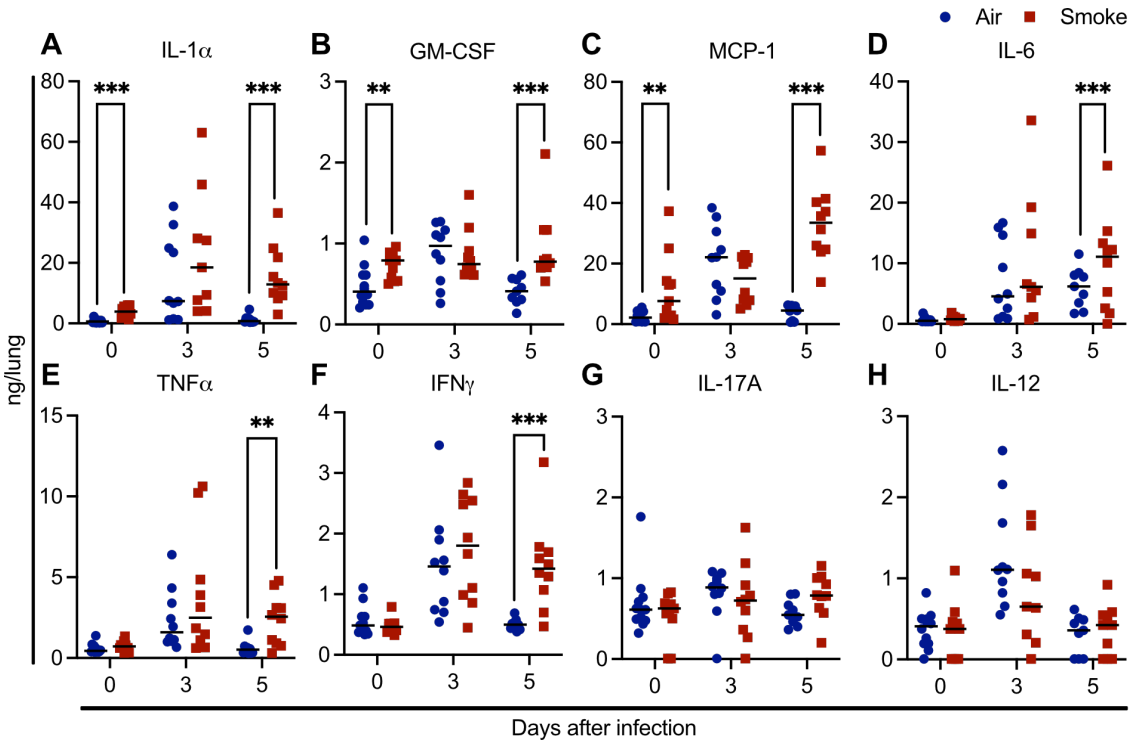

Figure 4.5: Increased levels of pro-inflammatory cytokines in smoke-treated mice before and after infection with *L. pneumophila*.
Lungs were harvested from air- and smoke-exposed mice at the indicated time points before and after infection with *L. pneumophila*. Lungs were homogenised, and the indicated cytokines and chemokines **(A-H)** were detected using a cytometric bead array. (A-H) Graphs show medians, with each dot representing an individual mouse. Data is pooled from two independent experiments (n ≥ 10 mice per group and time point). **p<0.01, ***p<0.001, Mann-Whitney-U test.

4.2.4 Cigarette smoke does not cause defective uptake or killing of *L. pneumophila* by neutrophils

Neutrophils engulf and degrade invading bacterial pathogens, and are essential in defence against *L. pneumophila* infection (LeibundGut-Landmann *et al.*, 2011; Ziltener *et al.*, 2016). However, cigarette smoke can cause defective phagocytosis in neutrophils (Stringer *et al.*, 2007; Tschernig *et al.*, 2015), or suppress their antimicrobial effector mechanisms (Dunn *et al.*, 2005; Xu *et al.*, 2008). Therefore, we investigated whether a reduced uptake of *L. pneumophila* by neutrophils in smoke-treated mice could contribute to more severe disease observed in these mice.

We assessed which cells initially phagocytosed the bacteria at approximately 16 hours after infection, and used heat-inactivated *L. pneumophila* to avoid the influence of any bacterial phagocytosis-promoting factors. Heat-inactivated *L. pneumophila* were delivered to air- and smoke-exposed mice to identify those cells ingesting *L. pneumophila* in absence of bacterial replication (Figure 4.6A). We observed the same changes to the pulmonary cellular composition as described before, with cigarette smoke causing AM depletion and neutrophil infiltration (Figure 4.6B). MC levels were slightly elevated in smoke-treated mice as well (Figure 4.6B), yet their contribution to overall bacterial uptake at this early time point after infection still remained much lower in comparison to AM or neutrophils (Figure 4.6C/E). The absolute numbers of cells staining positive for *L. pneumophila* closely reflected the changes in total cell numbers (Figure 4.6B/C). As a result, in smoke-treated mice, neutrophils were by far the predominant cell type to take up bacteria, and out of the three cell types investigated, almost 90 % of intracellular *L. pneumophila* was found within neutrophils (Figure 4.6E). In contrast, AM were clearly the main cell type to take up bacteria early after infection in air-exposed control mice, with more than 60 % of engulfed *L. pneumophila* found in AM in these mice (Figure 4.6C/E).

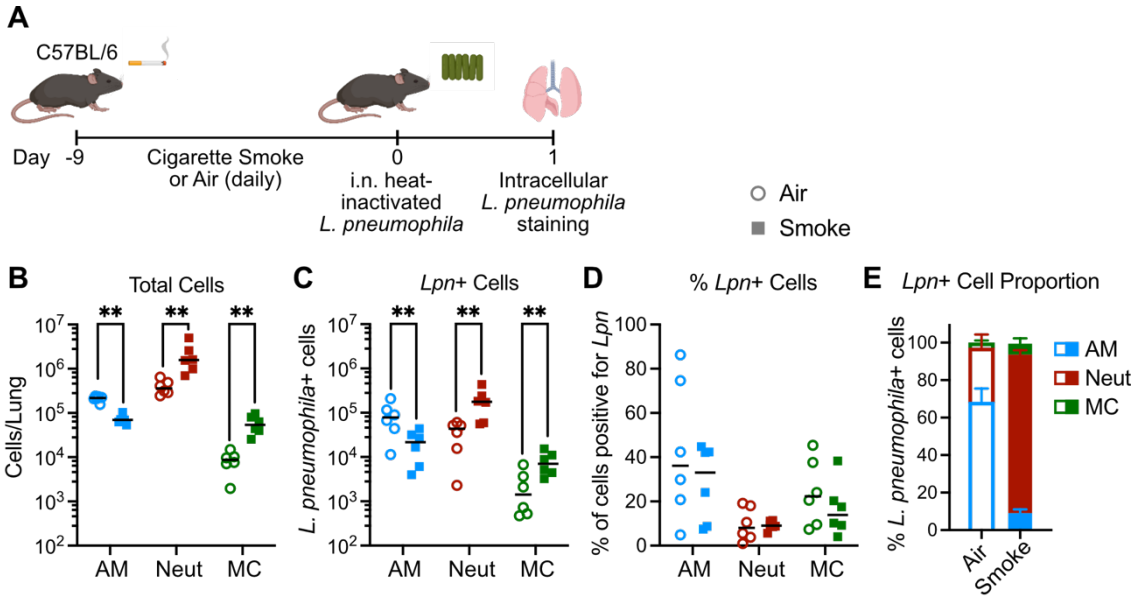

Figure 4.6: Cigarette smoke shifts uptake of *L. pneumophila* towards neutrophils.
(A) Mice were exposed to cigarette smoke or room air and infected with 2.5x10^6 CFU heat-inactivated *L. pneumophila*. Next day, lungs were harvested for intracellular bacterial staining. Flow cytometry was used to quantitate **(B)** the total amount of cells, **(C)** the total amount of *L. pneumophila* (*Lpn*)-positive cells, and **(D)** the percentage of *Lpn*-positive cells within a population. **(E)** Comparison of the proportions of *Lpn*-positive AM, neutrophils, and MC in air- and smoke-exposed mice. (B/C/D) Graphs show medians, with each dot representing an individual mouse. (E) Graph shows mean + SEM. (B-E) Data is pooled from two independent experiments (n = 6 mice per group). **p<0.01, Mann-Whitney-U test.

Neutrophils did not display defective uptake of *L. pneumophila* in smoke-exposed mice. In fact, they represented the major cell type to engulf the bacteria in the early stages after infection, most likely compensating for AM, which were depleted by cigarette smoke. Since phagocytosis of bacteria was not affected, we hypothesized that the increased overall bacterial load in smoke-exposed mice could be due to a loss of the bactericidal capability of neutrophils.

To test this, we purified neutrophils from air- and smoke-exposed mice after infection with *L. pneumophila* and cultured cell lysates to quantitate live intracellular bacteria in these cells. Neutrophils were gated as described previously and sorted with high purity from both air- and smoke-exposed mice (Figure 4.7A-C). The levels of live intracellular *L. pneumophila* within neutrophils remained similar between air- and smoke-treated mice on each day after infection (Figure 4.7D). Even though the decrease in live intracellular *L. pneumophila* in neutrophils between days 2 and 3 after infection appeared to be more pronounced in air-exposed control mice than in smoke-exposed mice, there was only a small but not significant trend towards more viable *L. pneumophila* per 10^4 neutrophils in smoke-treated mice on day 3 after infection (Figure 4.7D).

These results suggest that neutrophils retain their bactericidal properties despite cigarette smoke exposure.

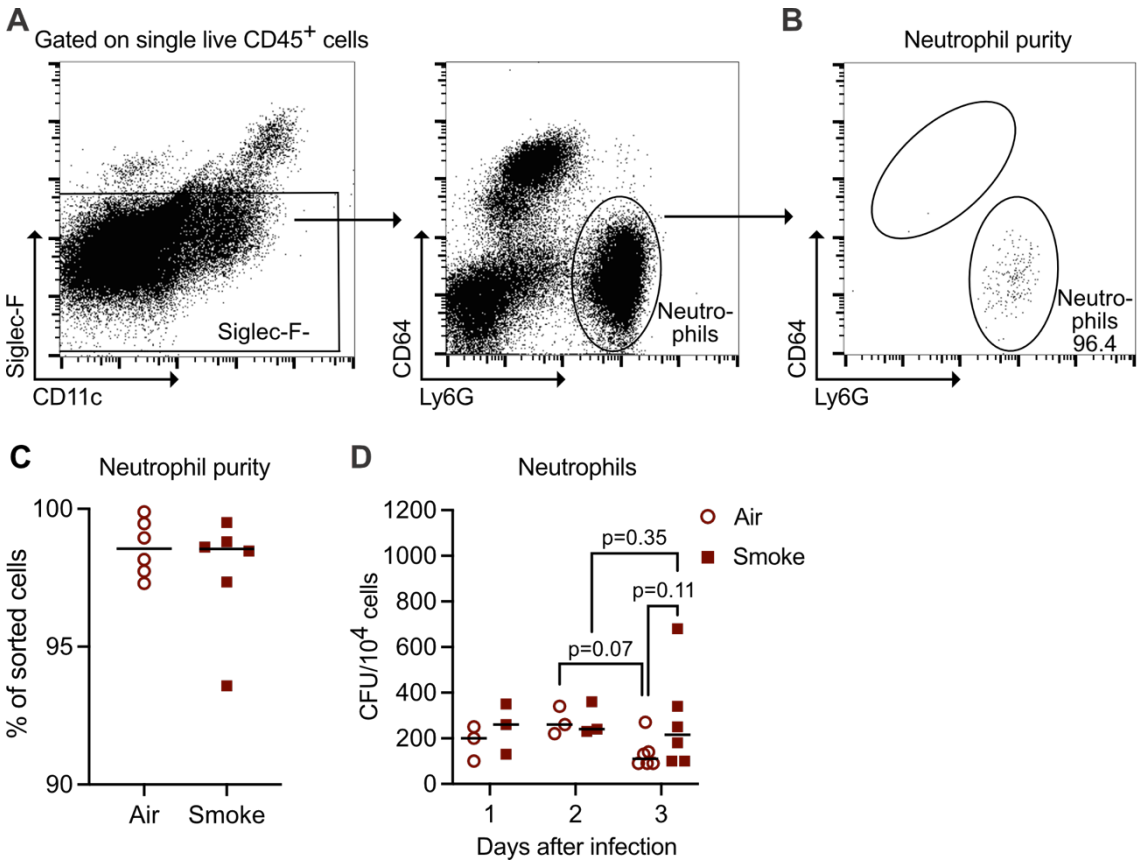

Figure 4.7: FACS-sorted neutrophils do not display increased live intracellular *L. pneumophila* in smoke-exposed mice.
Lungs were harvested from air- and smoke exposed mice and single cell suspensions were generated by enzymatic digest. Neutrophils were purified by fluorescent-activated cell sorting. **(A)** Representative gating strategy to purify neutrophils. **(B)** Representative flow cytometry plot confirming purity of sorted neutrophils. **(C)** Quantification of sorting purity of neutrophils on day 3 after infection. **(D)** Live intracellular *L. pneumophila* colony forming units (CFU) per 10^4 sorted neutrophils at the indicated time points after infection with *L. pneumophila*. (C/D) Graphs show medians, with each dot representing a pool of two mice. For day 1 and 2 after infection, data is from one experiment (n = 3 pools of mice per group and time point). For day 3 after infection, data is pooled from two independent experiments (n = 6 pools of mice per group). (D) Mann-Whitney-U test was used to compare air- and smoke-treated mice, paired t-test was used to compare days 2 and 3 after infection within the air- and smoke-treated groups.

Nevertheless, we performed further analyses of neutrophils to gain more detailed insight into their state on day 3 after infection during smoke exposure, when we observed a trend towards increased intracellular *L. pneumophila*.

We performed qPCR on neutrophils that were purified by FACS from air- and smoke-exposed mice 3 days after infection with *L. pneumophila*. We assessed the relative gene expression of *Tlr2*, which encodes for the Toll-like receptor 2 involved in *Legionella* recognition (Fuse *et al.*, 2007), *Spi1*, encoding the PU.1 transcription factor required for neutrophil terminal differentiation (Anderson *et al.*, 1998), as well as *Cyba*, which encodes a protein required for generation of reactive oxygen species by the NADPH oxidase (Belambri *et al.*, 2018). Relative gene expression in smoke-exposed neutrophils did not deviate from levels found in air-exposed control mice on day 3 after infection (Figure 4.8A). While this is only a small representation of gene expression in neutrophils, it is consistent with neutrophils not being majorly impaired by cigarette smoke.

We further analysed the levels of active neutrophil elastase, a serine protease involved in microbial killing by neutrophils (Korkmaz *et al.*, 2010), in purified neutrophils from air- and smoke-treated mice. Although the pulmonary levels of active neutrophil elastase were up-regulated during infection (Anderson *et al.*, 2019), we did not discover a smoke-dependent effect on the activity of neutrophil-specific neutrophil elastase after infection with *L. pneumophila* (Figure 4.8B/C).

These neutrophil-specific assays, in combination with the results obtained for bactericidal activity of these cells after purification, produced no evidence that neutrophils lost any ability to phagocytose and/or kill *L. pneumophila* after smoke exposure. They are therefore unlikely to serve as an enhanced niche for productive bacterial replication.

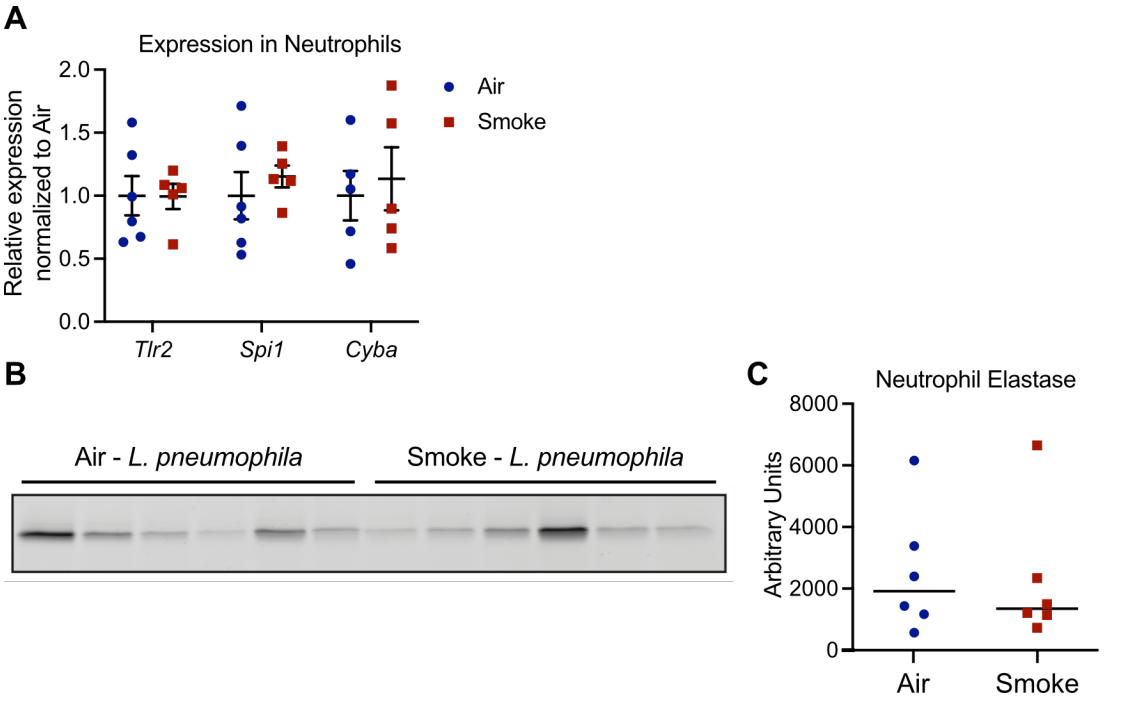

Figure 4.8: Cigarette smoke does not affect neutrophil gene expression or neutrophil elastase activity.
Neutrophils were FACS-sorted on day 3 after infection with *L. pneumophila* from air- or smoke-exposed mice. **(A)** RNA was isolated, transcribed into cDNA, and relative gene expression of the indicated genes was identified by qPCR. Expression was normalized to the reference gene *Rpl32* and expression levels of air-exposed mice. **(B)** Activity of neutrophil elastase was determined by labelling neutrophil lysates with the chemical probe PK105b. **(C)** Neutrophil elastase activity was quantified by densitometry based on in-gel fluorescence as identified in (B). (A) Graph shows mean ± SD, with each dot representing a pool of two mice. (B) Each lane represents a pool of two mice. (C) Graph shows median, with each dot representing a pool of two mice. (A/C) Data is pooled from two independent experiments, with n ≥ 5 pools of mice per group.

4.2.5 Cigarette smoke does not cause more severe disease after infection with *L. longbeachae*

We also investigated the effects of smoke treatment on the course of infection with a second *Legionella* species, *L. longbeachae*, the second-most common species to cause Legionnaires' Disease (Chambers *et al.*, 2021). Initial evidence suggests that smoking is associated with susceptibility to *L. longbeachae*-mediated Legionnaires' Disease (Kenagy *et al.*, 2017).

We exposed mice to cigarette smoke and concurrently infected them with *L. longbeachae* in a similar way as the *L. pneumophila* experiments described above (Figure 4.9A). As observed in previous experiments, all smoke-exposed mice displayed slightly lower body weight than air-exposed controls (Figure 4.9B). However, in contrast to the situation with *L. pneumophila*, we observed no significant difference in body weight loss between air- and smoke-treated mice after infection with *L. longbeachae* (Figure 4.9C). Both groups also recovered body weight on day 5 after infection to similar extent.

Cigarette smoke-exposed mice harboured almost 10-fold less pulmonary *L. longbeachae* when compared to control mice on day 3 after infection (Figure 4.9D). Both groups had sufficiently cleared infection by day 5 after infection, so that this difference was not detectable at that time point (Figure 4.9D).

In summary, the disease phenotype observed after infection with *L. pneumophila* was not recapitulated after infection with *L. longbeachae*, since smoke-treated mice did not display increased weight loss or pulmonary bacterial loads. In fact, cigarette smoke exposure may have the opposite effect on *L. longbeachae* pathogenesis as it appeared to slightly accelerate the clearance of infection.

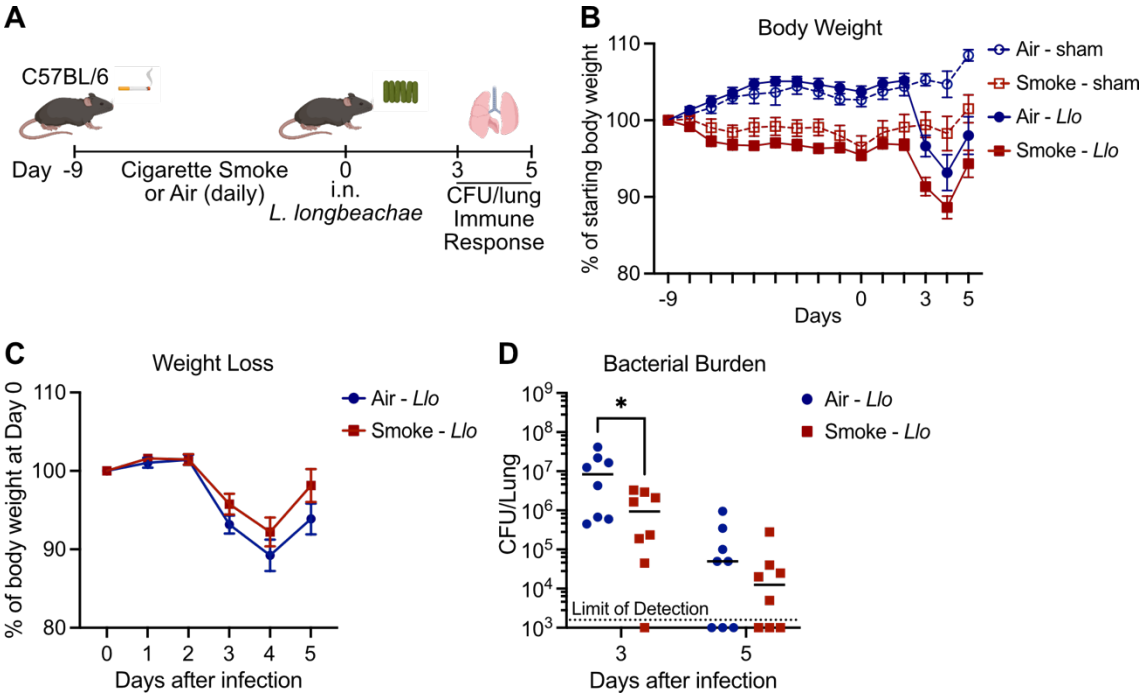

Figure 4.9: Cigarette smoke does not intensify disease after *L. longbeachae* infection.

(A) Scheme of cigarette smoke exposure. Mice were exposed to cigarette smoke or room air daily, and intranasally (i.n.) infected with $2.5x10^5$ CFU *L. longbeachae* NSW150 (*Llo*) on day 0. Body weight was monitored daily and at indicated time points after infection, pulmonary bacterial load was assessed. **(B)** Relative body weight of mice normalised to starting body weight on day -9. **(C)** Relative body weight of mice normalised to body weight on day 0, the day of infection. **(D)** Quantitation of *L. longbeachae* colony-forming units (CFU) in lungs of air- and smoke-exposed mice. (B/C) Graphs show mean ± SEM. (D) Graph shows median, with each dot representing an individual mouse. (B-D) Data is pooled from two independent experiments (n = 8 mice per group and time point). *p<0.05, Mann-Whitney-U test.

4.2.6 Cigarette smoke causes only minor changes in the cellular immune response towards *L. longbeachae*

We also examined the pulmonary cellular immune response in mice infected with *L. longbeachae* as we did for mice infected with *L. pneumophila*.

Infection with *L. longbeachae* caused an approximately 10-fold increase in pulmonary immune cells in both air- and smoke-exposed mice by day 5 after infection, but the total number of $CD45^+$ leukocytes was similar between the air- and smoke-exposed groups (Figure 4.10A). Consistent with previous experiments, smoke exposure reduced the numbers of AM, with around 40 % less AM identified in uninfected smoke-exposed mice compared to uninfected air-exposed controls. *L. longbeachae* infection itself caused a depletion of AM. This could be observed in both groups on day 3 after infection, but AM were replenished by day 5 after infection. The additional, smoke-induced AM depletion was still detectable on day 3, but not on day 5 after infection (Figure 4.10B).

L. longbeachae infection caused an accumulation of all other myeloid and lymphoid immune cells in the lung. Neutrophils represented the most abundant immune cell population in air- and smoke-exposed mice (Figure 4.10C), with MC being the second-most abundant population (Figure 4.10D). There were no differences between air- and smoke-exposed mice observed at any of the investigated time points for either cell type. Minor differences were seen in other immune cells, either elicited by cigarette smoke or infection (Figure 4.10E-K).

Intracellular flow cytometry staining was performed to detect those immune cells harbouring *L. longbeachae* after infection. Once again, these analyses focussed on AM, neutrophils and MC as the dominant phagocytes which contained bacteria (Figure 4.11). Neutrophils were by far the predominant *L. longbeachae*-positive cell type on both days after infection, followed by MC and AM (Figure 4.11A-C). A minor reduction in the absolute number and/or percentage of cells containing *L. longbeachae* was found in all cell types from smoke-exposed mice on day 3, but not on day 5 after infection (Figure 4.11A-F).

In summary, cigarette smoke caused only minor changes to the cellular immune response against *L. longbeachae*.

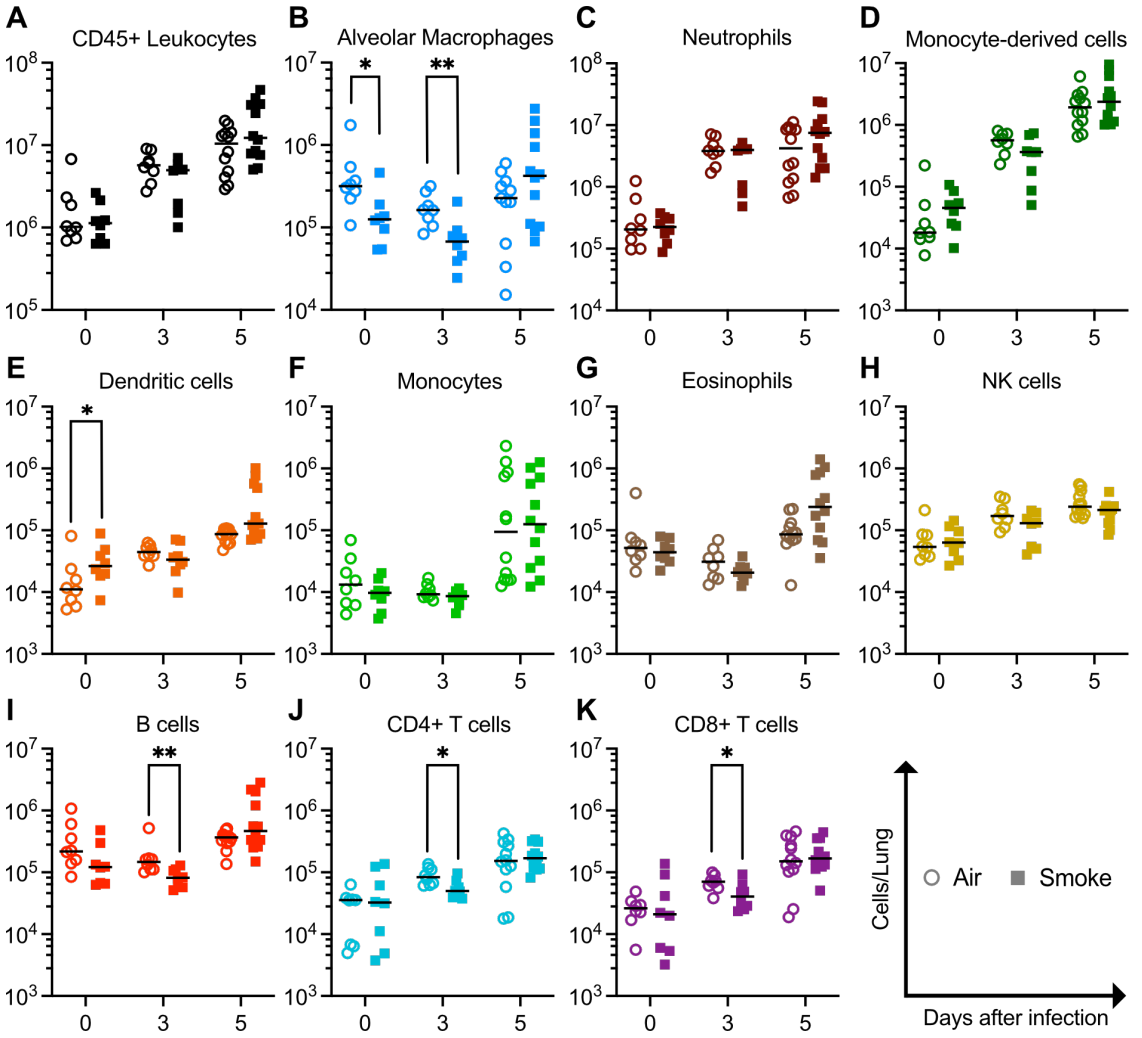

Figure 4.10: Cigarette smoke causes only minor changes in the cellular immune response towards *L. longbeachae*.
Lungs were harvested from air- and smoke exposed mice at indicated time points and single cell suspensions were generated by enzymatic digest. **(A)** Total CD45$^+$ leukocytes and **(B-K)** indicated individual immune cell populations were quantified by flow cytometry. (A-K) Graphs show medians, with each dot representing an individual mouse. Data is pooled from two or three independent experiments (n ≥ 8 mice per group and time point). *p<0.05, **p<0.01, Mann-Whitney-U test.

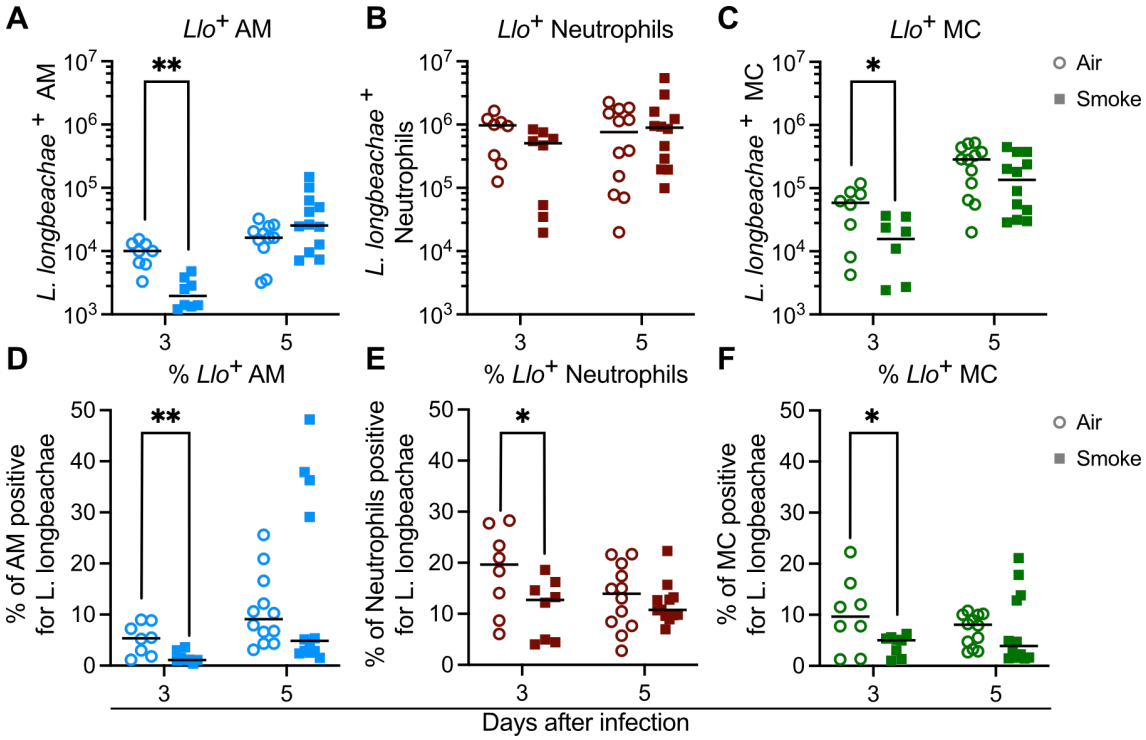

Figure 4.11: Fewer *L. longbeachae*-positive myeloid cells in smoke-exposed mice.
Lungs were harvested from air- and smoke exposed mice at indicated time points after infection and single cell suspensions were generated by enzymatic digest. **(A-C)** Total amounts of *L. longbeachae*-positive cells, and **(D-F)** the percentages of *L. longbeachae*-positive cells within the indicated cell population were identified by intracellular flow cytometry staining. (A-F) Graphs show medians, with each dot representing an individual mouse. Data is pooled from two or three independent experiments (n ≥ 8 mice per group and time point). *p<0.05, **p<0.01, Mann-Whitney-U test.

4.2.7 Clodronate-induced alveolar macrophage depletion mimics disease phenotypes observed in cigarette smoke models after *Legionella* infection

The two cell types that were affected by cigarette smoke the most were neutrophils and AM. Since neutrophils appeared to retain their bactericidal capacity against *L. pneumophila*, we focussed on AM, which were depleted as a result of smoke exposure prior to infection with either *L. pneumophila* or *L. longbeachae*. AM are the accepted replicative niche for both species, but how AM depletion at the time of infection with either species could change *Legionella* pathogenesis has not yet been reported. We therefore analysed the contribution of AM over the course of *Legionella* infection by treating mice with clodronate liposomes, a well-established method to deplete AM *in vivo* (Naito *et al.*, 1996). Three days later, we infected AM-depleted mice with *L. pneumophila* or *L. longbeachae* (Figure 4.12A).

AM were depleted by more than 80 % on average in clodronate-treated mice compared to PBS-treated mice, and PBS liposome-treated mice (Figure 4.12B). Due to the strong reduction in AM caused by *L. longbeachae* infection itself, the extent of AM depletion in clodronate-treated mice compared to either control group was less pronounced on day 3 and 5 after infection (Figure 4.12B). Clodronate-treated mice displayed strikingly decreased pulmonary *L. longbeachae* burden, with approximately 10-fold less bacteria on day 3 and almost 35-fold less bacteria on day 5 after infection compared to PBS-treated control mice (Figure 4.12C). This difference was not associated with changes in relative body weight (Figure 4.12D).

For *L. pneumophila* infection, pre-treatment with clodronate liposomes resulted in consistent AM depletion over the entire experiment (Figure 4.12E). Lungs of clodronate-treated mice contained, on average, only 10 – 35% of AM found in PBS-treated controls (Figure 4.12E). On day 1 after infection with *L. pneumophila*, we observed an approximate 4-fold reduction in the bacterial load present in clodronate-treated mice (Figure 4.12F). This result is consistent with what would be expected after the loss of the bacteria's replicative niche.

However, this initial decrease did not result in faster clearance of *L. pneumophila* at later timepoints. In fact, in clodronate-treated mice, we observed almost 3-fold higher bacterial loads of pulmonary *L. pneumophila* on day 5 and day 7 after infection compared to either control group (Figure 4.12F). Delayed bacterial clearance was accompanied by significantly delayed body weight recovery in AM-depleted mice (Figure 4.12G).

In summary, depletion of AM with clodronate liposomes largely reflected the disease phenotypes observed during cigarette smoke exposure. AM depletion appeared to be favourable during *L. longbeachae* infection, but delayed *L. pneumophila* clearance in later stages of infection.

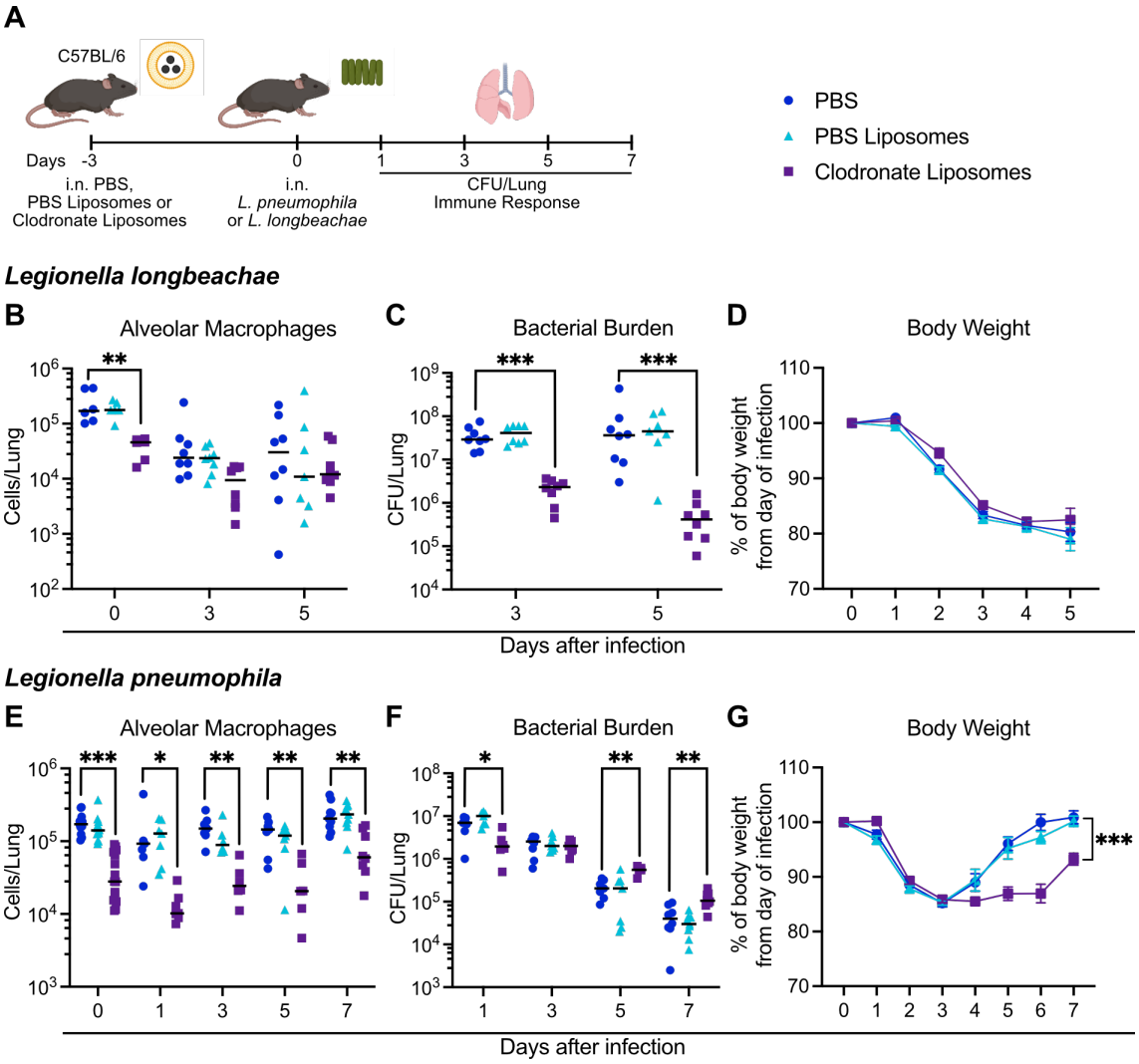

Figure 4.12: Clodronate-induced AM depletion differently affects disease progression after infection with *L. longbeachae* or *L. pneumophila*.
(A) Mice were treated with PBS, PBS liposomes or clodronate liposomes three days before intranasal infection with either $2.5x10^5$ CFU *L. longbeachae* NSW150, or $2.5x10^6$ CFU *L. pneumophila* 130b ΔflaA. Body weight of mice was monitored daily, and at the indicated time points, lungs were harvested for flow cytometry analyses and quantitation of pulmonary bacterial load. **(B/E)** AM were quantified by flow cytometry at the indicated time points. **(C/F)** Quantitation of pulmonary *L. longbeachae* or *L. pneumophila* colony-forming units (CFU) at the indicated time points. **(D/G)** Relative body weight progression of mice, normalized to body weight on the day of infection. (B/C/E/F) Graphs show medians, with each dot representing an individual mouse. (D/G) Graphs show mean ± SEM. (B-G) Data is pooled from two or three independent experiments, with n ≥ 6 mice per group and time point. *p<0.05, **p<0.01, ***p<0.001, One-Way ANOVA, displayed for differences between PBS and clodronate liposome groups.

4.3 Discussion

Cigarette smoke is a major known risk factor for many pulmonary viral and bacterial infections (Arcavi and Benowitz, 2004; Bagaitkar *et al.*, 2008; Bauer *et al.*, 2013), including Legionnaires' Disease (Straus *et al.*, 1996; Che *et al.*, 2008). Our mouse model of acute cigarette smoke exposure and concurrent *L. pneumophila* infection was consistent with the human epidemiological link between cigarette smoking and Legionnaires' Disease, and showed approximately 10-fold higher CFU in the lungs of smoke-treated mice and delayed recovery of body weight.

We originally believed that smoke-induced AM depletion was not the reason for more severe disease following *L. pneumophila* infection, given that AM are the replicative niche for *L. pneumophila*. However, when we specifically depleted AM by treating mice with clodronate liposomes prior to infection, bacterial clearance and disease recovery was significantly delayed as well. This suggests that the increase in *L. pneumophila* CFU in smoke-treated mice is, at least partially, the result of smoke-induced AM depletion. Additionally, AM have an underappreciated role in contributing to efficient clearance of *L. pneumophila* in the later stages of infection.

There are several possible explanations for the influence of AM on clearance of *L. pneumophila*. Ziltener *et al*. demonstrated that TNFα and TNFR1-signalling can induce bactericidal activity in AM *in vivo* (Ziltener *et al.*, 2016). It has also been shown that, *in vitro*, smoke-treated AM are not able to efficiently degrade intracellular *L. pneumophila* due to a down-regulation of TNFα (Matsunaga *et al.*, 2001; Matsunaga *et al.*, 2002). However, we observed that TNFα levels in the lungs of smoke-exposed mice infected with *L. pneumophila* were elevated on day 5 after infection. Furthermore, even from early stages after infection, AM represent only a minority of cells that take up *L. pneumophila*, with the far more numerous neutrophils and monocyte-derived cells constituting the major populations that phagocytose and degrade *L. pneumophila* (Brown *et al.*, 2016). This suggests that a potentially defective bactericidal activity by AM is unlikely to significantly contribute to the higher pulmonary bacterial loads in smoke-treated

mice, and it is more probable that AM influence the bactericidal activity of other phagocytes to combat *L. pneumophila* after the first few days of infection.

Depletion of AM could potentially delay the initiation of an adequate immune response. In line with previous reports, however, we observed distinct pro-inflammatory cytokine signalling and significantly increased numbers of neutrophils in lungs of smoke-treated mice before and after bacterial infection (Drannik *et al.*, 2004; Phipps *et al.*, 2010). It is possible that, in absence of AM, epithelial cells activated by cigarette smoke mediate the rapid influx of neutrophils due to the release of neutrophil chemotactic factors such as CXCL1, CXCL8, or leukotriene B_4 (Mio *et al.*, 1997; Barnes, 2009; Gao *et al.*, 2015; Barnes, 2016). Whether the levels of these chemokines remain significantly increased over the course of *Legionella* infection in our model, requires further investigation. As discussed in the previous chapter, smoke-induced inflammatory cell death of AM represents an additional trigger that likely contributes to the increased recruitment of different leukocyte populations to the lung, including neutrophils.

We confirmed that neutrophils are the predominant *L. pneumophila*-positive cell population in smoke-treated mice throughout the entire course of infection. Normally, neutrophils are able to restrict bacterial replication (Copenhaver *et al.*, 2014; Brown *et al.*, 2016) and are essential in the clearance of *L. pneumophila* as demonstrated in neutrophil-depleted mice (Tateda, *et al.*, 2001; LeibundGut-Landmann *et al.*, 2011). Since *L. pneumophila* is known to secrete effector proteins into neutrophils (Copenhaver *et al.*, 2014), we hypothesized that *L. pneumophila* could replicate in these cells during cigarette smoke exposure, thus contributing to the higher overall pulmonary CFU found in smoke-treated mice. Previous studies have shown impaired respiratory burst and bacterial killing capacity in smoke-treated neutrophils *in vitro* (Pabst *et al.*, 1995; Dunn *et al.*, 2005; Xu *et al.*, 2008; Y. Zhang *et al.*, 2018; Chien *et al.*, 2020). However, when we determined the amounts of viable intracellular bacteria in purified neutrophils, the amount of *L. pneumophila* per cell was similar on all days after infection in air- and smoke-exposed mice, suggesting there was no defect in bactericidal ability.

More recently, the epidemiological connection between cigarette smoking and Legionnaires' Disease was extended specifically to *L. longbeachae*-induced disease in New Zealand (Kenagy *et al.*, 2017), where *L. longbeachae* is the predominant causative species (Isenman *et al.*, 2016; Chambers *et al.*, 2021). In contrast to our findings using *L. pneumophila*, we did not observe a similar delay in body weight recovery or bacterial clearance when concurrently infecting smoke-treated mice with *L. longbeachae*. It has previously been reported that, in mouse models, *L. longbeachae* replicates very efficiently and causes higher pulmonary bacterial burden than *L. pneumophila* (Gobin *et al.*, 2009; Massis *et al.*, 2017). Species-specific microbial features such as the lack of flagellin, the presence of a capsule and specific repertoires of effector proteins secreted into host cells have been suggested to limit bacterial recognition and the immune response towards *L. longbeachae* (Kozak *et al.*, 2010; Cazalet *et al.*, 2010; Massis *et al.*, 2017). Despite using a *L. pneumophila* strain lacking flagellin to induce productive infection in C57BL/6 mice (Molofsky *et al.*, 2006; Asare *et al.*, 2007), and infecting with a lower dose of bacteria, *L. longbeachae* still reached far higher pulmonary bacterial loads than *L. pneumophila* in our hands. Treating mice with clodronate liposomes significantly limited *L. longbeachae* replication and was beneficial for bacterial clearance as evident by almost 35-fold less pulmonary *L. longbeachae* CFU in AM-depleted mice on day 5 after infection. Induction of AM apoptosis by inhibiting the pro-survival protein BCL-XL has been investigated as a therapeutic avenue to limit disease after *L. longbeachae* infection (Speir *et al.*, 2016). Importantly, our results suggest that this may not be a suitable approach for all *Legionella* species since AM depletion, either caused by cigarette smoke, or by clodronate liposome-treatment, significantly delayed bacterial clearance of *L. pneumophila*.

In human patients, the disease pattern and pathology is similar between cases caused by *L. longbeachae* or *L. pneumophila* (Amodeo *et al.*, 2010; Cameron *et al.*, 2016), and cigarette smoking remains a shared risk factor for Legionnaires' Disease. It has been shown that the extent of smoking history and the number of consumed cigarettes per day both correlated with higher susceptibility to disease caused by either species (Che *et al.*, 2008; Kenagy *et al.*, 2017). One limitation

in this study is the use of an acute model of cigarette smoke exposure that does not necessarily reproduce the pulmonary changes induced in humans that have smoked chronically for many years or decades. How chronic smoke exposure impacts the pathogenesis of different *Legionella* species has not yet been investigated in murine models, but it could provide additional insights into the smoke-induced perturbations of pulmonary immune responses towards infection. It may also help elucidating how smoke-induced AM depletion mechanistically delays bacterial clearance.

Overall, the results in this study suggest that smoke-induced AM depletion is an important contributor to more severe Legionnaires' Disease cause by *L. pneumophila*. Further experiments are required to understand whether this is a common feature across common pulmonary infections observed in smokers and to determine if this could be addressed pharmacologically.

5 Neutrophils promote proliferation of type II alveolar epithelial cells and functional lung recovery from pneumonia

5.1 Introduction

The lung is responsible for maintaining efficient gas exchange of O_2 and CO_2 between the air space and erythrocytes within the alveolar capillary bed (Torres *et al.*, 2021). To facilitate gas exchange, the alveolar epithelium is mostly comprised of structural, squamous type I AEC, which form the approximately 5 µm thin air-blood barrier together with endothelial cells. Secretory type II AEC constitute only about 5 % of the alveolar surface area and serve as local progenitors of type I AEC after epithelial injury (Barkauskas *et al.*, 2013; Desai *et al.*, 2014).

Beside the damage inflicted by invading lung pathogens themselves, the immune response may also be associated with significant tissue damage resulting from direct or bystander action of immune effector mechanisms on structural lung components such as the alveolar epithelium. Excessive transmigration of immune cells into the airways can cause a persisting breakdown of epithelial and endothelial barriers, resulting in vascular leakage into the alveoli (Matthay and Zimmerman, 2005; Zemans *et al.*, 2009).

The severity of lung damage observed after infection or during acute lung injury correlates particularly with the amount of neutrophils found in the airways, and could be reduced by inhibiting neutrophil migration (Grommes and Soehnlein, 2011). Within the alveolar space, activated neutrophils release ROS or tissue-degrading enzymes like neutrophil elastase or MMPs, which can directly induce epithelial cell death or down-regulate proteins that mediate AEC barrier interactions, for example E-Cadherin (Broermann *et al.*, 2011; Bhattacharya and Matthay, 2013; Boxio *et al.*, 2016). In case of pneumonia caused by influenza virus, cytotoxic $CD8^+$ T cells directly kill infected AECs, and excessive $CD8^+$ T cell activity can further exacerbate epithelial damage and confer severe lung pathology (Moskophidis and Kioussis, 1998; Schmidt and Varga, 2018).

Additionally, the processes that usually remove excess alveolar fluid are impaired during pneumonia as the inflammatory response causes a down-regulation of Na^+ or Cl^- channels that direct the water transport across the epithelium (Chen *et al.*, 2004; Lee *et al.*, 2007; Londino *et al.*, 2017). Consequently, pulmonary gas exchange is heavily compromised during pneumonia, which can lead to acute respiratory distress syndrome or respiratory failure.

In order to re-establish efficient oxygen uptake, repair processes are initiated alongside the immune response to mediate epithelial cell proliferation. An example for this is the active removal of dead cells from the alveolar space by AM and epithelial cells (Juncadella *et al.*, 2013; Allard *et al.*, 2018). AM and T_{reg} cells also produce a range of cytokines, including IL-10 and TGFβ, that control ongoing inflammatory processes (D'Alessio *et al.*, 2009; Herold *et al.*, 2011; Garbi and Lambrecht, 2017). Additionally, specific cytokines and growth factors that mediate tissue regeneration and type II AEC proliferation, such as amphiregulin, VEGFα, or IL-22, are released during the lung recovery phase (Varet *et al.*, 2010; Monticelli *et al.*, 2011; Kumar *et al.*, 2013; Zheng *et al.*, 2016; Croasdell Lucchini *et al.*, 2021a).

Most studies so far have predominantly investigated the protective roles of immune cells against invading pathogens, but in recent years, increased attention has been given to their role in tissue regeneration. Unlike T_{reg} cells, which promote epithelial cell repair by secreting amphiregulin (Li *et al.*, 2018), other conventional T cells, neutrophils or monocytes are still considered to mainly induce tissue damage due to their antimicrobial effector mechanisms. However, whether and how these cells contribute to pulmonary recovery remains largely unknown and requires further investigation.

Here, we addressed the role of immune cells in tissue repair and re-establishment of lung function following bacterial pneumonia by specific cell depletion during the resolution phase of inflammation in a mouse model of Legionnaires' disease.

5.2 Results

5.2.1 *Legionella* infection impairs lung function

We used the mouse model of Legionnaires' Disease to investigate the cellular mechanisms required for recovery of lung function following bacterial pneumonia. For this, we infected mice with *L. pneumophila* or *L. longbeachae* and compared lung function during the recovery phase 5 to 7 days after infection (Figure 5.1A), when most of the bacteria were cleared (Figure 4.1/4.9).

Despite similar disease progression after infection with either species as indicated by body weight loss (Figure 5.1B), we observed significantly reduced blood oxygen saturation (%SpO_2) only in mice infected with *L. longbeachae* (Figure 5.1C). These differences in blood oxygenation levels between the two species have been previously reported (Massis *et al.*, 2017). Importantly, %SpO_2 levels below 95 – 96 % are considered to be reduced in humans and mice (Lax *et al.*, 2014; Pretto *et al.*, 2014). All *L. longbeachae*-infected mice displayed levels below 96 %SpO_2 (average 93.1 %SpO_2) on day 5 after infection, but blood oxygen saturation returned to baseline levels above 96 %SpO_2 by day 7 after infection (Figure 5.1C). In contrast, infection with *L. pneumophila* caused a minor trend towards reduced %SpO_2 levels that was not statistically significant (Figure 5.1C).

Additionally, we detected significant changes to the respiratory parameters airway resistance, static compliance, and inspiratory capacity on day 5 after infection with either *L. longbeachae* or *L. pneumophila* (Figure 5.1D-F), indicating that infection impaired lung mechanics. Values of all investigated respiratory parameters returned to baseline levels of sham-infected control mice by day 7 after infection (Figure 5.1D-F).

In summary, despite similar changes to body weight and lung mechanics after infection with either *Legionella* species, only *L. longbeachae* infection resulted in significantly reduced blood oxygenation. We therefore focussed on the role of immune cells during functional lung recovery specifically after *L. longbeachae* infection.

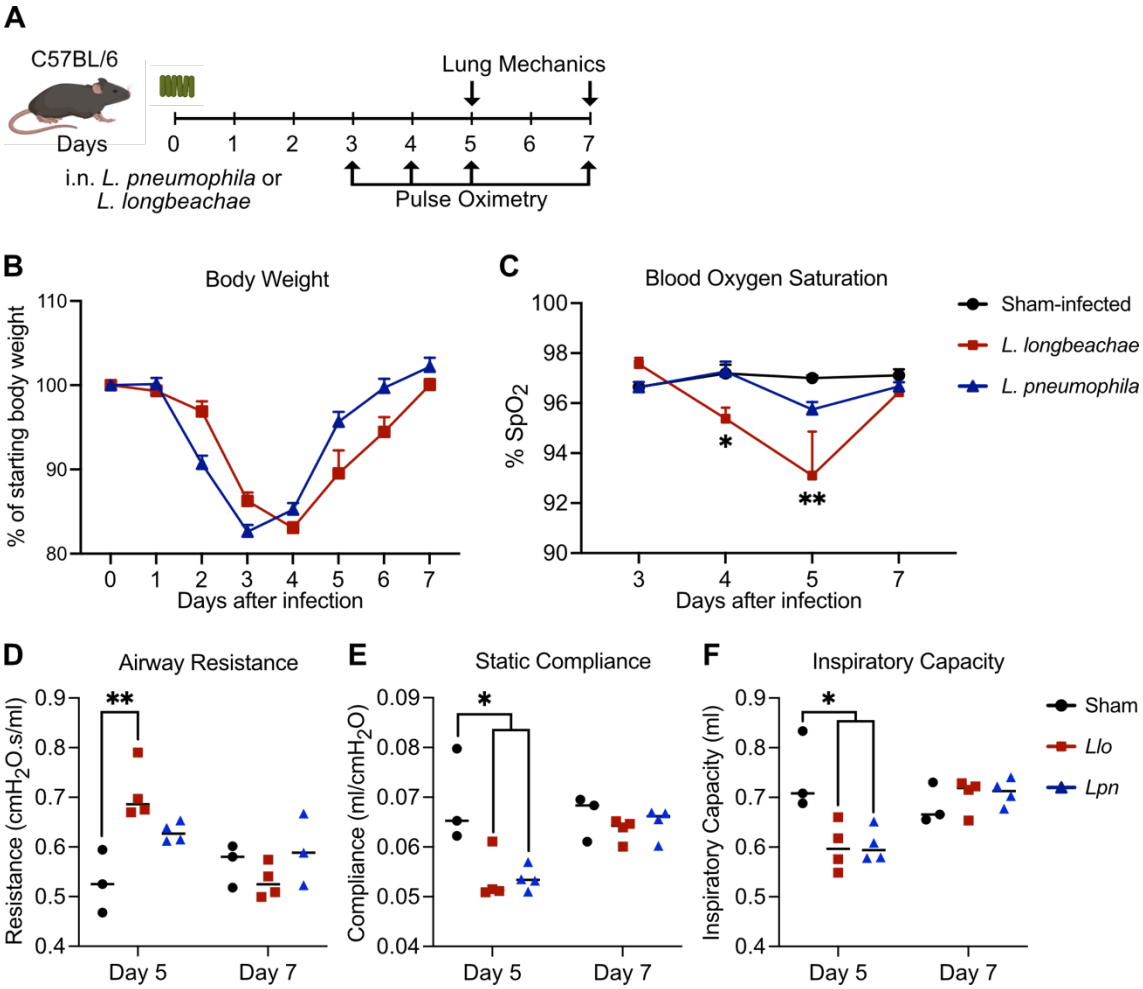

Figure 5.1: Legionella infection causes functional lung deficiency.
(A) Summary of experimental details. Mice were infected either with $2.5x10^4$ CFU *L. longbeachae*-mCherry or $2.5x10^5$ CFU *L. pneumophila* 130b ΔflaA and respiratory parameters were quantified at indicated times. Sham-infected mice received PBS. **(B)** Body weight kinetics of infected mice normalised to starting body weight on day 0. **(C)** Blood oxygen saturation ($\%SpO_2$) in mice at the indicated times after infection. **(D)** Airway resistance, **(E)** static compliance, and **(F)** inspiratory capacity of mice at the indicated times after infection. (B/C) Graphs show mean + SEM. (D-F) Graphs show median value, with each dot representing an individual mouse. Data are from one (*L. pneumophila*), or two pooled (*L. longbeachae*) independent experiments (n ≥ 3 mice per group and time point) (B/C) or one experiment (n ≥ 3 mice per group and time point) (D-F). *p<0.05, **p<0.01, One-way ANOVA. *Llo*, *L. longbeachae*; *Lpn*, *L. pneumophila*.

5.2.2 Neutrophil depletion during the resolution of *L. longbeachae* infection delays functional lung recovery

Impairment of lung function as indicated by blood oxygen saturation was most pronounced 5 days after infection with *L. longbeachae* before returning to normal levels on day 7. To investigate whether immune cells promoted the recovery of lung function, specific cell populations were depleted on day 5, and $\%SpO_2$ levels were quantified thereafter (Figure 5.2A). Clodronate liposomes were used to deplete macrophages (Figure 5.2B/C), and antibodies were used to deplete neutrophils (Figure 5.2D/E), $CD4^+$ T cells (Figure 5.2F/G), or $CD8^+$ T cells (Figure 5.2F/H). In contrast to the efficient depletion of neutrophils, $CD4^+$ T cells and $CD8^+$ T cells, treatment with clodronate liposomes at that point of infection did not cause a striking AM depletion. This is most likely due to the fact that AM counts are already strongly decreased as a result of *Legionella* infection itself (Figure 4.12B). Since we still observed a trend towards reduced AM compared to undepleted mice, we proceeded to analyse lung function in these mice.

Importantly, specific cell depletions during the recovery phase of *L. longbeachae* infection (Figure 5.3A) did not affect bacterial clearance from the lung. At the time of analysis, pulmonary *L. longbeachae* CFU levels were similar between all groups independently of whether specific immune cells populations had been depleted or not (Figure 5.3B). Furthermore, the abundance of total immune cells during the recovery phase from *L. longbeachae* infection was not significantly impacted by specific cell depletions since all infected groups displayed similar levels of pulmonary $CD45^+$ leukocyte counts at the time of analysis (Figure 5.3C).

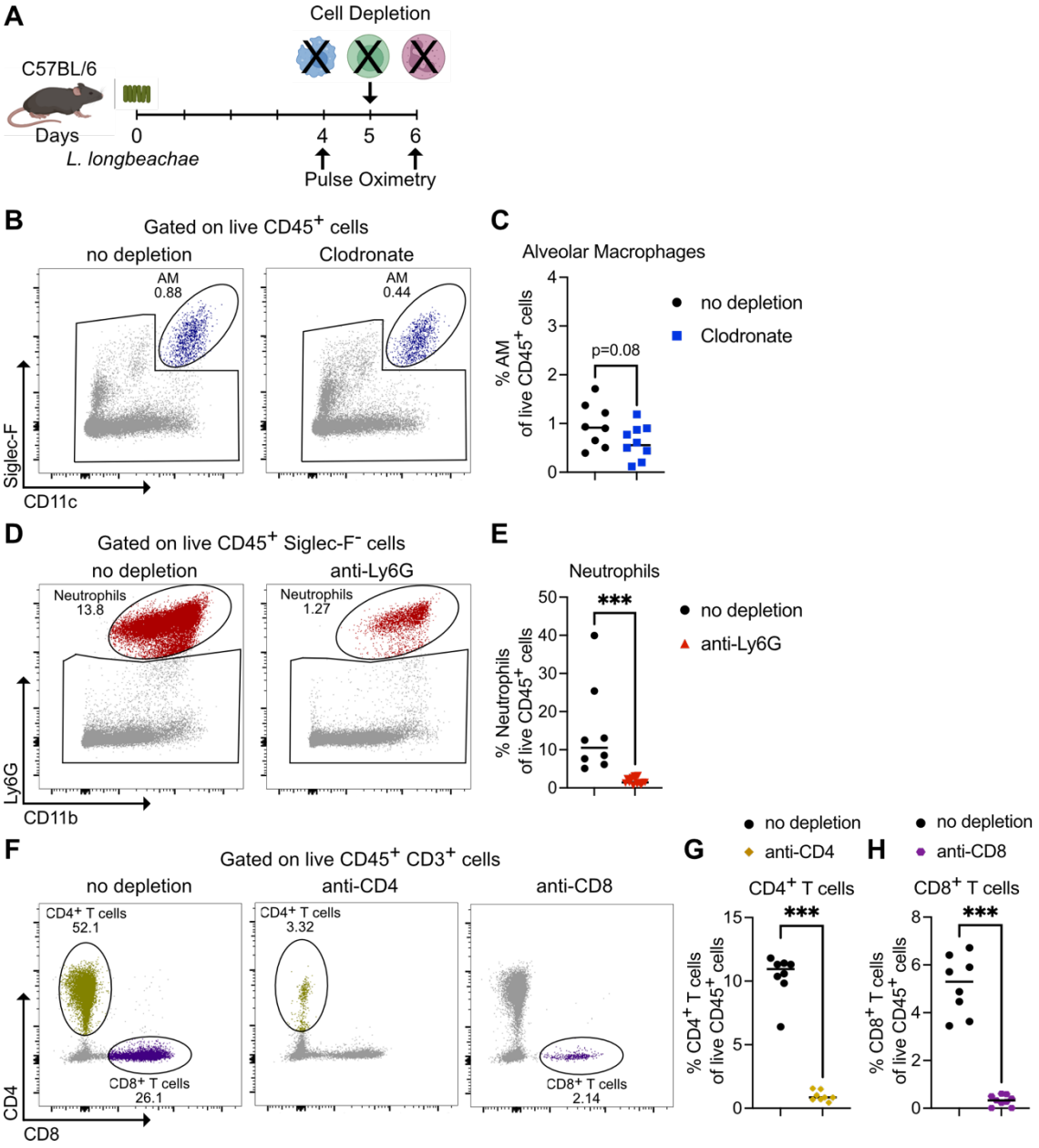

Figure 5.2: Depletion of specific immune cells during recovery phase from *L. longbeachae* infection.

(A) Summary of experimental details. Mice were infected with 2.5x10^4 CFU *L. longbeachae* mCherry. 5 days after infection, either AM, neutrophils, $CD4^+$ T cells, or $CD8^+$ T cells were depleted as described in the methods section. **(B-H)** Depletion of alveolar macrophages (C/D), neutrophils (E/F), $CD4^+$ T cells and $CD8^+$ T cells (F-H). (B/D/F) Representative flow cytometry plots showing depletion of the indicated cell populations in the lung in comparison to infected, undepleted mice. (C/E/G/H) Flow cytometry-based enumeration of immune cells in the lungs of mice treated with the indicated cell depletion methods. Graphs show medians, with each dot representing an individual mouse. Data is pooled from two independent experiments (n ≥ 8 mice per group). *p<0.05, **p<0.01, ***p<0.001, One-way ANOVA.

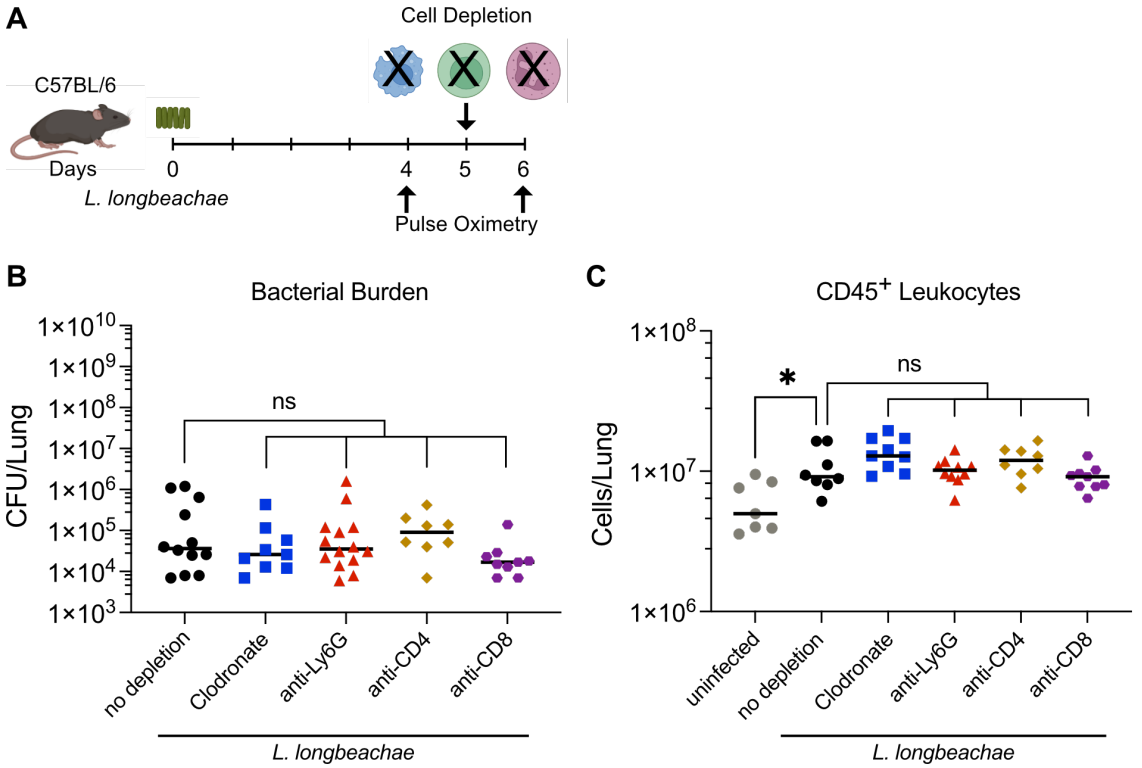

Figure 5.3: Cell depletion in recovery phase from *L. longbeachae* infection does not affect bacterial clearance and overall immune response.
(A) Summary of experimental details. Mice were infected with 2.5x10^4 CFU *L. longbeachae* mCherry. 5 days after infection, either AM, neutrophils, CD4$^+$ T cells, or CD8$^+$ T cells were depleted as described in the methods section. **(B)** Quantitation of *L. longbeachae* colony-forming units (CFU) in lungs of mice treated as indicated. **(C)** Total CD45$^+$ leukocytes in lungs of mice treated as indicated were enumerated by flow cytometry. (B/C) Graphs show medians, with each dot representing an individual mouse. Data is pooled from two (uninfected, clodronate, anti-CD4, anti-CD8) or three (no depletion, anti-Ly6G) independent experiments (n ≥ 7 mice per group and time point). *p<0.05, One-way ANOVA.

Having demonstrated that specific cell depletions did not change *Legionella* clearance, we measured blood oxygen saturation to determine whether particular immune cell populations promoted recovery of lung function (Figure 5.4A).

As expected, all groups of mice displayed significantly lower $\%SpO_2$ levels before cell depletion on day 4 after infection compared to uninfected control animals, confirming that *L. longbeachae* infection caused functional lung deficiency (Figure 5.4B). The average extent of reduction in oxygen saturation was comparable between all groups, with $\%SpO_2$ levels mostly ranging between approximately 92 – 96 %.

By day 6 after infection with *L. longbeachae*, $\%SpO_2$ levels in mice undergoing no cell depletion returned to similar levels compared to uninfected controls, even though some mice still displayed blood oxygen saturation below 96 $\%SpO_2$ (Figure 5.4C). Similarly, mice undergoing $CD4^+$ or $CD8^+$ T cell depletion displayed $\%SpO_2$ levels comparable to uninfected controls (Figure 5.4C), indicating that these cells did not have a major role in recovery of lung function at that stage. In contrast, $\%SpO_2$ levels of AM- or neutrophil-depleted mice were still significantly reduced compared to uninfected mice, indicating that functional lung recovery was impaired when these cells were absent in the resolution phase of *L. longbeachae* infection (Figure 5.4C).

In summary, these results surprisingly suggest that neutrophils contribute to the re-establishment of efficient oxygen uptake during the recovery phase from *L. longbeachae* infection. Additionally, clodronate-treated mice displayed a similar delay in the recovery of blood oxygen saturation, even though the treatment resulted only in a trend towards AM depletion. Importantly, these differences in functional lung recovery were most likely not due to changes in the immune response towards *Legionella* since bacterial clearance remained unaffected by specific cell depletions.

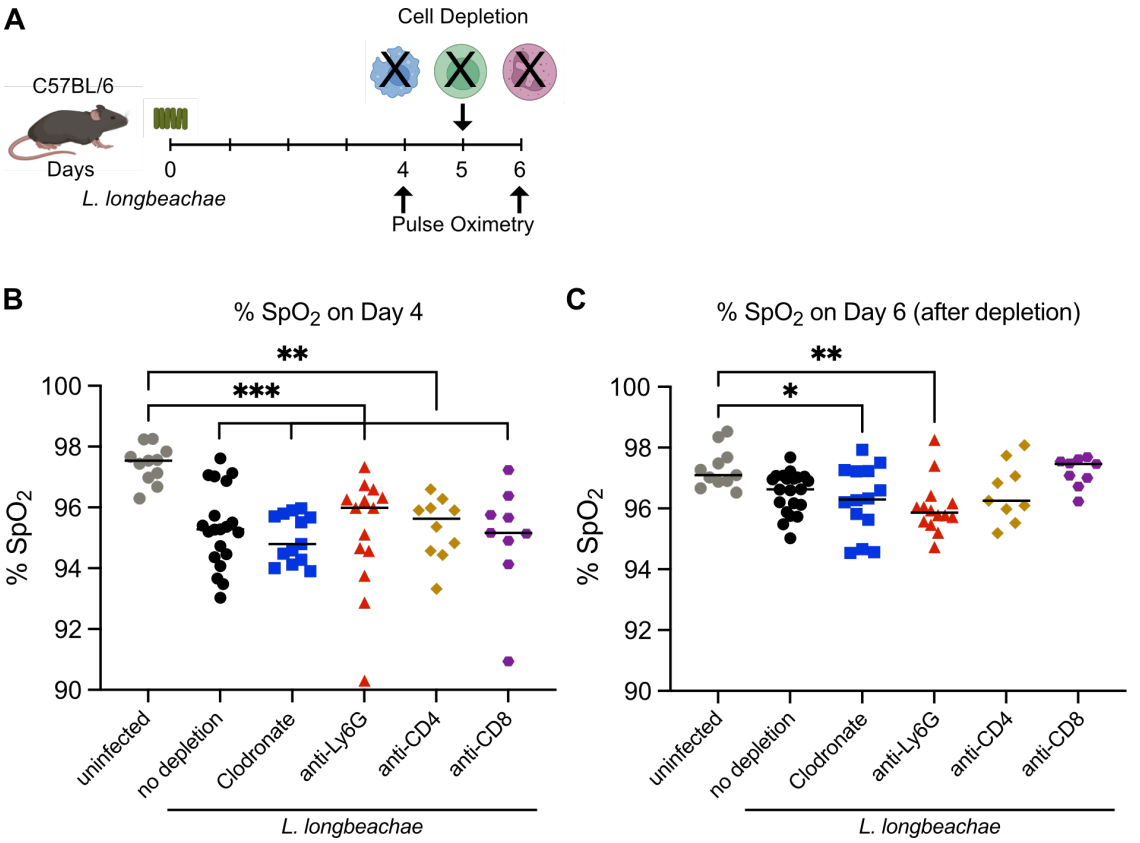

Figure 5.4: AM or neutrophil depletion during the resolution phase of *L. longbeachae* infection delays recovery of blood oxygen saturation.
(A) Summary of experimental details. Mice were infected with $2.5x10^4$ CFU *L. longbeachae*-mCherry. 5 days after infection, AM, neutrophils, $CD4^+$ T cells, or $CD8^+$ T cells were depleted as described in the methods section. Blood oxygen saturation was determined by pulse oximetry before and after cell depletion. **(B/C)** Levels of blood oxygen saturation on the day before (B) and after (C) cell depletion. Graphs show the group median, with each dot representing an individual mouse. Data is pooled from two (anti-CD4, anti-CD8) or three (uninfected, clodronate, no depletion, anti-Ly6G) independent experiments (n ≥ 9 mice per group). *p<0.05, **p<0.01, ***p<0.001, One-way ANOVA.

5.2.3 Delayed recovery of blood oxygenation in absence of neutrophils is independent of lung mechanics or edema

We next investigated the mechanisms by which neutrophils promote re-establishment of normal $\%SpO_2$ levels after *Legionella* infection. Impaired lung mechanics or excessive edema are two important factors negatively impacting blood oxygenation (Matthay and Zimmerman, 2005). Therefore, we assessed whether neutrophils modulated these two events during the recovery phase from *L. longbeachae* infection (Figure 5.5A).

Despite the previously described differences in blood oxygenation on the day of analysis (Figure 5.5B), we did not, by using computer-assisted forced respiratory manoeuvres, detect any differences in inspiratory capacity (Figure 5.5C), static compliance (Figure 5.5D), airway resistance (Figure 5.5E), or other secondary respiratory parameters such as tissue elastance and tissue damping after specific cell depletion (data not shown). Since infected mice, independently of cell depletion, showed similar respiratory parameter values compared to uninfected mice (Figure 5.5C-E), it is not certain whether infection with *L. longbeachae* in this experiment caused defects in lung mechanics as previously observed (Figure 5.1D-F). Nevertheless, these results indicate that the blood oxygenation levels found in mice were not impacted by changes to respiratory mechanics.

Next, we investigated whether neutrophils promoted edema clearance following *L. longbeachae* infection. For this, the wet-to-dry weight ratio of lungs was quantified as an indication of fluid accumulation. The wet/dry ratio in *L. longbeachae*-infected mice was increased on day 6 after infection compared to uninfected control mice, indicating that pulmonary edema was still present at that time (Figure 5.5F), even though infection was virtually cleared (Figure 5.3B). However, there were no striking differences between mice depleted for specific immune cell populations and their undepleted counterparts (Figure 5.5F).

Together, these results demonstrate that the delayed re-establishment of blood oxygenation in absence of neutrophils during the recovery from *L. longbeachae* infection was not due to changes in lung mechanics or unresolved edema.

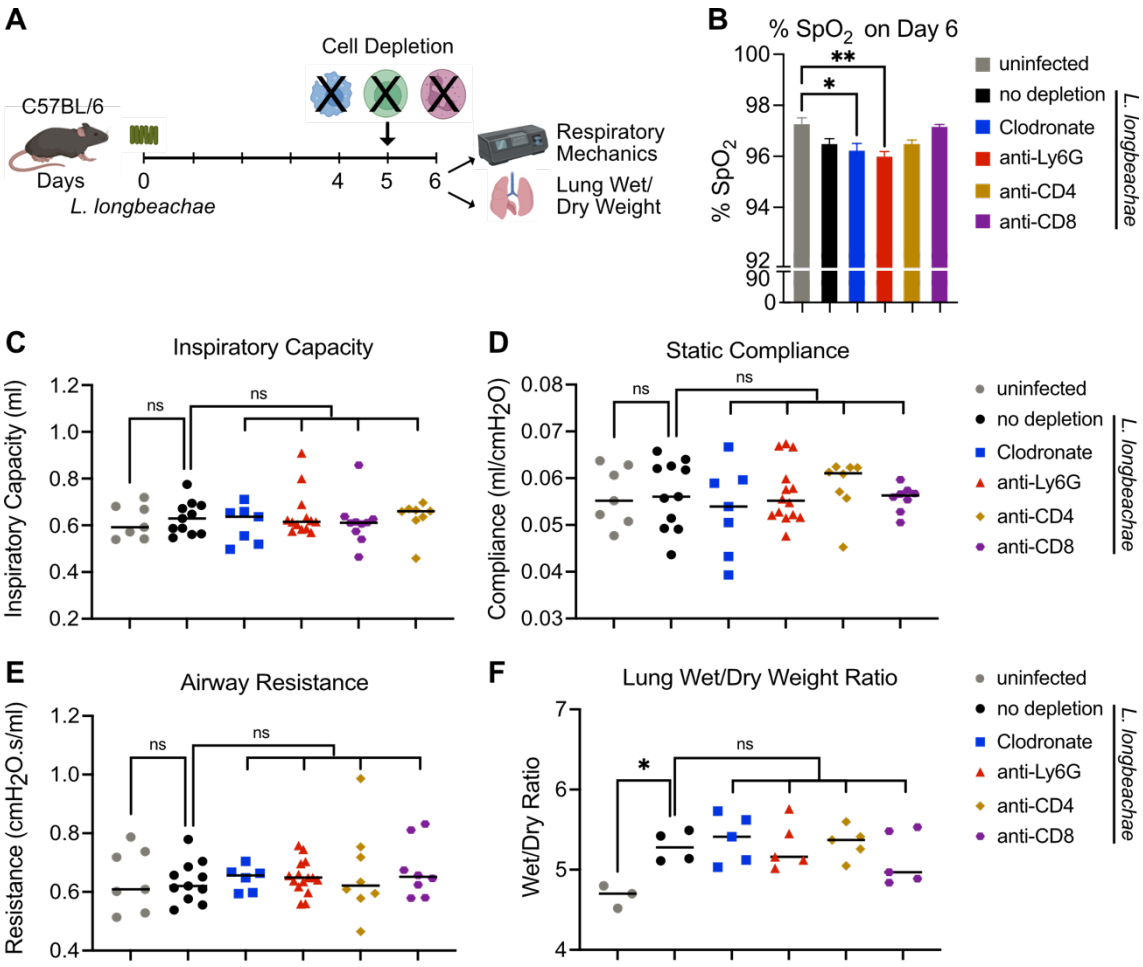

Figure 5.5: Cell depletions do not affect the lung mechanics or fluid accumulation in the lung.
(A) Summary of experimental details. Mice were infected with 2.5x10^4 CFU *L. longbeachae*-mCherry. 5 days after infection, either AM, neutrophils, $CD4^+$ T cells, or $CD8^+$ T cells were depleted. On day 6 after infection, lungs were retrieved for indicated analyses. **(B)** Blood oxygen saturation in indicated mice on day 6, shown as averages based on the values of individual mice depicted in Figure 5.4C. **(C-E)** The respiratory parameters inspiratory capacity (C), static compliance (D), and airway resistance (E) were quantified for mice depleted of the indicated cell population. **(F)** Wet/Dry weight ratio of lungs from mice depleted for the indicated cell population. (B) Graph shows mean + SEM. (C-F) Graphs show medians, with each dot representing an individual mouse. (C-E) Data is pooled from two (clodronate, anti-CD4, anti-CD8) or three (no depletion, anti-Ly6G) independent experiments (n ≥ 7 mice per group). (F) Experiment was performed once (n = 3-5 mice per group). *p<0.05, **p<0.01, One-way ANOVA.

5.2.4 Neutrophils contribute to proliferation of type II alveolar epithelial cells during recovery from *Legionella* infection

We therefore hypothesized that the delayed recovery of blood oxygen saturation in neutrophil-depleted mice was a result of reduced epithelial area across which oxygen exchange can take place due to alveoli disruption. Immune responses mounted to eradicate pathogens from the airways are associated with structural damage to the alveolar epithelium, and thus the air-blood barrier. Type II AEC serve as progenitors in the alveolar niche, proliferating and differentiating into type I AEC to regenerate respiratory epithelium (Barkauskas *et al.*, 2013; Desai *et al.*, 2014).

To investigate whether AM or neutrophils promoted type II AEC proliferation, we depleted these cells on day 5 after infection with *L. longbeachae* (Figure 5.6A) and quantified type II AEC proliferation by flow cytometry using Ki67 (Gerdes *et al.*, 1983; Major *et al.*, 2020) (Figure 5.6B/C). In uninfected control mice, only about 4 % of type II AEC were undergoing proliferation (Figure 5.6C/D), which is consistent with the low frequency of proliferating type II AEC in homeostasis (Barkauskas *et al.*, 2013; Major *et al.*, 2020). Infection with *L. longbeachae* clearly induced proliferation of these cells during the resolution phase of infection, with approximately 20 % of type II AEC staining positive for Ki67 on day 6 after infection (Figure 5.6C/D), indicating regeneration of alveolar epithelium. The rate of proliferation remained unchanged in mice treated with clodronate liposomes (Figure 5.6C/D), which had only caused a minor trend towards AM depletion (Figure 5.2C). However, in comparison to undepleted mice, the proportion of proliferating type II AEC was significantly diminished in neutrophil-depleted mice to about 13.5 % (Figure 5.6C/D), indicating that neutrophils promote proliferation of type II AEC during the recovery phase from *L. longbeachae* infection, a necessary step to regenerate alveolar epithelium during resolution of pneumonia.

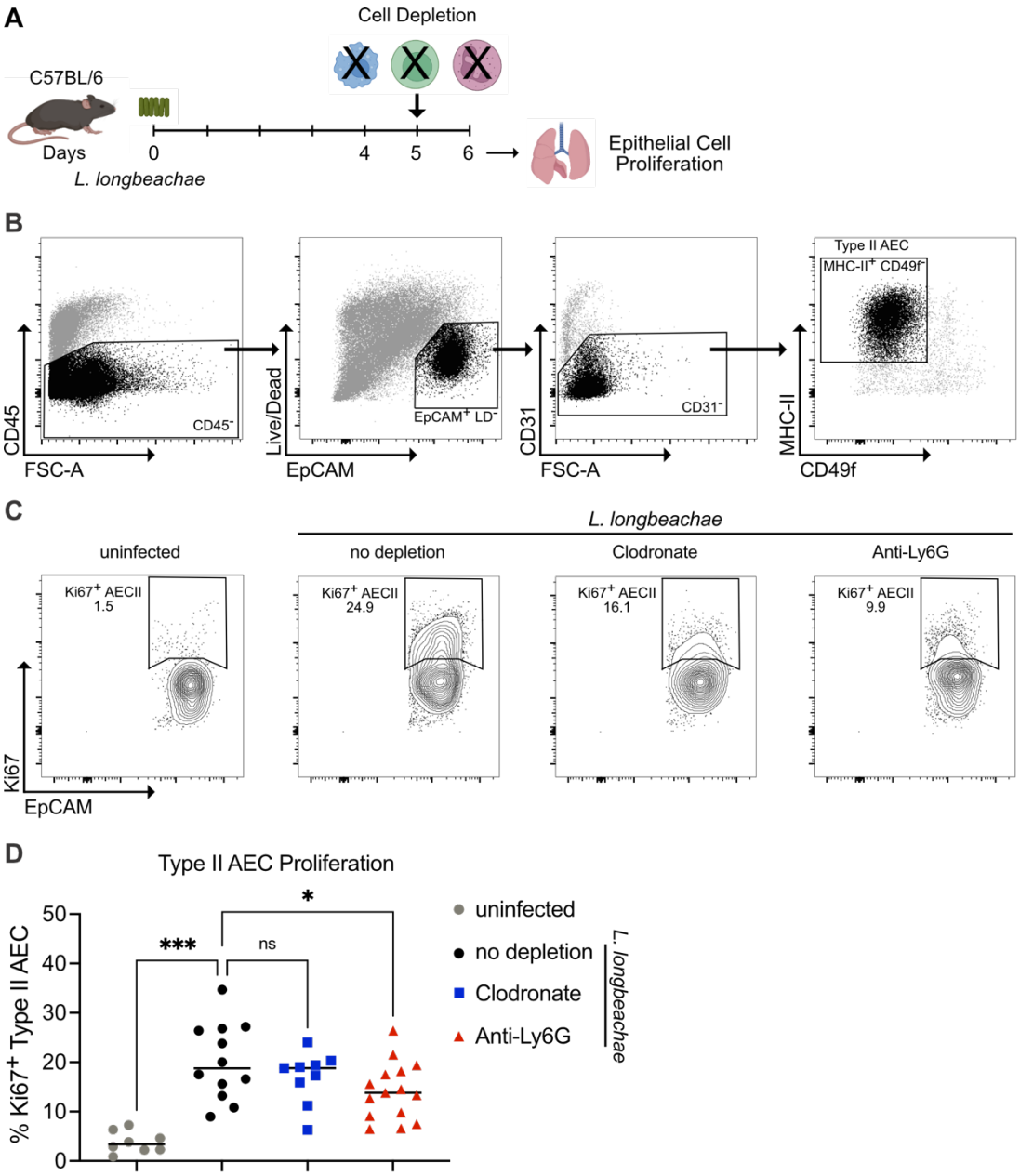

Figure 5.6: Reduced alveolar epithelial cell proliferation in neutrophil-depleted mice during recovery from *Legionella* infection.
(A) Summary of experimental details. Mice were infected with 2.5x10^4 CFU *L. longbeachae*-mCherry. Neutrophils or AM were depleted on day 5 after infection and lungs were enzymatically digested for flow cytometry analysis on day 6 after infection. **(B)** Gating strategy to identify type II alveolar epithelial cells (AEC) by flow cytometry (gated as single live CD45$^-$EpCAM$^+$CD31$^-$CD49f$^-$MHCII$^+$ cells). **(C)** Representative flow cytometry plots of intracellular Ki67 staining in type II AEC from indicated groups of mice. **(D)** Quantitation of proliferating, Ki67$^+$ type II AEC from indicated groups of mice. Graph shows median, with each dot representing an individual mouse. Data is pooled from two (clodronate) or three (uninfected, no depletion, anti-Ly6G) independent experiments (n ≥ 8 mice per group). *p<0.05, ***p<0.001, One-way ANOVA.

5.2.5 Neutrophils promote production of proliferation-enhancing growth factors and cytokines during recovery from *Legionella* infection

Since neutrophils promoted type II AEC proliferation required for epithelial regeneration during recovery from *L. longbeachae* infection, we next investigated whether neutrophils contributed to the production of cytokines or growth factors that are implicated with tissue repair or type II AEC proliferation.

For this, we pooled lung homogenates from undepleted mice and mice depleted of neutrophils in the recovery phase from *L. longbeachae* infection for a membrane-based cytokine screen. We identified several molecules that were up- or down-regulated by more than 15 % in lung homogenates of neutrophil-depleted mice compared to undepleted samples. Of note, the levels of the majority of screened cytokines or growth factors (71 out of 114 analytes) remained unchanged despite neutrophil depletion (data not shown).

Neutrophil depletion in the recovery phase from infection correlated with increased presence of several cytokines such as IL-2 and IL-5, and higher levels of G-CSF. Interestingly, molecules involved in angiogenesis, for example Endoglin and Angiopoietin-1, appeared to be upregulated in absence of neutrophils during the recovery phase as well (Figure 5.7A).

As expected, the levels of several molecules almost exclusively produced by neutrophils, for example MMP-9, were found to be strongly downregulated after neutrophil depletion (Figure 5.7B). Furthermore, we detected reduced pulmonary presence of neutrophil-associated cytokines like IL-1α or IL-17A, lower levels of several chemokines of the CXCL or CCL families, as well as downregulation of growth factors like HGF or FGF1 (Figure 5.7B). Interestingly, absence of neutrophils also appeared to be associated with lower pulmonary presence of amphiregulin (AREG) and IL-22 (Figure 5.7B), both of which are directly implicated with type II AEC epithelial proliferation and tissue repair (Kumar *et al.*, 2013; Zaiss *et al.*, 2015).

We validated the data obtained from the membrane-based screen for selected analytes, using a more sensitive and quantitative cytokine assay. We found that

pulmonary levels of VEGFα (Figure 5.7C) or GM-CSF (Figure 5.7D) were unchanged in neutrophil-depleted mice, consistent with the results from the membrane-based screen (data not shown). A slight downregulation of IL-10 (Figure 5.7E) and IL-22 (Figure 5.7F), which was observed in lung homogenates of neutrophil-depleted mice in the cytokine screen, could not be confirmed in the quantitative cytokine assay. However, we detected additional changes by identifying reduced IL-1β (Figure 5.7G) and TNFα (Figure 5.7H) concentrations following neutrophil depletion, both of which are associated with epithelial repair in the lung (Katsura *et al.*, 2019).

These results suggest that neutrophils promote the production of several growth factors and cytokines which are associated with type II AEC proliferation. Whether neutrophils themselves directly secrete these molecules in recovering lungs, or whether neutrophils induced the production of these molecules by other immune cells or epithelial cells in our model, requires further investigation.

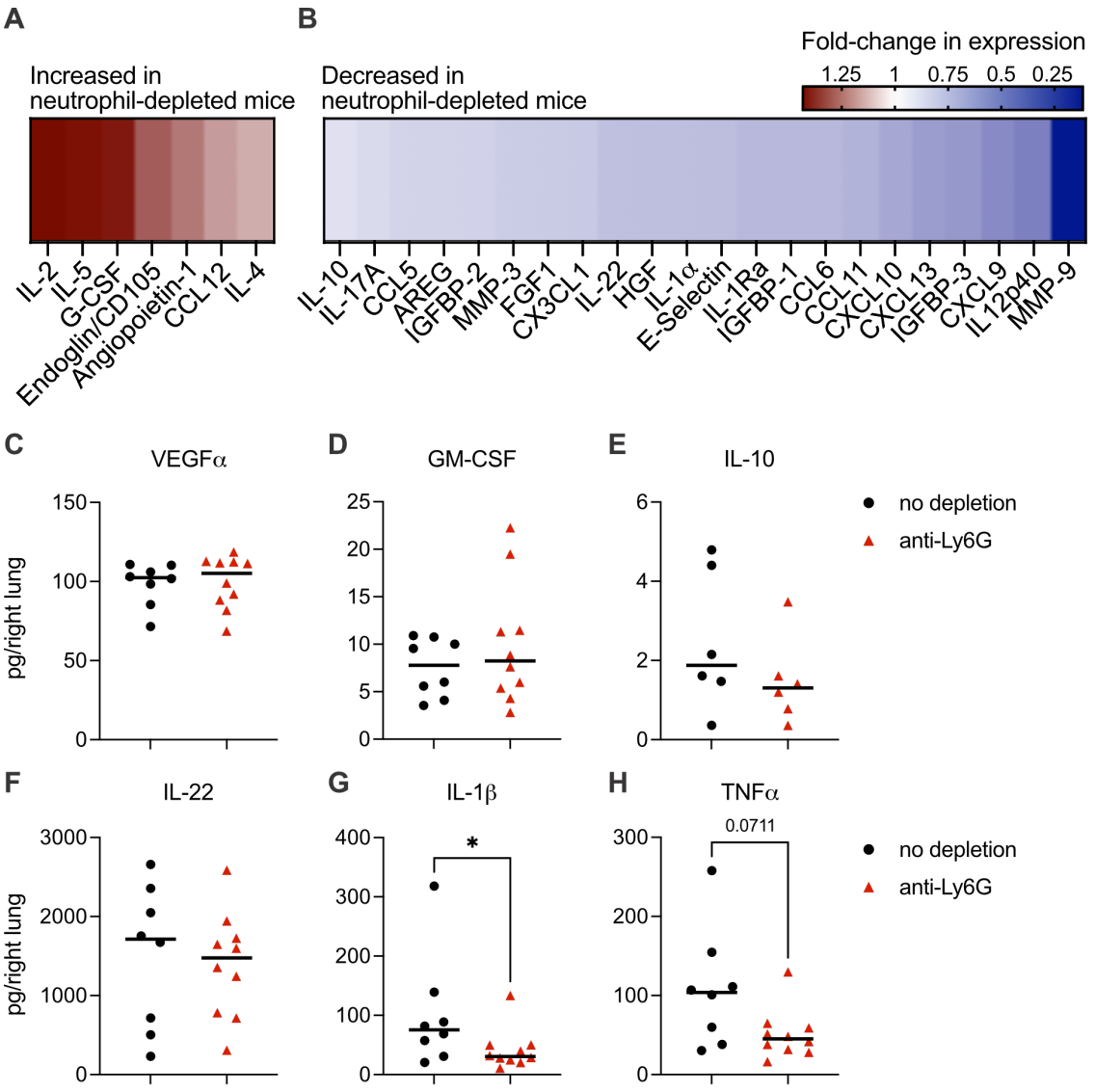

Figure 5.7: Lower production of IL-1β and TNFα in neutrophil-depleted mice recovering from *L. longbeachae* infection.
Mice were infected with 2.5x10^4 CFU *L. longbeachae*-mCherry. Neutrophils were depleted on day 5 after infection and lungs were homogenized on day 6 after infection. **(A/B)** Lung homogenates from 5 undepleted or 5 neutrophil-depleted mice were pooled and screened using a ProteomeProfiler™ Mouse Cytokine Array as described in the methods section. Heatmaps show relative expression of upregulated (A) or downregulated (B) molecules in neutrophil-depleted mice relative to undepleted mice. **(C-H)** Quantitation of indicated cytokines in lung homogenates of undepleted or neutrophil-depleted mice by ProcartaPlex™ Mouse Mix & Match Array. Graphs show medians, with each dot representing an individual mouse. Data is pooled from two independent experiments (n ≥ 8 mice per group). *p<0.05, Mann-Whitney-U test.

5.3 Discussion

Neutrophils are essential in the pulmonary innate immune response against bacterial infections such as *Legionella* (LeibundGut-Landmann *et al.*, 2011). However, their transmigration from the pulmonary vasculature into the airways and their subsequent bactericidal activities are associated with epithelial damage that can impair oxygen exchange across a compromised air-blood barrier (Zemans *et al.*, 2009; Bhattacharya and Matthay, 2013). Thus, neutrophils are generally considered to be harmful to their microenvironment, and unchecked pro-inflammatory neutrophil activity has been shown to play a central role in the pathology of acute and chronic lung diseases such as ARDS (Grommes and Soehnlein, 2011), influenza (Brandes *et al.*, 2013), and COPD (Hoenderdos and Condliffe, 2013).

In contrast to this, the work in this chapter provides evidence that neutrophils, aside from bacterial clearance, promote functional lung recovery during the resolution phase of bacterial pneumonia. Neutrophils induced the production of cytokines and growth factors that are known to enhance type II AEC proliferation, a process required to repair damaged respiratory epithelium to improve gas exchange and increase $\%SpO_2$ levels. This is consistent with some published reports showing that neutrophils are important for tissue repair and regeneration following infection or acute lung injury (Zemans *et al.*, 2011; Neudecker *et al.*, 2017; Blázquez-Prieto, López-Alonso, Huidobro, *et al.*, 2018).

MMP-9 has previously been shown to facilitate matrix processing and epithelial repair in a mouse model of ventilator-induced lung injury (Blázquez-Prieto, López-Alonso, Amado-Rodríguez, *et al.*, 2018). In our model, MMP-9 was the most strongly down-regulated molecule in neutrophil-depleted mice, suggesting that it may have contributed to delayed functional lung recovery after *Legionella* infection as well. Similarly, proteomic analyses linked neutrophil-associated MMP-9, together with FGF1, with enhanced type II AEC proliferation in a model of acid-induced acute lung injury (Paris *et al.*, 2016). FGF1 is a known inducer of epithelial cell proliferation (Louzier *et al.*, 2004; Shimbori *et al.*, 2016), and, thus, the reduced FGF1 expression observed in our model during the recovery phase

of *Legionella* infection may also have contributed to the impaired type II AEC proliferation in absence of neutrophils. Another molecule strongly linked with tissue repair that was down-regulated in neutrophil-depleted mice was amphiregulin, a ligand of the epidermal growth factor receptor (Berasain and Avila, 2014; Zaiss *et al.*, 2015). In the lung, group II ILC-derived amphiregulin proved critical in tissue repair and remodelling, as well as blood oxygenation after Influenza infection (Monticelli *et al.*, 2011). In a model of naphthalene-induced lung injury, amphiregulin production by pulmonary macrophages promoted epithelial cell proliferation after an epithelium-macrophage crosstalk as well (Lucas *et al.*, 2022). While neutrophils themselves have not yet been identified as direct source of amphiregulin, they express amphiregulin at mRNA level (Tecchio *et al.*, 2014), which we also observed by mRNA sequencing of neutrophils infected with *L. longbeachae* for five days (Oberkircher *et al.*, manuscript in preparation). If not directly produced by neutrophils, their absence could still impair amphiregulin production by bystander immune or epithelial cells, as suggested in a model of colitis (Chen *et al.*, 2018).

Additionally, we found TNFα and IL-1β levels to be reduced in the absence of neutrophils during recovery from *Legionella* infection, suggesting that they may play a beneficial role to induce epithelial proliferation. Even though these cytokines are predominantly associated with pro-inflammatory processes that contribute to lung disease (Mukhopadhyay *et al.*, 2006; Borthwick, 2016), TNFα and IL-1β, and IL-1/NF-κB signalling in general, were recently found to promote proliferation of type II AEC *in vitro* and *in vivo* after Influenza infection, similar to our results (Katsura *et al.*, 2019). It is therefore possible, that the mechanistic role of TNFα and IL-1 signalling during lung recovery depends on the type of induced damage, as well as on the timing and location of cytokine release. IL-1 and IL-1R signalling during *Legionella* infection have mainly been investigated at the onset of infection (Barry *et al.*, 2013b). But since neutrophils are a known source of TNFα in later stages of infection (Ziltener *et al.*, 2016), a lack of neutrophil-derived TNFα is one possible explanation by which neutrophil depletion may limit type II AEC proliferation during lung recovery from Legionnaires' Disease.

Our results also revealed that neutrophil depletion during the recovery phase from *L. longbeachae* infection did not change the levels of several other molecules associated with epithelial proliferation. These include IL-22, which has been found to be crucial in lung repair after influenza infection (Kumar *et al.*, 2013), IL-33, which is released after epithelial damage to induce anti-inflammatory and tissue repair processes (Monticelli *et al.*, 2011; Monticelli *et al.*, 2015), or VEGFα, a known contributor of alveolar development and recovery (Brown *et al.*, 2001; Dao *et al.*, 2018). Nevertheless, neutrophils promoted the production of several other cytokines and growth factors in the recovery phase from *L. longbeachae* infection, and their potential roles in lung recovery have yet to be elucidated. Whether the molecules discussed above can be mechanistically linked to the reduced type II AEC proliferation and delayed recovery of blood oxygenation observed in neutrophil-depleted mice, requires further investigation as well.

Notably, we did not observe a similar effect after depletion of T cells, even though T_{reg} cells, a sub-population of $CD4^+$ T cells, possess important anti-inflammatory properties and have been shown to contribute to tissue repair in the lung after infection or acute injury (D'Alessio *et al.*, 2009; Arpaia *et al.*, 2015). However, T cells only play a minor role during *Legionella* infection, and its eradication mostly depends on an efficient innate immune response mediated by myeloid cells. Therefore, the relatively minor increase in $CD4^+$ T cells induced after infection with *L. longbeachae* may not contain a large enough number of T_{reg} cells to notably affect growth factor secretion and type II AEC proliferation. Similarly, mice depleted in $CD8^+$ T cells during recovery from *Legionella* infection still efficiently re-established baseline levels of blood oxygen saturation.

Pulmonary macrophages are a heterogenous cell population, comprising AM, interstitial macrophages, and monocyte-derived cells (Hou *et al.*, 2021). These sub-populations contribute differently to pulmonary injury or repair after infection or tissue damage, depending on their distinct inflammatory profiles (Wynn and Vannella, 2016; Kulikauskaite and Wack, 2020). Clodronate-based macrophage depletion during the recovery phase of *L. longbeachae* infection resulted in reduced blood oxygen saturation compared to untreated mice. However, the

cause for this phenotype could not be clearly identified because depletion was inefficient and, in fact, not statistically significant. The partial AM depletion was not associated with reduced epithelial cell proliferation as observed in neutrophil-depleted mice. Therefore, further experiments are required to dissect whether macrophages affect type II AEC proliferation in the resolution phase of bacterial pneumonia, and how specific macrophage subsets contribute to lung recovery.

In summary, the work in this chapter provides novel insights into the regenerative role of neutrophils during the resolution of bacterial pneumonia. Our results suggest that these cells are required for the efficient recovery of blood oxygen levels and promote type II AEC proliferation, which is likely to contribute to the important re-establishment of functional alveolar epithelium.

6 General discussion

Legionnaires' Disease remains a global health burden, and its incidence has been continuously rising over the past decades despite the implementation of surveillance and prevention measures (Beauté, 2017; Chambers *et al.*, 2021). As with many other pulmonary infections, susceptibility to Legionnaires' Disease is strongly linked with cigarette smoking (Straus *et al.*, 1996; Den Boer *et al.*, 2006; Che *et al.*, 2008), which significantly impacts the immune response directed against lung pathogens (Stämpfli and Anderson, 2009; Strzelak *et al.*, 2018). Cigarette smoking is estimated to cause more than 8 million deaths per year, mediating countless adverse health effects and contributing to a large range of diseases such as COPD, lung cancer, asthma, and pneumonia (Murray *et al.*, 2020; Reitsma *et al.*, 2021).

Maintaining AM function and viability is of particular importance in the context of pulmonary infections, since AM are the main phagocyte within the airways, where they engulf invading pathogens and initiate immune responses (Guilliams *et al.*, 2013; Hussell and Bell, 2014). The first part of this work investigated the fundamental ways by which cigarette smoke affects immune cells in the lung. These studies showed that acute cigarette smoke actually depletes AM in a manner dependent on pyroptosis, an inflammatory type of cell death. Pyroptosis is a common outcome of the activation of inflammasomes and results in the release of the pro-inflammatory mediators IL-1β and IL-18 (Schroder and Tschopp, 2010), which are known to contribute to chronic lung disease (Botelho *et al.*, 2011; Dima *et al.*, 2015). Consequently, reducing IL-1β and IL-18 concentrations in the lung, for example by using specific blocking antibodies, is currently being investigated as a therapeutical avenue in patients with COPD (Mistry *et al.*, 2014; Rogliani *et al.*, 2015; Dima *et al.*, 2015). Additionally, strategies to prevent inflammasome activation in the first place are currently explored. MCC950 is a selective small-molecule inhibitor of the NLRP3 inflammasome and reduces the production of IL-1β (Coll *et al.*, 2015). It has been successfully used as treatment in mouse models of inflammatory diseases such as experimental autoimmune encephalomyelitis (Coll *et al.*, 2015), colitis (Perera

et al., 2018), or atherosclerosis (van der Heijden *et al.*, 2017). Similarly, MCC950-mediated inflammasome blockade ameliorated pulmonary inflammation and leukocyte recruitment in mice after LPS delivery (Wang *et al.*, 2021) or in the late stages of influenza infection (Tate *et al.*, 2016). Cigarette smoking causes significant oxidative stress in exposed cells which can activate, amongst others, the NLRP3 inflammasome and subsequently cause pro-inflammatory cell death (Kirkham and Barnes, 2013; Zuo *et al.*, 2014; Swanson *et al.*, 2019). An important target for pharmacological interventions aiming to reduce oxidative stress in cells is the master regulator of cellular oxidative stress responses, Nrf2 (Vomund *et al.*, 2017, p.2). Therapeutic targeting of Nrf2 has been shown to balance the oxidant-to-antioxidant ratio in smoke-exposed cells and has been able limit smoke-induced epithelial cell death *in vivo* (Rangasamy *et al.*, 2004; Sussan *et al.*, 2009, p.2; Rahman and Kinnula, 2012; Vomund *et al.*, 2017; Dianat *et al.*, 2018). Whether such treatments could reverse the observed smoke-induced cell death of AM in our model and reverse the increased susceptibility to infection remains to be investigated and could be a topic for future studies.

Cigarette smoking exacerbates numerous bacterial or viral infections including Legionnaires' Disease, but many of the underlying mechanisms remain unknown (Arcavi and Benowitz, 2004; Bauer *et al.*, 2013). However, it could be easily imagined that the AM depletion we observed in our model would favour extracellular accumulation of common bacterial pathogens such as *S. pneumoniae* or *P. aeruginosa*, which could replicate to higher numbers and cause more severe disease. In contrast to pathogens able to survive extracellularly in the lung environment, *Legionella*, which are the causative agents of Legionnaires' Disease, depend on the establishment of an intracellular replicative niche within AM (Newton *et al.*, 2010). Nevertheless, we found that AM may have a so far underappreciated role in the clearance of *L. pneumophila*. During *L. pneumophila* infection, AM are normally transiently depleted in the lung by cellular sensing of bacterial flagellin by the NAIP5/NLRC4 inflammasome and subsequent caspase-1-dependent pyroptosis (Zamboni *et al.*, 2006; Molofsky *et al.*, 2006), or by flagellin-independent activation of caspase-11 and NLRP3-inflammasome-dependent pyroptosis (Case *et al.*, 2013; Casson *et al.*, 2013).

Restoration of AM in the later stages of infection correlates with bacterial clearance (Brown *et al.*, 2016). AM are repopulated either by self-proliferation, or by circulating monocytes that can infiltrate the accessible alveolar niche and rapidly adopt a pro-inflammatory AM phenotype (Hashimoto *et al.*, 2013; van de Laar *et al.*, 2016; Aegerter *et al.*, 2020). Due to their origin, monocyte-derived AM retain a different transcriptomic profile compared to resident AM (Aegerter *et al.*, 2020), enabling them to mount efficient immune responses and potentially conveying resistance against intracellular bacterial replication (Brown *et al.*, 2016). Under normal circumstances, the accumulation of such pro-inflammatory monocyte-derived AM may be an important contributor to *L. pneumophila* clearance. In fact, direct bactericidal activity by AM in later stages of infection has been reported previously, even though the AM population was not further specified (Ziltener *et al.*, 2016). However, during cigarette smoke exposure, AM remained strongly depleted throughout the entire experiment. It is conceivable that cigarette smoke induces cell death in infiltrating and differentiating monocyte-derived AM as well, and thus abrogates their beneficial effects during *L. pneumophila* clearance. AM may also promote bactericidal activity of immune cells that are recruited to the airways, such as neutrophils, which heavily infiltrated the lungs after cigarette smoke exposure. However, we did not observe specific defects in the antimicrobial capacity of neutrophils due to cigarette smoke treatment as previously suggested by others (Pabst *et al.*, 1995; Dunn *et al.*, 2005; Xu *et al.*, 2008). Future experiments are required to define the mechanisms by which AM contribute to clearance of *L. pneumophila*, and if depletion of these cells by cigarette smoke is a common mechanism of susceptibility to infection.

The second focus of this study was the role of immune cells during the recovery from Legionnaires' Disease. Immune resistance mechanisms directed against pathogens that invade the lung are associated with tissue-damaging side effects that compromise proper lung function (Matthay and Zimmerman, 2005). Re-establishment of lung structure and function, particularly efficient oxygen uptake from the inhaled air, are crucial processes to prevent lung pathology, and lessons

from the ongoing COVID-19 pandemic clearly reiterated how excessive and unchecked pulmonary inflammation can lead to increased morbidity and mortality (Merad and Martin, 2020).

Neutrophils and monocytes are two major innate immune cell populations that are recruited to the airways in response to infection, and contribute to bacterial clearance by employing a range of antimicrobial effector mechanisms that can be harmful to the surrounding environment (Brown *et al.*, 2017; McKenna *et al.*, 2021). In the context of pulmonary infections, this dual role of neutrophils remains a major issue that limits effectiveness of neutrophil-targeted therapies, since cell depletion or suppression of effector functions closely correlates with increased pathogen burden. However, emerging evidence suggests that neutrophils display distinct tissue-regenerative features that may potentially be harnessed in the future (Zemans *et al.*, 2009; Neudecker *et al.*, 2017). The work in this study expands this knowledge by showing that neutrophils promote type II AEC proliferation and re-establishment of blood oxygenation in the recovery phase from *Legionella* infection.

Specific depletion of neutrophils in the recovery phase of infection caused the reduced production of a several growth factors and cytokines that are implicated with tissue repair and epithelial cell proliferation, including MMP-9 (Blázquez-Prieto, López-Alonso, Amado-Rodríguez, *et al.*, 2018), amphiregulin (Monticelli *et al.*, 2011), IL-1β, or TNFα (Katsura *et al.*, 2019). Whether all of these molecules were directly produced by neutrophils remains to be further investigated. Neutrophils are a known source of MMP9 (McKenna *et al.*, 2021) and a likely source of TNFα during *L. longbeachae* infection (Massis *et al.*, 2017), but have so far never been shown to secrete amphiregulin (Tecchio *et al.*, 2014). Secretion of other growth factors and cytokines in the lung during recovery from infection may have been indirectly induced by neutrophils, for example after efferocytosis, a process by which AM remove immune effector cells such as neutrophils from the lung and that initiates the release of several anti-inflammatory cytokines (Allard *et al.*, 2018).

It is feasible that the lower cytokine and growth factor levels in absence of neutrophils negatively affected the proliferation rate of type II AEC, an

observation made in our model by staining for the proliferation marker Ki67. Since type II AEC serve as progenitors in the alveoli and differentiate into type I AEC upon epithelial injury (Barkauskas *et al.*, 2013; Desai *et al.*, 2014), a reduced area of functional alveolar epithelium may have caused the lower blood oxygenation levels found in neutrophil-depleted mice compared to undepleted mice.
Whether causative links between these processes exist, and how neutrophils may mechanistically promote epithelial proliferation and functional lung recovery in our model requires further investigation. Nevertheless, these results add to the growing body of studies that provide new insights into the tissue-regenerative mechanisms of neutrophils aiding in the recovery of lung function after pulmonary infection.

In summary, the work in this thesis showed that acute cigarette smoke depleted AM *in vivo* with the contribution of NLRP3-dependent pyroptosis, and that smoke-induced cell death was associated with more severe disease and delayed bacterial clearance in a mouse model of Legionnaires' Disease. Additionally, neutrophils were shown to play an important role not only in bacterial clearance but also in the functional lung recovery from Legionnaires' Disease.

References

Aegerter, H. *et al.* (2020) 'Influenza-Induced Monocyte-Derived Alveolar Macrophages Confer Prolonged Antibacterial Protection'. *Nature Immunology*, 21(2), pp. 145–157. DOI: 10.1038/s41590-019-0568-x.

Alcón, A., Fàbregas, N. and Torres, A. (2005) 'Pathophysiology of Pneumonia'. *Clinics in Chest Medicine*, 26(1), pp. 39–46. DOI: 10.1016/j.ccm.2004.10.013.

Allard, B., Panariti, A. and Martin, J.G. (2018) 'Alveolar Macrophages in the Resolution of Inflammation, Tissue Repair, and Tolerance to Infection'. *Frontiers in Immunology*, 9, p. 1777. DOI: 10.3389/fimmu.2018.01777.

Alli, O.A.T. *et al.* (2000) 'Temporal Pore Formation-Mediated Egress from Macrophages and Alveolar Epithelial Cells by Legionella Pneumophila'. *Infection and Immunity*, 68(11), pp. 6431–6440. DOI: 10.1128/IAI.68.11.6431-6440.2000.

Amich, J. *et al.* (2020) 'Three-Dimensional Light Sheet Fluorescence Microscopy of Lungs To Dissect Local Host Immune- *Aspergillus Fumigatus* Interactions' Goldman, G.H. (ed.). *MBio*, 11(1), pp. e02752-19, /mbio/11/1/mBio.02752-19.atom. DOI: 10.1128/mBio.02752-19.

Amodeo, M.R., Murdoch, D.R. and Pithie, A.D. (2010) 'Legionnaires' Disease Caused by Legionella Longbeachae and Legionella Pneumophila: Comparison of Clinical Features, Host-Related Risk Factors, and Outcomes'. *Clinical Microbiology and Infection*, 16(9), pp. 1405–1407. DOI: 10.1111/j.1469-0691.2009.03125.x.

Anderson, B.M. *et al.* (2019) 'Application of a Chemical Probe to Detect Neutrophil Elastase Activation during Inflammatory Bowel Disease'. *Scientific Reports*, 9(1), p. 13295. DOI: 10.1038/s41598-019-49840-4.

Anderson, K.L. *et al.* (1998) 'Neutrophils Deficient in PU.1 Do Not Terminally Differentiate or Become Functionally Competent'. *Blood*, 92(5), pp. 1576–1585.

Andrews, H.L., Vogel, J.P. and Isberg, R.R. (1998) 'Identification of Linked Legionella Pneumophila Genes Essential for Intracellular Growth and Evasion of the Endocytic Pathway'. *Infection and Immunity*, 66(3), pp. 950–958.

Ang, D.K.Y. *et al.* (2010) 'Cutting Edge: Pulmonary Legionella Pneumophila Is Controlled by Plasmacytoid Dendritic Cells but Not Type I IFN'. *Journal of Immunology (Baltimore, Md.: 1950)*, 184(10), pp. 5429–5433. DOI: 10.4049/jimmunol.1000128.

Aoshiba, K., Tamaoki, J. and Nagai, A. (2001) 'Acute Cigarette Smoke Exposure Induces Apoptosis of Alveolar Macrophages'. *American Journal of Physiology-Lung Cellular and Molecular Physiology*, 281(6), pp. L1392–L1401. DOI: 10.1152/ajplung.2001.281.6.L1392.

Arango Duque, G. and Descoteaux, A. (2014) 'Macrophage Cytokines: Involvement in Immunity and Infectious Diseases'. *Frontiers in Immunology*, 5. DOI: 10.3389/fimmu.2014.00491.

Arcavi, L. and Benowitz, N.L. (2004) 'Cigarette Smoking and Infection'. *Archives of Internal Medicine*, 164(20), pp. 2206–2216. DOI: 10.1001/archinte.164.20.2206.

Archer, K.A. *et al.* (2010) 'Cooperation between Multiple Microbial Pattern Recognition Systems Is Important for Host Protection against the Intracellular Pathogen Legionella Pneumophila'. *Infection and Immunity*, 78(6), pp. 2477–2487. DOI: 10.1128/IAI.00243-10.

Archer, K.A. *et al.* (2009) 'Multiple MyD88-Dependent Responses Contribute to Pulmonary Clearance of Legionella Pneumophila'. *Cellular Microbiology*, 11(1), pp. 21–36. DOI: 10.1111/j.1462-5822.2008.01234.x.

Archer, K.A. and Roy, C.R. (2006) 'MyD88-Dependent Responses Involving Toll-like Receptor 2 Are Important for Protection and Clearance of Legionella Pneumophila in a Mouse Model of Legionnaires' Disease'. *Infection and Immunity*, 74(6), pp. 3325–3333. DOI: 10.1128/IAI.02049-05.

Arpaia, N. *et al.* (2015) 'A Distinct Function of Regulatory T Cells in Tissue Protection'. *Cell*, 162(5), pp. 1078–1089. DOI: 10.1016/j.cell.2015.08.021.

Arredouani, M. *et al.* (2004) 'The Scavenger Receptor MARCO Is Required for Lung Defense against Pneumococcal Pneumonia and Inhaled Particles'. *Journal of Experimental Medicine*, 200(2), pp. 267–272. DOI: 10.1084/jem.20040731.

Asare, R. *et al.* (2007) 'Genetic Susceptibility and Caspase Activation in Mouse and Human Macrophages Are Distinct for Legionella Longbeachae and L. Pneumophila'. *Infection and Immunity*, 75(4), pp. 1933–1945. DOI: 10.1128/IAI.00025-07.

Asare, R. and Abu Kwaik, Y. (2007) 'Early Trafficking and Intracellular Replication of Legionella Longbeachaea within an ER-Derived Late Endosome-like Phagosome'. *Cellular Microbiology*, 9(6), pp. 1571–1587. DOI: 10.1111/j.1462-5822.2007.00894.x.

Asrat, S., Dugan, A.S. and Isberg, R.R. (2014) 'The Frustrated Host Response to Legionella Pneumophila Is Bypassed by MyD88-Dependent Translation of pro-Inflammatory Cytokines'. *PLoS Pathogens*, 10(7), p. e1004229. DOI: 10.1371/journal.ppat.1004229.

Audrain-McGovern, J. and Benowitz, N.L. (2011) 'Cigarette Smoking, Nicotine, and Body Weight'. *Clinical Pharmacology & Therapeutics*, 90(1), pp. 164–168. DOI: 10.1038/clpt.2011.105.

Bagaitkar, J., Demuth, D.R. and Scott, D.A. (2008) 'Tobacco Use Increases Susceptibility to Bacterial Infection'. *Tobacco Induced Diseases*, 4(1), p. 12. DOI: 10.1186/1617-9625-4-12.

Bals, R. *et al.* (1998) 'The Peptide Antibiotic LL-37/HCAP-18 Is Expressed in Epithelia of the Human Lung Where It Has Broad Antimicrobial Activity at the Airway Surface'. *Proceedings of the National Academy of Sciences*, 95(16), pp. 9541–9546. DOI: 10.1073/pnas.95.16.9541.

Barbagelata, E. *et al.* (2020) 'Gender Differences in Community-Acquired Pneumonia'. *Minerva Medica*, 111(2). DOI: 10.23736/S0026-4806.20.06448-4.

Barkauskas, C.E. *et al.* (2013) 'Type 2 Alveolar Cells Are Stem Cells in Adult Lung'. *Journal of Clinical Investigation*, 123(7), pp. 3025–3036. DOI: 10.1172/JCI68782.

Barnes, P.J. (2016) 'Inflammatory Mechanisms in Patients with Chronic Obstructive Pulmonary Disease'. *Journal of Allergy and Clinical Immunology*, 138(1), pp. 16–27. DOI: 10.1016/j.jaci.2016.05.011.

Barnes, P.J. (2009) 'The Cytokine Network in Chronic Obstructive Pulmonary Disease'. *American Journal of Respiratory Cell and Molecular Biology*, 41(6), pp. 631–638. DOI: 10.1165/rcmb.2009-0220TR.

Barry, K.C. *et al.* (2013a) 'IL-1α Signaling Initiates the Inflammatory Response to Virulent Legionella Pneumophila in Vivo'. *Journal of Immunology (Baltimore, Md.: 1950)*, 190(12), pp. 6329–6339. DOI: 10.4049/jimmunol.1300100.

Barry, K.C. *et al.* (2013b) 'IL-1α Signaling Initiates the Inflammatory Response to Virulent *Legionella Pneumophila* In Vivo'. *The Journal of Immunology*, 190(12), pp. 6329–6339. DOI: 10.4049/jimmunol.1300100.

Barskey, A.E., Derado, G. and Edens, C. (2022) 'Rising Incidence of Legionnaires' Disease and Associated Epidemiologic Patterns, United States, 1992-2018'. *Emerging Infectious Diseases*, 28(3), pp. 527–538. DOI: 10.3201/eid2803.211435.

Bartram, U. and Speer, C.P. (2004) 'The Role of Transforming Growth Factor β in Lung Development and Disease'. *Chest*, 125(2), pp. 754–765. DOI: 10.1378/chest.125.2.754.

Bauer, C.M.T. *et al.* (2008) 'Cigarette Smoke Suppresses Type I Interferon-Mediated Antiviral Immunity in Lung Fibroblast and Epithelial Cells'. *Journal of Interferon & Cytokine Research*, 28(3), pp. 167–179. DOI: 10.1089/jir.2007.0054.

Bauer, C.M.T., Morissette, M.C. and Stämpfli, M.R. (2013) 'The Influence of Cigarette Smoking on Viral Infections'. *Chest*, 143(1), pp. 196–206. DOI: 10.1378/chest.12-0930.

Beauté, J. *et al.* (2020) 'Healthcare-Associated Legionnaires' Disease, Europe, 2008−2017'. *Emerging Infectious Diseases*, 26(10), pp. 2309–2318. DOI: 10.3201/eid2610.181889.

Beauté, J. (2017) 'Legionnaires' Disease in Europe, 2011 to 2015'. *Euro Surveillance: Bulletin Europeen Sur Les Maladies Transmissibles = European Communicable Disease Bulletin*, 22(27). DOI: 10.2807/1560-7917.ES.2017.22.27.30566.

Belambri, S.A. *et al.* (2018) 'NADPH Oxidase Activation in Neutrophils: Role of the Phosphorylation of Its Subunits'. *European Journal of Clinical Investigation*, 48, p. e12951. DOI: 10.1111/eci.12951.

Berasain, C. and Avila, M.A. (2014) 'Amphiregulin'. *Seminars in Cell & Developmental Biology*, 28, pp. 31–41. DOI: 10.1016/j.semcdb.2014.01.005.

Berenson, C.S. *et al.* (2006) 'Impaired Phagocytosis of Nontypeable *Haemophilus Influenzae* by Human Alveolar Macrophages in Chronic Obstructive Pulmonary Disease'. *The Journal of Infectious Diseases*, 194(10), pp. 1375–1384. DOI: 10.1086/508428.

Berenson, C.S. *et al.* (2013) 'Phagocytic Dysfunction of Human Alveolar Macrophages and Severity of Chronic Obstructive Pulmonary Disease'. *The Journal of Infectious Diseases*, 208(12), pp. 2036–2045. DOI: 10.1093/infdis/jit400.

Berger, K.H. and Isberg, R.R. (1993) 'Two Distinct Defects in Intracellular Growth Complemented by a Single Genetic Locus in Legionella Pneumophila'. *Molecular Microbiology*, 7(1), pp. 7–19.

Berrington, W.R. *et al.* (2013) 'Nucleotide-Binding Oligomerization Domain Containing-like Receptor Family, Caspase Recruitment Domain (CARD) Containing 4 (NLRC4) Regulates Intrapulmonary Replication of Aerosolized Legionella Pneumophila'. *BMC Infectious Diseases*, 13, p. 371. DOI: 10.1186/1471-2334-13-371.

Bhan, U. *et al.* (2008) 'Toll-Like Receptor 9 Regulates the Lung Macrophage Phenotype and Host Immunity in Murine Pneumonia Caused by Legionella Pneumophila'. *Infection and Immunity*, 76(7), pp. 2895–2904. DOI: 10.1128/IAI.01489-07.

Bharat, A. *et al.* (2016) 'Flow Cytometry Reveals Similarities Between Lung Macrophages in Humans and Mice'. *American Journal of Respiratory Cell and Molecular Biology*, 54(1), pp. 147–149. DOI: 10.1165/rcmb.2015-0147LE.

Bhattacharya, J. and Matthay, M.A. (2013) 'Regulation and Repair of the Alveolar-Capillary Barrier in Acute Lung Injury'. *Annual Review of Physiology*, 75, pp. 593–615. DOI: 10.1146/annurev-physiol-030212-183756.

Bhattacharya, J. and Westphalen, K. (2016) 'Macrophage-Epithelial Interactions in Pulmonary Alveoli'. *Seminars in Immunopathology*, 38(4), pp. 461–469. DOI: 10.1007/s00281-016-0569-x.

Blázquez-Prieto, J., López-Alonso, I., Amado-Rodríguez, L., *et al.* (2018) 'Impaired Lung Repair during Neutropenia Can Be Reverted by Matrix Metalloproteinase-9'. *Thorax*, 73(4), pp. 321–330. DOI: 10.1136/thoraxjnl-2017-210105.

Blázquez-Prieto, J., López-Alonso, I., Huidobro, C., *et al.* (2018) 'The Emerging Role of Neutrophils in Repair after Acute Lung Injury'. *American Journal of Respiratory Cell and Molecular Biology*, 59(3), pp. 289–294. DOI: 10.1165/rcmb.2018-0101PS.

Boamah, D.K. *et al.* (2017) 'From Many Hosts, One Accidental Pathogen: The Diverse Protozoan Hosts of Legionella'. *Frontiers in Cellular and Infection Microbiology*, 7, p. 477. DOI: 10.3389/fcimb.2017.00477.

de Boer, W.I. *et al.* (2000) 'Monocyte Chemoattractant Protein 1, Interleukin 8, and Chronic Airways Inflammation in COPD'. *The Journal of Pathology*, 190(5), pp. 619–626. DOI: 10.1002/(SICI)1096-9896(200004)190:5<619::AID-PATH555>3.0.CO;2-6.

Boivin, G. *et al.* (2020) 'Durable and Controlled Depletion of Neutrophils in Mice'. *Nature Communications*, 11(1), p. 2762. DOI: 10.1038/s41467-020-16596-9.

Borgerding, M. and Klus, H. (2005) 'Analysis of Complex Mixtures – Cigarette Smoke'. *Experimental and Toxicologic Pathology*, 57, pp. 43–73. DOI: 10.1016/j.etp.2005.05.010.

Borthwick, L.A. (2016) 'The IL-1 Cytokine Family and Its Role in Inflammation and Fibrosis in the Lung'. *Seminars in Immunopathology*, 38(4), pp. 517–534. DOI: 10.1007/s00281-016-0559-z.

Botelho, F.M. *et al.* (2011) 'IL-1α/IL-1R1 Expression in Chronic Obstructive Pulmonary Disease and Mechanistic Relevance to Smoke-Induced Neutrophilia in Mice' Chu, H.W. (ed.). *PLoS ONE*, 6(12), p. e28457. DOI: 10.1371/journal.pone.0028457.

Botelho, F.M. *et al.* (2010) 'Innate Immune Processes Are Sufficient for Driving Cigarette Smoke-Induced Inflammation in Mice'. *American Journal of Respiratory Cell and Molecular Biology*, 42(4), pp. 394–403. DOI: 10.1165/rcmb.2008-0301OC.

Boxio, R. *et al.* (2016) 'Neutrophil Elastase Cleaves Epithelial Cadherin in Acutely Injured Lung Epithelium'. *Respiratory Research*, 17(1), p. 129. DOI: 10.1186/s12931-016-0449-x.

Bozinovski, S. *et al.* (2015) 'Innate Cellular Sources of Interleukin-17A Regulate Macrophage Accumulation in Cigarette- Smoke-Induced Lung Inflammation in Mice'. *Clinical Science (London, England: 1979)*, 129(9), pp. 785–796. DOI: 10.1042/CS20140703.

Bracke, K.R. *et al.* (2006) 'Cigarette Smoke-Induced Pulmonary Inflammation and Emphysema Are Attenuated in CCR6-Deficient Mice'. *The Journal of Immunology*, 177(7), pp. 4350–4359. DOI: 10.4049/jimmunol.177.7.4350.

Brandes, M. *et al.* (2013) 'A Systems Analysis Identifies a Feedforward Inflammatory Circuit Leading to Lethal Influenza Infection'. *Cell*, 154(1), pp. 197–212. DOI: 10.1016/j.cell.2013.06.013.

Brenner, D., Blaser, H. and Mak, T.W. (2015) 'Regulation of Tumour Necrosis Factor Signalling: Live or Let Die'. *Nature Reviews Immunology*, 15(6), pp. 362–374. DOI: 10.1038/nri3834.

Brieland, J.K. *et al.* (2000) 'Immunomodulatory Role of Endogenous Interleukin-18 in Gamma Interferon-Mediated Resolution of Replicative Legionella Pneumophila Lung Infection'. *Infection and Immunity*, 68(12), pp. 6567–6573.

Brieland, J.K. *et al.* (1998) 'In Vivo Regulation of Replicative Legionella Pneumophila Lung Infection by Endogenous Interleukin-12'. *Infection and Immunity*, 66(1), pp. 65–69.

Brinkmann, V. *et al.* (2004) 'Neutrophil Extracellular Traps Kill Bacteria'. *Science*, 303(5663), pp. 1532–1535. DOI: 10.1126/science.1092385.

Broermann, A. *et al.* (2011) 'Dissociation of VE-PTP from VE-Cadherin Is Required for Leukocyte Extravasation and for VEGF-Induced Vascular Permeability in Vivo'. *The Journal of Experimental Medicine*, 208(12), pp. 2393–2401. DOI: 10.1084/jem.20110525.

Brown, A.S. *et al.* (2016) 'Cooperation between Monocyte-Derived Cells and Lymphoid Cells in the Acute Response to a Bacterial Lung Pathogen'. *PLoS Pathogens*, 12(6), p. e1005691. DOI: 10.1371/journal.ppat.1005691.

Brown, A.S. *et al.* (2017) 'The Regulation of Acute Immune Responses to the Bacterial Lung Pathogen *Legionella Pneumophila*'. *Journal of Leukocyte Biology*, 101(4), pp. 875–886. DOI: 10.1189/jlb.4MR0816-340R.

Brown, K.R. *et al.* (2001) 'VEGF Induces Airway Epithelial Cell Proliferation in Human Fetal Lung in Vitro'. *American Journal of Physiology. Lung Cellular and Molecular Physiology*, 281(4), pp. L1001-1010. DOI: 10.1152/ajplung.2001.281.4.L1001.

Broz, P. and Dixit, V.M. (2016) 'Inflammasomes: Mechanism of Assembly, Regulation and Signalling'. *Nature Reviews Immunology*, 16(7), pp. 407–420. DOI: 10.1038/nri.2016.58.

Bruggemann, H. *et al.* (2006) 'Virulence Strategies for Infecting Phagocytes Deduced from the in Vivo Transcriptional Program of Legionella Pneumophila'. *Cellular Microbiology*, 8(8), pp. 1228–1240. DOI: 10.1111/j.1462-5822.2006.00703.x.

Bruin, J.P. *et al.* (2014) 'Isolation of Ciprofloxacin-Resistant Legionella Pneumophila in a Patient with Severe Pneumonia'. *The Journal of Antimicrobial Chemotherapy*, 69(10), pp. 2869–2871. DOI: 10.1093/jac/dku196.

Busch, C.J.-L. *et al.* (2019) 'Isolation and Long-Term Cultivation of Mouse Alveolar Macrophages'. *Bio-Protocol*, 9(14). DOI: 10.21769/BioProtoc.3302.

Byrne, A.J. *et al.* (2015) 'Pulmonary Macrophages: Key Players in the Innate Defence of the Airways'. *Thorax*, 70(12), pp. 1189–1196. DOI: 10.1136/thoraxjnl-2015-207020.

Cai, S. *et al.* (2016) 'IFN-γ Induction by Neutrophil-Derived IL-17A Homodimer Augments Pulmonary Antibacterial Defense'. *Mucosal Immunology*, 9(3), pp. 718–729. DOI: 10.1038/mi.2015.95.

Cai, X., Chiu, Y.-H. and Chen, Z.J. (2014) 'The CGAS-CGAMP-STING Pathway of Cytosolic DNA Sensing and Signaling'. *Molecular Cell*, 54(2), pp. 289–296. DOI: 10.1016/j.molcel.2014.03.040.

Cameron, R.L. *et al.* (2016) 'Comparison of Legionella Longbeachae and Legionella Pneumophila Cases in Scotland; Implications for Diagnosis, Treatment and Public Health Response'. *Journal of Medical Microbiology*, 65(2), pp. 142–146. DOI: 10.1099/jmm.0.000215.

Case, C.L. *et al.* (2013) 'Caspase-11 Stimulates Rapid Flagellin-Independent Pyroptosis in Response to Legionella Pneumophila'. *Proceedings of the National Academy of Sciences of the United States of America*, 110(5), pp. 1851–1856. DOI: 10.1073/pnas.1211521110.

Case, C.L., Shin, S. and Roy, C.R. (2009) 'Asc and Ipaf Inflammasomes Direct Distinct Pathways for Caspase-1 Activation in Response to Legionella Pneumophila'. *Infection and Immunity*, 77(5), pp. 1981–1991. DOI: 10.1128/IAI.01382-08.

Cass, S.P. *et al.* (2021) 'Increased Monocyte-Derived CD11b+ Macrophage Subpopulations Following Cigarette Smoke Exposure Are Associated With Impaired Bleomycin-Induced Tissue Remodelling'. *Frontiers in Immunology*, 12, p. 740330. DOI: 10.3389/fimmu.2021.740330.

Casson, C.N. *et al.* (2013) 'Caspase-11 Activation in Response to Bacterial Secretion Systems That Access the Host Cytosol' Isberg, R.R. (ed.). *PLoS Pathogens*, 9(6), p. e1003400. DOI: 10.1371/journal.ppat.1003400.

Castro, S.M., Chakraborty, K. and Guerrero-Plata, A. (2011) 'Cigarette Smoke Suppresses TLR-7 Stimulation in Response to Virus Infection in Plasmacytoid Dendritic Cells'. *Toxicology in Vitro*, 25(5), pp. 1106–1113. DOI: 10.1016/j.tiv.2011.03.011.

Cazalet, C. *et al.* (2010) 'Analysis of the Legionella Longbeachae Genome and Transcriptome Uncovers Unique Strategies to Cause Legionnaires' Disease'. *PLoS Genetics*, 6(2), p. e1000851. DOI: 10.1371/journal.pgen.1000851.

Chambers, S.T. *et al.* (2021) 'Legionellosis Caused by Non-Legionella Pneumophila Species, with a Focus on Legionella Longbeachae'. *Microorganisms*, 9(2), p. 291. DOI: 10.3390/microorganisms9020291.

Chapman, H.A. *et al.* (2011) 'Integrin A6β4 Identifies an Adult Distal Lung Epithelial Population with Regenerative Potential in Mice'. *Journal of Clinical Investigation*, 121(7), pp. 2855–2862. DOI: 10.1172/JCI57673.

Che, D. *et al.* (2008) 'Sporadic Community-Acquired Legionnaires' Disease in France: A 2-Year National Matched Case-Control Study'. *Epidemiology and Infection*, 136(12), pp. 1684–1690. DOI: 10.1017/S0950268807000283.

Chen, F. *et al.* (2018) 'Neutrophils Promote Amphiregulin Production in Intestinal Epithelial Cells through TGF-β and Contribute to Intestinal Homeostasis'. *The Journal of Immunology*, 201(8), pp. 2492–2501. DOI: 10.4049/jimmunol.1800003.

Chen, H. *et al.* (2007) 'Tobacco Smoking Inhibits Expression of Proinflammatory Cytokines and Activation of IL-1R-Associated Kinase, P38, and NF-KappaB in Alveolar Macrophages Stimulated with TLR2 and TLR4 Agonists'. *Journal of Immunology (Baltimore, Md.: 1950)*, 179(9), pp. 6097–6106.

Chen, X.-J. *et al.* (2004) 'Influenza Virus Inhibits ENaC and Lung Fluid Clearance'. *American Journal of Physiology. Lung Cellular and Molecular Physiology*, 287(2), pp. L366-373. DOI: 10.1152/ajplung.00011.2004.

Chien, J. *et al.* (2020) 'Cigarette Smoke Exposure Promotes Virulence of Pseudomonas Aeruginosa and Induces Resistance to Neutrophil Killing' Torres, V.J. (ed.). *Infection and Immunity*, 88(11), pp. e00527-20. DOI: 10.1128/IAI.00527-20.

Clemens, D.L., Lee, B.-Y. and Horwitz, M.A. (2000) 'Deviant Expression of Rab5 on Phagosomes Containing the Intracellular Pathogens Mycobacterium Tuberculosis and Legionella Pneumophila Is Associated with Altered Phagosomal Fate'. *Infection and Immunity*, 68(5), pp. 2671–2684. DOI: 10.1128/IAI.68.5.2671-2684.2000.

Cloutier, M.M. (2019) *Respiratory Physiology*. 2nd edition. Philadelphia, PA: Elsevier.

Cohen, N.A. *et al.* (2009) 'Cigarette Smoke Condensate Inhibits Transepithelial Chloride Transport and Ciliary Beat Frequency'. *The Laryngoscope*, 119(11), pp. 2269–2274. DOI: 10.1002/lary.20223.

Coll, R.C. *et al.* (2015) 'A Small-Molecule Inhibitor of the NLRP3 Inflammasome for the Treatment of Inflammatory Diseases'. *Nature Medicine*, 21(3), pp. 248–255. DOI: 10.1038/nm.3806.

Copenhaver, A.M. *et al.* (2014) 'Alveolar Macrophages and Neutrophils Are the Primary Reservoirs for Legionella Pneumophila and Mediate Cytosolic Surveillance of Type IV Secretion'. *Infection and Immunity*, 82(10), pp. 4325–4336. DOI: 10.1128/IAI.01891-14.

Copenhaver, A.M. *et al.* (2015) 'IL-1R Signaling Enables Bystander Cells to Overcome Bacterial Blockade of Host Protein Synthesis'. *Proceedings of the National Academy of Sciences of the United States of America*, 112(24), pp. 7557–7562. DOI: 10.1073/pnas.1501289112.

Correia, A.M. *et al.* (2016) 'Probable Person-to-Person Transmission of Legionnaires' Disease'. *New England Journal of Medicine*, 374(5), pp. 497–498. DOI: 10.1056/NEJMc1505356.

Croasdell Lucchini, A. *et al.* (2021a) 'Epithelial Cells and Inflammation in Pulmonary Wound Repair'. *Cells*, 10(2). DOI: 10.3390/cells10020339.

Croasdell Lucchini, A. *et al.* (2021b) 'Epithelial Cells and Inflammation in Pulmonary Wound Repair'. *Cells*, 10(2), p. 339. DOI: 10.3390/cells10020339.

Crotta, S. *et al.* (2013) 'Type I and Type III Interferons Drive Redundant Amplification Loops to Induce a Transcriptional Signature in Influenza-Infected Airway Epithelia' Kawaoka, Y. (ed.). *PLoS Pathogens*, 9(11), p. e1003773. DOI: 10.1371/journal.ppat.1003773.

Crouse, J., Kalinke, U. and Oxenius, A. (2015) 'Regulation of Antiviral T Cell Responses by Type I Interferons'. *Nature Reviews Immunology*, 15(4), pp. 231–242. DOI: 10.1038/nri3806.

Cunha, B.A., Burillo, A. and Bouza, E. (2016) 'Legionnaires' Disease'. *The Lancet*, 387(10016), pp. 376–385. DOI: 10.1016/S0140-6736(15)60078-2.

Dalebroux, Z.D., Edwards, R.L. and Swanson, M.S. (2009) 'SpoT Governs *Legionella Pneumophila* Differentiation in Host Macrophages'. *Molecular Microbiology*, 71(3), pp. 640–658. DOI: 10.1111/j.1365-2958.2008.06555.x.

D'Alessio, F.R. *et al.* (2009) 'CD4+CD25+Foxp3+ Tregs Resolve Experimental Lung Injury in Mice and Are Present in Humans with Acute Lung Injury'. *The Journal of Clinical Investigation*, 119(10), pp. 2898–2913. DOI: 10.1172/JCI36498.

Dao, D.T. *et al.* (2018) 'Intranasal Delivery of VEGF Enhances Compensatory Lung Growth in Mice' Kou, Y.R. (ed.). *PLOS ONE*, 13(6), p. e0198700. DOI: 10.1371/journal.pone.0198700.

Demedts, I.K. *et al.* (2007) 'Accumulation of Dendritic Cells and Increased CCL20 Levels in the Airways of Patients with Chronic Obstructive Pulmonary Disease'. *American Journal of Respiratory and Critical Care Medicine*, 175(10), pp. 998–1005. DOI: 10.1164/rccm.200608-1113OC.

Den Boer, J.W., Nijhof, J. and Friesema, I. (2006) 'Risk Factors for Sporadic Community-Acquired Legionnaires' Disease. A 3-Year National Case-Control Study'. *Public Health*, 120(6), pp. 566–571. DOI: 10.1016/j.puhe.2006.03.009.

Desai, T.J., Brownfield, D.G. and Krasnow, M.A. (2014) 'Alveolar Progenitor and Stem Cells in Lung Development, Renewal and Cancer'. *Nature*, 507(7491), pp. 190–194. DOI: 10.1038/nature12930.

D'hulst, A.I. (2005) 'Time Course of Cigarette Smoke-Induced Pulmonary Inflammation in Mice'. *European Respiratory Journal*, 26(2), pp. 204–213. DOI: 10.1183/09031936.05.00095204.

Dianat, M. *et al.* (2018) 'Crocin Attenuates Cigarette Smoke-Induced Lung Injury and Cardiac Dysfunction by Anti-Oxidative Effects: The Role of Nrf2 Antioxidant System in Preventing Oxidative Stress'. *Respiratory Research*, 19(1), p. 58. DOI: 10.1186/s12931-018-0766-3.

Dickson, R.P., Erb-Downward, J.R. and Huffnagle, G.B. (2014) 'Towards an Ecology of the Lung: New Conceptual Models of Pulmonary Microbiology and Pneumonia Pathogenesis'. *The Lancet Respiratory Medicine*, 2(3), pp. 238–246. DOI: 10.1016/S2213-2600(14)70028-1.

Dima, E. *et al.* (2015) 'Implication of Interleukin (IL)-18 in the Pathogenesis of Chronic Obstructive Pulmonary Disease (COPD)'. *Cytokine*, 74(2), pp. 313–317. DOI: 10.1016/j.cyto.2015.04.008.

Dinarello, C.A. (2018) 'Overview of the IL-1 Family in Innate Inflammation and Acquired Immunity'. *Immunological Reviews*, 281(1), pp. 8–27. DOI: 10.1111/imr.12621.

Dominguez, A. *et al.* (2009) 'Factors Influencing the Case-Fatality Rate of Legionnaires' Disease'. *The International Journal of Tuberculosis and Lung Disease: The Official Journal of the International Union Against Tuberculosis and Lung Disease*, 13(3), pp. 407–412.

Drannik, A.G. *et al.* (2004) 'Impact of Cigarette Smoke on Clearance and Inflammation after Pseudomonas Aeruginosa Infection'. *American Journal of Respiratory and Critical Care Medicine*, 170(11), pp. 1164–1171. DOI: 10.1164/rccm.200311-1521OC.

Droemann, D. *et al.* (2005) 'Toll-like Receptor 2 Expression Is Decreased on Alveolar Macrophages in Cigarette Smokers and COPD Patients'. *Respiratory Research*, 6(1), p. 68. DOI: 10.1186/1465-9921-6-68.

Drouin, M., Saenz, J. and Chiffoleau, E. (2020) 'C-Type Lectin-Like Receptors: Head or Tail in Cell Death Immunity'. *Frontiers in Immunology*, 11, p. 251. DOI: 10.3389/fimmu.2020.00251.

Dunn, J.S. *et al.* (2005) 'Inhibition of Human Neutrophil Reactive Oxygen Species Production and P67phox Translocation by Cigarette Smoke Extract'. *Atherosclerosis*, 179(2), pp. 261–267. DOI: 10.1016/j.atherosclerosis.2004.11.011.

Fitzgerald, K.A. and Kagan, J.C. (2020) 'Toll-like Receptors and the Control of Immunity'. *Cell*, 180(6), pp. 1044–1066. DOI: 10.1016/j.cell.2020.02.041.

Fleetwood, A.J., Cook, A.D. and Hamilton, J.A. (2005) 'Functions of Granulocyte-Macrophage Colony-Stimulating Factor'. *Critical Reviews in Immunology*, 25(5), pp. 405–428. DOI: 10.1615/CritRevImmunol.v25.i5.50.

Fliermans, C.B. *et al.* (1979) 'Isolation of Legionella Pneumophila from Nonepidemic-Related Aquatic Habitats'. *Applied and Environmental Microbiology*, 37(6), pp. 1239–1242.

Fontana, M.F. *et al.* (2011) 'Secreted Bacterial Effectors That Inhibit Host Protein Synthesis Are Critical for Induction of the Innate Immune Response to Virulent Legionella Pneumophila' Roy, C.R. (ed.). *PLoS Pathogens*, 7(2), p. e1001289. DOI: 10.1371/journal.ppat.1001289.

Fraser, D.W. *et al.* (1977) 'Legionnaires' Disease: Description of an Epidemic of Pneumonia'. *The New England Journal of Medicine*, 297(22), pp. 1189–1197. DOI: 10.1056/NEJM197712012972201.

Frutuoso, M.S. *et al.* (2010) 'The Pattern Recognition Receptors Nod1 and Nod2 Account for Neutrophil Recruitment to the Lungs of Mice Infected with Legionella Pneumophila'. *Microbes and Infection*, 12(11), pp. 819–827. DOI: 10.1016/j.micinf.2010.05.006.

Fujita, M. *et al.* (2008) 'TNF Receptor 1 and 2 Contribute in Different Ways to Resistance to Legionella Pneumophila-Induced Mortality in Mice'. *Cytokine*, 44(2), pp. 298–303. DOI: 10.1016/j.cyto.2008.08.015.

Fuse, E.T. *et al.* (2007) 'Role of Toll-like Receptor 2 in Recognition of Legionella Pneumophila in a Murine Pneumonia Model'. *Journal of Medical Microbiology*, 56(Pt 3), pp. 305–312. DOI: 10.1099/jmm.0.46913-0.

Galluzzi, L. *et al.* (2018) 'Molecular Mechanisms of Cell Death: Recommendations of the Nomenclature Committee on Cell Death 2018'. *Cell Death & Differentiation*, 25(3), pp. 486–541. DOI: 10.1038/s41418-017-0012-4.

Gangl, K. *et al.* (2009) 'Cigarette Smoke Facilitates Allergen Penetration across Respiratory Epithelium'. *Allergy*, 64(3), pp. 398–405. DOI: 10.1111/j.1398-9995.2008.01861.x.

Gao, W. *et al.* (2015) 'Bronchial Epithelial Cells: The Key Effector Cells in the Pathogenesis of Chronic Obstructive Pulmonary Disease?: Bronchial Epithelial Cells in COPD'. *Respirology*, 20(5), pp. 722–729. DOI: 10.1111/resp.12542.

Garbi, N. and Lambrecht, B.N. (2017) 'Location, Function, and Ontogeny of Pulmonary Macrophages during the Steady State'. *Pflügers Archiv - European Journal of Physiology*, 469(3–4), pp. 561–572. DOI: 10.1007/s00424-017-1965-3.

Gaschler, G.J. *et al.* (2008) 'Cigarette Smoke Exposure Attenuates Cytokine Production by Mouse Alveolar Macrophages'. *American Journal of Respiratory Cell and Molecular Biology*, 38(2), pp. 218–226. DOI: 10.1165/rcmb.2007-0053OC.

Gaspar, A.H. and Machner, M.P. (2014) 'VipD Is a Rab5-Activated Phospholipase A $_1$ That Protects *Legionella Pneumophila* from Endosomal Fusion'. *Proceedings of the*

National Academy of Sciences, 111(12), pp. 4560–4565. DOI: 10.1073/pnas.1316376111.

Gebhardt, M.J., Jacobson, R.K. and Shuman, H.A. (2017) 'Seeing Red; the Development of PON.MCherry, a Broad-Host Range Constitutive Expression Plasmid for Gram-Negative Bacteria' Zamboni, D.S. (ed.). *PLOS ONE*, 12(3), p. e0173116. DOI: 10.1371/journal.pone.0173116.

George, T.C. *et al.* (2004) 'Distinguishing Modes of Cell Death Using the ImageStream® Multispectral Imaging Flow Cytometer: Imaging Apoptotic and Necrotic Cells in Flow'. *Cytometry Part A*, 59A(2), pp. 237–245. DOI: 10.1002/cyto.a.20048.

Gerdes, J. *et al.* (1983) 'Production of a Mouse Monoclonal Antibody Reactive with a Human Nuclear Antigen Associated with Cell Proliferation'. *International Journal of Cancer*, 31(1), pp. 13–20. DOI: 10.1002/ijc.2910310104.

Gerhardt, T. and Ley, K. (2015) 'Monocyte Trafficking across the Vessel Wall'. *Cardiovascular Research*, 107(3), pp. 321–330. DOI: 10.1093/cvr/cvv147.

Ghosh, M.C. *et al.* (2013) 'Insulin-like Growth Factor-I Stimulates Differentiation of ATII Cells to ATI-like Cells through Activation of Wnt5a'. *American Journal of Physiology-Lung Cellular and Molecular Physiology*, 305(3), pp. L222–L228. DOI: 10.1152/ajplung.00014.2013.

Girard, R. *et al.* (2003) 'Lipopolysaccharides from Legionella and Rhizobium Stimulate Mouse Bone Marrow Granulocytes via Toll-like Receptor 2'. *Journal of Cell Science*, 116(Pt 2), pp. 293–302.

Girardin, S.E. *et al.* (2003) 'Peptidoglycan Molecular Requirements Allowing Detection by Nod1 and Nod2'. *Journal of Biological Chemistry*, 278(43), pp. 41702–41708. DOI: 10.1074/jbc.M307198200.

Givi, M.E. *et al.* (2015) 'Cigarette Smoke Differentially Modulates Dendritic Cell Maturation and Function in Time'. *Respiratory Research*, 16. DOI: 10.1186/s12931-015-0291-6.

Gobin, I. *et al.* (2009) 'Experimental Legionella Longbeachae Infection in Intratracheally Inoculated Mice'. *Journal of Medical Microbiology*, 58(Pt 6), pp. 723–730. DOI: 10.1099/jmm.0.007476-0.

Gong, T. *et al.* (2020) 'DAMP-Sensing Receptors in Sterile Inflammation and Inflammatory Diseases'. *Nature Reviews Immunology*, 20(2), pp. 95–112. DOI: 10.1038/s41577-019-0215-7.

Griffin, G.K. *et al.* (2012) 'IL-17 and TNF-α Sustain Neutrophil Recruitment during Inflammation through Synergistic Effects on Endothelial Activation'. *The Journal of Immunology*, 188(12), pp. 6287–6299. DOI: 10.4049/jimmunol.1200385.

Griffith, J.W., Sokol, C.L. and Luster, A.D. (2014) 'Chemokines and Chemokine Receptors: Positioning Cells for Host Defense and Immunity'. *Annual Review of Immunology*, 32(1), pp. 659–702. DOI: 10.1146/annurev-immunol-032713-120145.

Grommes, J. and Soehnlein, O. (2011) 'Contribution of Neutrophils to Acute Lung Injury'. *Molecular Medicine*, 17(3–4), pp. 293–307. DOI: 10.2119/molmed.2010.00138.

Groom, J.R. and Luster, A.D. (2011) 'CXCR3 Ligands: Redundant, Collaborative and Antagonistic Functions'. *Immunology & Cell Biology*, 89(2), pp. 207–215. DOI: 10.1038/icb.2010.158.

de Groot, P.M. *et al.* (2018) 'The Epidemiology of Lung Cancer'. *Translational Lung Cancer Research*, 7(3), pp. 220–233. DOI: 10.21037/tlcr.2018.05.06.

Guilliams, M., Lambrecht, B.N. and Hammad, H. (2013) 'Division of Labor between Lung Dendritic Cells and Macrophages in the Defense against Pulmonary Infections'. *Mucosal Immunology*, 6(3), pp. 464–473. DOI: 10.1038/mi.2013.14.

Guilliams, M., Mildner, A. and Yona, S. (2018) 'Developmental and Functional Heterogeneity of Monocytes'. *Immunity*, 49(4), pp. 595–613. DOI: 10.1016/j.immuni.2018.10.005.

Guzik, K. *et al.* (2011) 'Cigarette Smoke-Exposed Neutrophils Die Unconventionally but Are Rapidly Phagocytosed by Macrophages'. *Cell Death & Disease*, 2, p. e131. DOI: 10.1038/cddis.2011.13.

Hackstein, H. *et al.* (2013) 'Modulation of Respiratory Dendritic Cells during Klebsiella Pneumonia Infection'. *Respiratory Research*, 14, p. 91. DOI: 10.1186/1465-9921-14-91.

Haley, P.J. *et al.* (1991) 'Comparative Morphology and Morphometry of Alveolar Macrophages from Six Species'. *The American Journal of Anatomy*, 191(4), pp. 401–407. DOI: 10.1002/aja.1001910407.

Hardison, S.E. and Brown, G.D. (2012) 'C-Type Lectin Receptors Orchestrate Antifungal Immunity'. *Nature Immunology*, 13(9), pp. 817–822. DOI: 10.1038/ni.2369.

Harris, J.O. *et al.* (1975) 'Comparison of Proteolytic Enzyme Activity in Pulmonary Alveolar Macrophages and Blood Leukocytes in Smokers and Nonsmokers'. *The American Review of Respiratory Disease*, 111(5), pp. 579–586. DOI: 10.1164/arrd.1975.111.5.579.

Harvey, C.J. *et al.* (2011) 'Targeting Nrf2 Signaling Improves Bacterial Clearance by Alveolar Macrophages in Patients with COPD and in a Mouse Model'. *Science Translational Medicine*, 3(78), p. 78ra32. DOI: 10.1126/scitranslmed.3002042.

Hashimoto, D. *et al.* (2013) 'Tissue-Resident Macrophages Self-Maintain Locally throughout Adult Life with Minimal Contribution from Circulating Monocytes'. *Immunity*, 38(4), pp. 792–804. DOI: 10.1016/j.immuni.2013.04.004.

Hawn, T.R. *et al.* (2007) 'Altered Inflammatory Responses in TLR5-Deficient Mice Infected with *Legionella Pneumophila*'. *The Journal of Immunology*, 179(10), pp. 6981–6987. DOI: 10.4049/jimmunol.179.10.6981.

Hawn, T.R. *et al.* (2006) 'Myeloid Differentiation Primary Response Gene (88)- and Toll-like Receptor 2-Deficient Mice Are Susceptible to Infection with Aerosolized Legionella Pneumophila'. *The Journal of Infectious Diseases*, 193(12), pp. 1693–1702. DOI: 10.1086/504525.

Heath, W.R. and Carbone, F.R. (2009) 'Dendritic Cell Subsets in Primary and Secondary T Cell Responses at Body Surfaces'. *Nature Immunology*, 10(12), pp. 1237–1244. DOI: 10.1038/ni.1822.

van der Heijden, T. *et al.* (2017) 'NLRP3 Inflammasome Inhibition by MCC950 Reduces Atherosclerotic Lesion Development in Apolipoprotein E–Deficient Mice—Brief Report'. *Arteriosclerosis, Thrombosis, and Vascular Biology*, 37(8), pp. 1457–1461. DOI: 10.1161/ATVBAHA.117.309575.

Heijink, I.H. *et al.* (2012) 'Cigarette Smoke Impairs Airway Epithelial Barrier Function and Cell-Cell Contact Recovery'. *European Respiratory Journal*, 39(2), pp. 419–428. DOI: 10.1183/09031936.00193810.

Herb, M. and Schramm, M. (2021) 'Functions of ROS in Macrophages and Antimicrobial Immunity'. *Antioxidants*, 10(2), p. 313. DOI: 10.3390/antiox10020313.

Herold, S. *et al.* (2011) 'Exudate Macrophages Attenuate Lung Injury by the Release of IL-1 Receptor Antagonist in Gram-Negative Pneumonia'. *American Journal of Respiratory and Critical Care Medicine*, 183(10), pp. 1380–1390. DOI: 10.1164/rccm.201009-1431OC.

Herr, C. *et al.* (2009) 'Suppression of Pulmonary Innate Host Defence in Smokers'. *Thorax*, 64(2), pp. 144–149. DOI: 10.1136/thx.2008.102681.

Hoang, T. *et al.* (2018) 'Stereological Analysis of Individual Lung Lobes during Normal and Aberrant Mouse Lung Alveolarisation'. *Journal of Anatomy*, 232(3), pp. 472–484. DOI: 10.1111/joa.12773.

Hodge, S. *et al.* (2007) 'Smoking Alters Alveolar Macrophage Recognition and Phagocytic Ability: Implications in Chronic Obstructive Pulmonary Disease'. *American Journal of Respiratory Cell and Molecular Biology*, 37(6), pp. 748–755. DOI: 10.1165/rcmb.2007-0025OC.

Hoenderdos, K. and Condliffe, A. (2013) 'The Neutrophil in Chronic Obstructive Pulmonary Disease'. *American Journal of Respiratory Cell and Molecular Biology*, 48(5), pp. 531–539. DOI: 10.1165/rcmb.2012-0492TR.

Hogan, B.L.M. *et al.* (2014) 'Repair and Regeneration of the Respiratory System: Complexity, Plasticity, and Mechanisms of Lung Stem Cell Function'. *Cell Stem Cell*, 15(2), pp. 123–138. DOI: 10.1016/j.stem.2014.07.012.

Honda, Y. *et al.* (1996) 'Decreased Contents of Surfactant Proteins A and D in BAL Fluids of Healthy Smokers'. *Chest*, 109(4), pp. 1006–1009.

Hopfner, K.-P. and Hornung, V. (2020) 'Molecular Mechanisms and Cellular Functions of CGAS–STING Signalling'. *Nature Reviews Molecular Cell Biology*, 21(9), pp. 501–521. DOI: 10.1038/s41580-020-0244-x.

Horwitz, M.A. (1983) 'The Legionnaires' Disease Bacterium (Legionella Pneumophila) Inhibits Phagosome-Lysosome Fusion in Human Monocytes'. *The Journal of Experimental Medicine*, 158(6), pp. 2108–2126. DOI: 10.1084/jem.158.6.2108.

Hou, F. *et al.* (2021) 'Diversity of Macrophages in Lung Homeostasis and Diseases'. *Frontiers in Immunology*, 12, p. 753940. DOI: 10.3389/fimmu.2021.753940.

von Hoven, G. *et al.* (2019) 'Staphylococcus Aureus α-Toxin: Small Pore, Large Consequences'. *Biological Chemistry*, 400(10), pp. 1261–1276. DOI: 10.1515/hsz-2018-0472.

Hoving, J.C., Wilson, G.J. and Brown, G.D. (2014) 'Signalling C -Type Lectin Receptors, Microbial Recognition and Immunity'. *Cellular Microbiology*, 16(2), pp. 185–194. DOI: 10.1111/cmi.12249.

Hughes, C.E. and Nibbs, R.J.B. (2018) 'A Guide to Chemokines and Their Receptors'. *The FEBS Journal*, 285(16), pp. 2944–2971. DOI: 10.1111/febs.14466.

Hussell, T. and Bell, T.J. (2014) 'Alveolar Macrophages: Plasticity in a Tissue-Specific Context'. *Nature Reviews Immunology*, 14(2), pp. 81–93. DOI: 10.1038/nri3600.

Ibrahim-Granet, O. *et al.* (2003) 'Phagocytosis and Intracellular Fate of *Aspergillus Fumigatus* Conidia in Alveolar Macrophages'. *Infection and Immunity*, 71(2), pp. 891–903. DOI: 10.1128/IAI.71.2.891-903.2003.

Innes, A.L. *et al.* (2006) 'Epithelial Mucin Stores Are Increased in the Large Airways of Smokers With Airflow Obstruction'. *CHEST*, 130(4), pp. 1102–1108. DOI: 10.1378/chest.130.4.1102.

Isaac, D.T. *et al.* (2015) 'MavN Is a *Legionella Pneumophila* Vacuole-Associated Protein Required for Efficient Iron Acquisition during Intracellular Growth'. *Proceedings of the National Academy of Sciences*, 112(37). DOI: 10.1073/pnas.1511389112.

Isenman, H.L. *et al.* (2016) 'Legionnaires' Disease Caused by *Legionella Longbeachae* : Clinical Features and Outcomes of 107 Cases from an Endemic Area: *Legionella Longbeachae* Pneumonia'. *Respirology*, 21(7), pp. 1292–1299. DOI: 10.1111/resp.12808.

Jain, S. *et al.* (2015) 'Community-Acquired Pneumonia Requiring Hospitalization among U.S. Adults'. *New England Journal of Medicine*, 373(5), pp. 415–427. DOI: 10.1056/NEJMoa1500245.

Jakubzick, C.V., Randolph, G.J. and Henson, P.M. (2017) 'Monocyte Differentiation and Antigen-Presenting Functions'. *Nature Reviews Immunology*, 17(6), pp. 349–362. DOI: 10.1038/nri.2017.28.

Jha, P. and Peto, R. (2014) 'Global Effects of Smoking, of Quitting, and of Taxing Tobacco'. *New England Journal of Medicine*, 370(1), pp. 60–68. DOI: 10.1056/NEJMra1308383.

Jimenez Ruiz, C.A. *et al.* (1998) 'Bronchoalveolar Lavage in Smokers: Quantification of Alveolar Macrophages and Neutrophils as Markers of Bronchial Obstruction'. *In Vivo (Athens, Greece)*, 12(4), pp. 427–430.

Joller, N. *et al.* (2007) 'Induction and Protective Role of Antibodies in Legionella Pneumophila Infection'. *European Journal of Immunology*, 37(12), pp. 3414–3423. DOI: 10.1002/eji.200737591.

Jones, J.G. *et al.* (1980) 'Increased Alveolar Epithelial Permeability in Cigarette Smokers'. *The Lancet*, 315(8159), pp. 66–68. DOI: 10.1016/S0140-6736(80)90493-6.

Juncadella, I.J. *et al.* (2013) 'Apoptotic Cell Clearance by Bronchial Epithelial Cells Critically Influences Airway Inflammation'. *Nature*, 493(7433), pp. 547–551. DOI: 10.1038/nature11714.

Kagan, J.C. *et al.* (2004) 'Legionella Subvert the Functions of Rab1 and Sec22b to Create a Replicative Organelle'. *The Journal of Experimental Medicine*, 199(9), pp. 1201–1211. DOI: 10.1084/jem.20031706.

Kak, G., Raza, M. and Tiwari, B.K. (2018) 'Interferon-Gamma (IFN-γ): Exploring Its Implications in Infectious Diseases'. *Biomolecular Concepts*, 9(1), pp. 64–79. DOI: 10.1515/bmc-2018-0007.

Kanai, K. *et al.* (2015) 'Cigarette Smoke Augments MUC5AC Production via the TLR3-EGFR Pathway in Airway Epithelial Cells'. *Respiratory Investigation*, 53(4), pp. 137–148. DOI: 10.1016/j.resinv.2015.01.007.

Kapellos, T.S. *et al.* (2018) 'Dysregulated Functions of Lung Macrophage Populations in COPD'. *Journal of Immunology Research*, 2018, pp. 1–19. DOI: 10.1155/2018/2349045.

Kaplanski, G. (2018) 'Interleukin-18: Biological Properties and Role in Disease Pathogenesis'. *Immunological Reviews*, 281(1), pp. 138–153. DOI: 10.1111/imr.12616.

Karimi, R. *et al.* (2012) 'Cell Recovery in Bronchoalveolar Lavage Fluid in Smokers Is Dependent on Cumulative Smoking History' Idzko, M. (ed.). *PLoS ONE*, 7(3), p. e34232. DOI: 10.1371/journal.pone.0034232.

Katsura, H. *et al.* (2019) 'IL-1 and TNFα Contribute to the Inflammatory Niche to Enhance Alveolar Regeneration'. *Stem Cell Reports*, 12(4), pp. 657–666. DOI: 10.1016/j.stemcr.2019.02.013.

Kawasaki, T. and Kawai, T. (2014) 'Toll-Like Receptor Signaling Pathways'. *Frontiers in Immunology*, 5. DOI: 10.3389/fimmu.2014.00461.

Kelly, D.F., Moxon, E.R. and Pollard, A.J. (2004) 'Haemophilus Influenzae Type b Conjugate Vaccines'. *Immunology*, 113(2), pp. 163–174. DOI: 10.1111/j.1365-2567.2004.01971.x.

Kenagy, E. *et al.* (2017) 'Risk Factors for Legionella Longbeachae Legionnaires' Disease, New Zealand'. *Emerging Infectious Diseases*, 23(7), pp. 1148–1154. DOI: 10.3201/eid2307.161429.

Kimura, T. *et al.* (2012) 'Oxidized Phospholipid, 1-Palmitoyl-2-(9′-Oxo-Nonanoyl)-Glycerophosphocholine (PON-GPC), Produced in the Lung Due to Cigarette Smoking, Impairs Immune Function in Macrophages'. *Lung*, 190(2), pp. 169–182. DOI: 10.1007/s00408-011-9331-2.

King, T.E., Savici, D. and Campbell, P.A. (1988) 'Phagocytosis and Killing of Listeria Monocytogenes by Alveolar Macrophages: Smokers versus Nonsmokers'. *The Journal of Infectious Diseases*, 158(6), pp. 1309–1316.

Kirby, J.E. *et al.* (1998) 'Evidence for Pore-Forming Ability by Legionella Pneumophila'. *Molecular Microbiology*, 27(2), pp. 323–336. DOI: 10.1046/j.1365-2958.1998.00680.x.

Kirkham, P.A. and Barnes, P.J. (2013) 'Oxidative Stress in COPD'. *Chest*, 144(1), pp. 266–273. DOI: 10.1378/chest.12-2664.

Knudsen, L. and Ochs, M. (2018) 'The Micromechanics of Lung Alveoli: Structure and Function of Surfactant and Tissue Components'. *Histochemistry and Cell Biology*, 150(6), pp. 661–676. DOI: 10.1007/s00418-018-1747-9.

Knust, J. *et al.* (2009) 'Stereological Estimates of Alveolar Number and Size and Capillary Length and Surface Area in Mice Lungs'. *The Anatomical Record: Advances in Integrative Anatomy and Evolutionary Biology*, 292(1), pp. 113–122. DOI: 10.1002/ar.20747.

Kopf, M., Schneider, C. and Nobs, S.P. (2015) 'The Development and Function of Lung-Resident Macrophages and Dendritic Cells'. *Nature Immunology*, 16(1), pp. 36–44. DOI: 10.1038/ni.3052.

Korkmaz, B. *et al.* (2010) 'Neutrophil Elastase, Proteinase 3, and Cathepsin G as Therapeutic Targets in Human Diseases' Sibley, D. (ed.). *Pharmacological Reviews*, 62(4), pp. 726–759. DOI: 10.1124/pr.110.002733.

Kozak, N.A. *et al.* (2010) 'Virulence Factors Encoded by *Legionella Longbeachae* Identified on the Basis of the Genome Sequence Analysis of Clinical Isolate D-4968'. *Journal of Bacteriology*, 192(4), pp. 1030–1044. DOI: 10.1128/JB.01272-09.

Kraev, T.A. *et al.* (2009) 'Indoor Concentrations of Nicotine in Low-Income, Multi-Unit Housing: Associations with Smoking Behaviours and Housing Characteristics'. *Tobacco Control*, 18(6), pp. 438–444. DOI: 10.1136/tc.2009.029728.

Kroening, P.R. *et al.* (2008) 'Cigarette Smoke-Induced Oxidative Stress Suppresses Generation of Dendritic Cell IL-12 and IL-23 through ERK-Dependent Pathways'. *The Journal of Immunology*, 181(2), pp. 1536–1547. DOI: 10.4049/jimmunol.181.2.1536.

Kruger, P. *et al.* (2015) 'Neutrophils: Between Host Defence, Immune Modulation, and Tissue Injury' Dehio, C. (ed.). *PLOS Pathogens*, 11(3), p. e1004651. DOI: 10.1371/journal.ppat.1004651.

Kulikauskaite, J. and Wack, A. (2020) 'Teaching Old Dogs New Tricks? The Plasticity of Lung Alveolar Macrophage Subsets'. *Trends in Immunology*, 41(10), pp. 864–877. DOI: 10.1016/j.it.2020.08.008.

Kulkarni, R. *et al.* (2010) 'Cigarette Smoke Inhibits Airway Epithelial Cell Innate Immune Responses to Bacteria'. *Infection and Immunity*, 78(5), pp. 2146–2152. DOI: 10.1128/IAI.01410-09.

Kumar, P. *et al.* (2013) 'IL-22 from Conventional NK Cells Is Epithelial Regenerative and Inflammation Protective during Influenza Infection'. *Mucosal Immunology*, 6(1), pp. 69–82. DOI: 10.1038/mi.2012.49.

Lax, S. *et al.* (2014) 'Using a Non-Invasive Assessment of Lung Injury in a Murine Model of Acute Lung Injury'. *BMJ Open Respiratory Research*, 1(1), p. e000014. DOI: 10.1136/bmjresp-2013-000014.

Lecaille, F., Lalmanach, G. and Andrault, P.-M. (2016) 'Antimicrobial Proteins and Peptides in Human Lung Diseases: A Friend and Foe Partnership with Host Proteases'. *Biochimie*, 122, pp. 151–168. DOI: 10.1016/j.biochi.2015.08.014.

Lee, J.W. *et al.* (2007) 'Acute Lung Injury Edema Fluid Decreases Net Fluid Transport across Human Alveolar Epithelial Type II Cells'. *Journal of Biological Chemistry*, 282(33), pp. 24109–24119. DOI: 10.1074/jbc.M700821200.

Lee, M. *et al.* (2018) 'Tissue-Specific Role of CX $_3$ CR1 Expressing Immune Cells and Their Relationships with Human Disease'. *Immune Network*, 18(1), p. e5. DOI: 10.4110/in.2018.18.e5.

LeibundGut-Landmann, S. *et al.* (2011) 'Nonhematopoietic Cells Are Key Players in Innate Control of Bacterial Airway Infection'. *Journal of Immunology (Baltimore, Md.: 1950)*, 186(5), pp. 3130–3137. DOI: 10.4049/jimmunol.1003565.

Leiva-Juárez, M.M., Kolls, J.K. and Evans, S.E. (2018) 'Lung Epithelial Cells: Therapeutically Inducible Effectors of Antimicrobial Defense'. *Mucosal Immunology*, 11(1), pp. 21–34. DOI: 10.1038/mi.2017.71.

Leopold, P.L. *et al.* (2009) 'Smoking Is Associated with Shortened Airway Cilia'. *PloS One*, 4(12), p. e8157. DOI: 10.1371/journal.pone.0008157.

Li, J. *et al.* (2018) 'Regulatory T-Cells: Potential Regulator of Tissue Repair and Regeneration'. *Frontiers in Immunology*, 9, p. 585. DOI: 10.3389/fimmu.2018.00585.

Lin, J. *et al.* (2013) 'Oxidized Low Density Lipoprotein Induced Caspase-1 Mediated Pyroptotic Cell Death in Macrophages: Implication in Lesion Instability?' Mohanraj, R. (ed.). *PLoS ONE*, 8(4), p. e62148. DOI: 10.1371/journal.pone.0062148.

Linna, M.S. *et al.* (2008) 'Smoking and Low Serum Testosterone Associates with High Concentration of Oxidized LDL'. *Annals of Medicine*, 40(8), pp. 634–640. DOI: 10.1080/07853890802161007.

Lippmann, J. *et al.* (2011) 'Dissection of a Type I Interferon Pathway in Controlling Bacterial Intracellular Infection in Mice'. *Cellular Microbiology*, 13(11), pp. 1668–1682. DOI: 10.1111/j.1462-5822.2011.01646.x.

Liu, B.C. *et al.* (2018) 'Constitutive Interferon Maintains GBP Expression Required for Release of Bacterial Components Upstream of Pyroptosis and Anti-DNA Responses'. *Cell Reports*, 24(1), pp. 155-168.e5. DOI: 10.1016/j.celrep.2018.06.012.

Liu, Q. *et al.* (2019) 'Lung Regeneration by Multipotent Stem Cells Residing at the Bronchioalveolar-Duct Junction'. *Nature Genetics*, 51(4), pp. 728–738. DOI: 10.1038/s41588-019-0346-6.

Liu, X. *et al.* (2020) 'Legionella-Infected Macrophages Engage the Alveolar Epithelium to Metabolically Reprogram Myeloid Cells and Promote Antibacterial Inflammation'. *Cell Host & Microbe*, 28(5), pp. 683-698.e6. DOI: 10.1016/j.chom.2020.07.019.

Löfdahl, J.M., Wahlström, J. and Sköld, C.M. (2006) 'Different Inflammatory Cell Pattern and Macrophage Phenotype in Chronic Obstructive Pulmonary Disease Patients, Smokers and Non-Smokers'. *Clinical and Experimental Immunology*, 145(3), pp. 428–437. DOI: 10.1111/j.1365-2249.2006.03154.x.

Londino, J.D. *et al.* (2017) 'Influenza Virus Infection Alters Ion Channel Function of Airway and Alveolar Cells: Mechanisms and Physiological Sequelae'. *American Journal of Physiology-Lung Cellular and Molecular Physiology*, 313(5), pp. L845–L858. DOI: 10.1152/ajplung.00244.2017.

Louzier, V. *et al.* (2004) 'Adenovirus-Mediated Fibroblast Growth Factor 1 Expression in the Lung Induces Epithelial Cell Proliferation: Consequences to Hyperoxic Lung Injury in Rats'. *Human Gene Therapy*, 15(8), pp. 793–804. DOI: 10.1089/1043034041648390.

Lu, L.-M. *et al.* (2007) 'Cigarette Smoke Impairs NK Cell-Dependent Tumor Immune Surveillance'. *The Journal of Immunology*, 178(2), pp. 936–943. DOI: 10.4049/jimmunol.178.2.936.

Lucas, C.D. *et al.* (2022) 'Pannexin 1 Drives Efficient Epithelial Repair after Tissue Injury'. *Science Immunology*, 7(71), p. eabm4032. DOI: 10.1126/sciimmunol.abm4032.

Lugg, S.T. *et al.* (2022) 'Cigarette Smoke Exposure and Alveolar Macrophages: Mechanisms for Lung Disease'. *Thorax*, 77(1), pp. 94–101. DOI: 10.1136/thoraxjnl-2020-216296.

Ma, Y., Long, Y. and Chen, Y. (2021) 'Roles of Inflammasome in Cigarette Smoke-Related Diseases and Physiopathological Disorders: Mechanisms and Therapeutic Opportunities'. *Frontiers in Immunology*, 12, p. 720049. DOI: 10.3389/fimmu.2021.720049.

Machner, M.P. and Isberg, R.R. (2006) 'Targeting of Host Rab GTPase Function by the Intravacuolar Pathogen Legionella Pneumophila'. *Developmental Cell*, 11(1), pp. 47–56. DOI: 10.1016/j.devcel.2006.05.013.

Major, J. *et al.* (2020) 'Type I and III Interferons Disrupt Lung Epithelial Repair during Recovery from Viral Infection'. *Science*, 369(6504), pp. 712–717. DOI: 10.1126/science.abc2061.

Manzel, L.J. *et al.* (2011) 'Inhibition by Cigarette Smoke of Nuclear Factor-KB-Dependent Response to Bacteria in the Airway'. *American Journal of Respiratory Cell and Molecular Biology*, 44(2), pp. 155–165. DOI: 10.1165/rcmb.2009-0454OC.

Marston, B.J., Lipman, H.B. and Breiman, R.F. (1994) 'Surveillance for Legionnaires' Disease. Risk Factors for Morbidity and Mortality'. *Archives of Internal Medicine*, 154(21), pp. 2417–2422.

Martí-Lliteras, P. *et al.* (2009) 'Nontypeable Haemophilus Influenzae Clearance by Alveolar Macrophages Is Impaired by Exposure to Cigarette Smoke'. *Infection and Immunity*, 77(10), pp. 4232–4242. DOI: 10.1128/IAI.00305-09.

Maruta, K. *et al.* (1998) 'Entry and Intracellular Growth of Legionella Dumoffii in Alveolar Epithelial Cells'. *American Journal of Respiratory and Critical Care Medicine*, 157(6 Pt 1), pp. 1967–1974. DOI: 10.1164/ajrccm.157.6.9710108.

Mascarenhas, D.P.A. *et al.* (2015) 'Interleukin 1 Receptor-Driven Neutrophil Recruitment Accounts to MyD88-Dependent Pulmonary Clearance of Legionella Pneumophila Infection in Vivo'. *The Journal of Infectious Diseases*, 211(2), pp. 322–330. DOI: 10.1093/infdis/jiu430.

Masomian, M. *et al.* (2020) 'Development of Next Generation Streptococcus Pneumoniae Vaccines Conferring Broad Protection'. *Vaccines*, 8(1), p. 132. DOI: 10.3390/vaccines8010132.

Masselink, W. *et al.* (2019) 'Broad Applicability of a Streamlined Ethyl Cinnamate-Based Clearing Procedure'. *Development*, 146(3), p. dev166884. DOI: 10.1242/dev.166884.

Massis, L.M. *et al.* (2017) 'Legionella Longbeachae Is Immunologically Silent and Highly Virulent In Vivo'. *The Journal of Infectious Diseases*, 215(3), pp. 440–451. DOI: 10.1093/infdis/jiw560.

Matsunaga, K. *et al.* (2002) 'Epigallocatechin Gallate, a Potential Immunomodulatory Agent of Tea Components, Diminishes Cigarette Smoke Condensate-Induced Suppression of Anti- *Legionella Pneumophila* Activity and Cytokine Responses of Alveolar Macrophages'. *Clinical and Vaccine Immunology*, 9(4), pp. 864–871. DOI: 10.1128/CDLI.9.4.864-871.2002.

Matsunaga, K. *et al.* (2001) 'Involvement of Nicotinic Acetylcholine Receptors in Suppression of Antimicrobial Activity and Cytokine Responses of Alveolar Macrophages to *Legionella Pneumophila* Infection by Nicotine'. *The Journal of Immunology*, 167(11), pp. 6518–6524. DOI: 10.4049/jimmunol.167.11.6518.

Matthay, M.A. and Zimmerman, G.A. (2005) 'Acute Lung Injury and the Acute Respiratory Distress Syndrome: Four Decades of Inquiry into Pathogenesis and Rational Management'. *American Journal of Respiratory Cell and Molecular Biology*, 33(4), pp. 319–327. DOI: 10.1165/rcmb.F305.

McDade, J.E. *et al.* (1977) 'Legionnaires' Disease: Isolation of a Bacterium and Demonstration of Its Role in Other Respiratory Disease'. *The New England Journal of Medicine*, 297(22), pp. 1197–1203. DOI: 10.1056/NEJM197712012972202.

McKenna, E. *et al.* (2021) 'Neutrophils: Need for Standardized Nomenclature'. *Frontiers in Immunology*, 12, p. 602963. DOI: 10.3389/fimmu.2021.602963.

McKinney, R.M. *et al.* (1981) 'Legionella Longbeachae Species Nova, Another Etiologic Agent of Human Pneumonia'. *Annals of Internal Medicine*, 94(6), pp. 739–743. DOI: 10.7326/0003-4819-94-6-739.

Melo-Gonzalez, F. and Hepworth, M.R. (2017) 'Functional and Phenotypic Heterogeneity of Group 3 Innate Lymphoid Cells'. *Immunology*, 150(3), pp. 265–275. DOI: 10.1111/imm.12697.

Merad, M. and Martin, J.C. (2020) 'Pathological Inflammation in Patients with COVID-19: A Key Role for Monocytes and Macrophages'. *Nature Reviews Immunology*, 20(6), pp. 355–362. DOI: 10.1038/s41577-020-0331-4.

Mercante, J.W. and Winchell, J.M. (2015) 'Current and Emerging Legionella Diagnostics for Laboratory and Outbreak Investigations'. *Clinical Microbiology Reviews*, 28(1), pp. 95–133. DOI: 10.1128/CMR.00029-14.

Mian, M.F. *et al.* (2009) 'Exposure to Cigarette Smoke Suppresses IL-15 Generation and Its Regulatory NK Cell Functions in Poly I:C-Augmented Human PBMCs'. *Molecular Immunology*, 46(15), pp. 3108–3116. DOI: 10.1016/j.molimm.2009.06.009.

Mian, M.F. *et al.* (2008) 'Impairment of Human NK Cell Cytotoxic Activity and Cytokine Release by Cigarette Smoke'. *Journal of Leukocyte Biology*, 83(3), pp. 774–784. DOI: 10.1189/jlb.0707481.

Mio, T. *et al.* (1997) 'Cigarette Smoke Induces Interleukin-8 Release from Human Bronchial Epithelial Cells'. *American Journal of Respiratory and Critical Care Medicine*, 155(5), pp. 1770–1776. DOI: 10.1164/ajrccm.155.5.9154890.

Misharin, A.V. *et al.* (2013) 'Flow Cytometric Analysis of Macrophages and Dendritic Cell Subsets in the Mouse Lung'. *American Journal of Respiratory Cell and Molecular Biology*, 49(4), pp. 503–510. DOI: 10.1165/rcmb.2013-0086MA.

Mistry, P. *et al.* (2014) 'Safety, Tolerability, Pharmacokinetics, and Pharmacodynamics of Single-Dose Antiinterleukin- 18 MAb GSK1070806 in Healthy and Obese Subjects'. *International Journal of Clinical Pharmacology and Therapeutics*, 52(10), pp. 867–879. DOI: 10.5414/CP202087.

Miyashita, N. *et al.* (2020) 'Distribution of Legionella Species and Serogroups in Patients with Culture-Confirmed Legionella Pneumonia'. *Journal of Infection and Chemotherapy*, 26(5), pp. 411–417. DOI: 10.1016/j.jiac.2019.12.016.

Moazed, F. *et al.* (2016) 'Cigarette Smokers Have Exaggerated Alveolar Barrier Disruption in Response to Lipopolysaccharide Inhalation'. *Thorax*, 71(12), pp. 1130–1136. DOI: 10.1136/thoraxjnl-2015-207886.

Modestou, M.A. *et al.* (2010) 'Inhibition of IFN-γ-Dependent Antiviral Airway Epithelial Defense by Cigarette Smoke'. *Respiratory Research*, 11(1), p. 64. DOI: 10.1186/1465-9921-11-64.

Mody, C.H. *et al.* (1993) 'Legionella Pneumophila Replicates within Rat Alveolar Epithelial Cells'. *The Journal of Infectious Diseases*, 167(5), pp. 1138–1145. DOI: 10.1093/infdis/167.5.1138.

Molmeret, M. *et al.* (2004) 'Disruption of the Phagosomal Membrane and Egress of Legionella Pneumophila into the Cytoplasm during the Last Stages of Intracellular Infection of Macrophages and Acanthamoeba Polyphaga'. *Infection and Immunity*, 72(7), pp. 4040–4051. DOI: 10.1128/IAI.72.7.4040-4051.2004.

Molofsky, A.B. *et al.* (2006) 'Cytosolic Recognition of Flagellin by Mouse Macrophages Restricts Legionella Pneumophila Infection'. *The Journal of Experimental Medicine*, 203(4), pp. 1093–1104. DOI: 10.1084/jem.20051659.

Mondino, S. *et al.* (2020) 'Legionnaires' Disease: State of the Art Knowledge of Pathogenesis Mechanisms of *Legionella*'. *Annual Review of Pathology: Mechanisms of Disease*, 15(1), pp. 439–466. DOI: 10.1146/annurev-pathmechdis-012419-032742.

Monroe, K.M., McWhirter, S.M. and Vance, R.E. (2009) 'Identification of Host Cytosolic Sensors and Bacterial Factors Regulating the Type I Interferon Response to Legionella Pneumophila' Isberg, R.R. (ed.). *PLoS Pathogens*, 5(11), p. e1000665. DOI: 10.1371/journal.ppat.1000665.

Monticelli, L.A. *et al.* (2015) 'IL-33 Promotes an Innate Immune Pathway of Intestinal Tissue Protection Dependent on Amphiregulin-EGFR Interactions'. *Proceedings of the National Academy of Sciences of the United States of America*, 112(34), pp. 10762–10767. DOI: 10.1073/pnas.1509070112.

Monticelli, L.A. *et al.* (2011) 'Innate Lymphoid Cells Promote Lung-Tissue Homeostasis after Infection with Influenza Virus'. *Nature Immunology*, 12(11), pp. 1045–1054. DOI: 10.1031/ni.2131.

Morris, A. *et al.* (2008) 'Comparison of Cigarette Smoke-Induced Acute Inflammation in Multiple Strains of Mice and the Effect of a Matrix Metalloproteinase Inhibitor on These Responses'. *Journal of Pharmacology and Experimental Therapeutics*, 327(3), pp. 851–862. DOI: 10.1124/jpet.108.140848.

Moskophidis, D. and Kioussis, D. (1998) 'Contribution of Virus-Specific CD8+ Cytotoxic T Cells to Virus Clearance or Pathologic Manifestations of Influenza Virus Infection in a T Cell Receptor Transgenic Mouse Model'. *Journal of Experimental Medicine*, 188(2), pp. 223–232. DOI: 10.1084/jem.188.2.223.

Motz, G.T. *et al.* (2010) 'Chronic Cigarette Smoke Exposure Primes NK Cell Activation in a Mouse Model of Chronic Obstructive Pulmonary Disease'. *Journal of Immunology (Baltimore, Md.: 1950)*, 184(8), pp. 4460–4469. DOI: 10.4049/jimmunol.0903654.

Mu, M. *et al.* (2020) 'Alveolar Epithelial Cells Promote IGF-1 Production by Alveolar Macrophages Through TGF-β to Suppress Endogenous Inflammatory Signals'. *Frontiers in Immunology*, 11, p. 1585. DOI: 10.3389/fimmu.2020.01585.

Mukhopadhyay, S., Hoidal, J.R. and Mukherjee, T.K. (2006) 'Role of TNFα in Pulmonary Pathophysiology'. *Respiratory Research*, 7(1), p. 125. DOI: 10.1186/1465-9921-7-125.

Muñoz-Planillo, R. *et al.* (2013) 'K+ Efflux Is the Common Trigger of NLRP3 Inflammasome Activation by Bacterial Toxins and Particulate Matter'. *Immunity*, 38(6), pp. 1142–1153. DOI: 10.1016/j.immuni.2013.05.016.

Murata, T. *et al.* (2006) 'The Legionella Pneumophila Effector Protein DrrA Is a Rab1 Guanine Nucleotide-Exchange Factor'. *Nature Cell Biology*, 8(9), pp. 971–977. DOI: 10.1038/ncb1463.

Murphy, J.M. *et al.* (2013) 'The Pseudokinase MLKL Mediates Necroptosis via a Molecular Switch Mechanism'. *Immunity*, 39(3), pp. 443–453. DOI: 10.1016/j.immuni.2013.06.018.

Murray, C.J.L. *et al.* (2020) 'Global Burden of 87 Risk Factors in 204 Countries and Territories, 1990–2019: A Systematic Analysis for the Global Burden of Disease Study 2019'. *The Lancet*, 396(10258), pp. 1223–1249. DOI: 10.1016/S0140-6736(20)30752-2.

Murray, L.A. *et al.* (2011) 'TGF-Beta Driven Lung Fibrosis Is Macrophage Dependent and Blocked by Serum Amyloid P'. *The International Journal of Biochemistry & Cell Biology*, 43(1), pp. 154–162. DOI: 10.1016/j.biocel.2010.10.013.

Nagai, H. *et al.* (2002) 'A Bacterial Guanine Nucleotide Exchange Factor Activates ARF on Legionella Phagosomes'. *Science (New York, N.Y.)*, 295(5555), pp. 679–682. DOI: 10.1126/science.1067025.

Naito, M. *et al.* (1996) 'Liposome-Encapsulated Dichloromethylene Diphosphonate Induces Macrophage Apoptosis in Vivo and in Vitro'. *Journal of Leukocyte Biology*, 60(3), pp. 337–344. DOI: 10.1002/jlb.60.3.337.

Nakayama, T. *et al.* (1985) 'Cigarette Smoke Induces DNA Single-Strand Breaks in Human Cells'. *Nature*, 314(6010), pp. 462–464. DOI: 10.1038/314462a0.

Naujoks, J. *et al.* (2016) 'IFNs Modify the Proteome of Legionella-Containing Vacuoles and Restrict Infection Via IRG1-Derived Itaconic Acid'. *PLoS Pathogens*, 12(2), p. e1005408. DOI: 10.1371/journal.ppat.1005408.

Naujoks, J. *et al.* (2018) 'Innate Sensing and Cell-Autonomous Resistance Pathways in Legionella Pneumophila Infection'. *International Journal of Medical Microbiology*, 308(1), pp. 161–167. DOI: 10.1016/j.ijmm.2017.10.004.

Neudecker, V. *et al.* (2017) 'Neutrophil Transfer of *MiR-223* to Lung Epithelial Cells Dampens Acute Lung Injury in Mice'. *Science Translational Medicine*, 9(408), p. eaah5360. DOI: 10.1126/scitranslmed.aah5360.

Newton, H.J. *et al.* (2010) 'Molecular Pathogenesis of Infections Caused by Legionella Pneumophila'. *Clinical Microbiology Reviews*, 23(2), pp. 274–298. DOI: 10.1128/CMR.00052-09.

Nishimoto, A.T., Rosch, J.W. and Tuomanen, E.I. (2020) 'Pneumolysin: Pathogenesis and Therapeutic Target'. *Frontiers in Microbiology*, 11, p. 1543. DOI: 10.3389/fmicb.2020.01543.

Noda, N. *et al.* (2013) 'Cigarette Smoke Impairs Phagocytosis of Apoptotic Neutrophils by Alveolar Macrophages via Inhibition of the Histone Deacetylase/Rac/CD9 Pathways'. *International Immunology*, 25(11), pp. 643–650. DOI: 10.1093/intimm/dxt033.

Ochs, M. *et al.* (2004) 'The Number of Alveoli in the Human Lung'. *American Journal of Respiratory and Critical Care Medicine*, 169(1), pp. 120–124. DOI: 10.1164/rccm.200308-1107OC.

O'Connor, T.J. *et al.* (2016) 'Iron Limitation Triggers Early Egress by the Intracellular Bacterial Pathogen Legionella Pneumophila'. *Infection and Immunity*, 84(8), pp. 2185–2197. DOI: 10.1128/IAI.01306-15.

O'Leary, S.M. *et al.* (2014) 'Cigarette Smoking Impairs Human Pulmonary Immunity to Mycobacterium Tuberculosis'. *American Journal of Respiratory and Critical Care Medicine*, 190(12), pp. 1430–1436. DOI: 10.1164/rccm.201407-1385OC.

Oliva, G., Sahr, T. and Buchrieser, C. (2018) 'The Life Cycle of L. Pneumophila: Cellular Differentiation Is Linked to Virulence and Metabolism'. *Frontiers in Cellular and Infection Microbiology*, 8, p. 3. DOI: 10.3389/fcimb.2018.00003.

Oliveira da Silva, C. *et al.* (2017) 'Time Course of the Phenotype of Blood and Bone Marrow Monocytes and Macrophages in the Lung after Cigarette Smoke Exposure In Vivo'. *International Journal of Molecular Sciences*, 18(9), p. E1940. DOI: 10.3390/ijms18091940.

Opitz, B. *et al.* (2006) 'Legionella Pneumophila Induces IFNβ in Lung Epithelial Cells via IPS-1 and IRF3, Which Also Control Bacterial Replication'. *Journal of Biological Chemistry*, 281(47), pp. 36173–36179. DOI: 10.1074/jbc.M604638200.

Overbeek, S.A. *et al.* (2011) 'Cigarette Smoke Induces B2-Integrin-Dependent Neutrophil Migration across Human Endothelium'. *Respiratory Research*, 12(1), p. 75. DOI: 10.1186/1465-9921-12-75.

Pabst, M.J. *et al.* (1995) 'Inhibition of Neutrophil and Monocyte Defensive Functions by Nicotine'. *Journal of Periodontology*, 66(12), pp. 1047–1055. DOI: 10.1902/jop.1995.66.12.1047.

Paris, A.J. *et al.* (2016) 'Neutrophils Promote Alveolar Epithelial Regeneration by Enhancing Type II Pneumocyte Proliferation in a Model of Acid-Induced Acute Lung Injury'. *American Journal of Physiology-Lung Cellular and Molecular Physiology*, 311(6), pp. L1062–L1075. DOI: 10.1152/ajplung.00327.2016.

Park, E.-J. *et al.* (2018) 'Cigarette Smoke Condensate May Disturb Immune Function with Apoptotic Cell Death by Impairing Function of Organelles in Alveolar Macrophages'. *Toxicology in Vitro*, 52, pp. 351–364. DOI: 10.1016/j.tiv.2018.07.014.

Pereira, M.S.F. *et al.* (2011) 'Activation of NLRC4 by Flagellated Bacteria Triggers Caspase-1-Dependent and -Independent Responses To Restrict Legionella Pneumophila Replication in Macrophages and In Vivo'. *The Journal of Immunology*, 187(12), pp. 6447–6455. DOI: 10.4049/jimmunol.1003784.

Perera, A.P. *et al.* (2018) 'MCC950, a Specific Small Molecule Inhibitor of NLRP3 Inflammasome Attenuates Colonic Inflammation in Spontaneous Colitis Mice'. *Scientific Reports*, 8(1), p. 8618. DOI: 10.1038/s41598-018-26775-w.

Pérez-Rial, S. *et al.* (2013) 'Role of Recently Migrated Monocytes in Cigarette Smoke-Induced Lung Inflammation in Different Strain of Mice' Morty, R.E. (ed.). *PLoS ONE*, 8(9), p. e72975. DOI: 10.1371/journal.pone.0072975.

Peteranderl, C. *et al.* (2017) 'Inflammatory Responses Regulating Alveolar Ion Transport during Pulmonary Infections'. *Frontiers in Immunology*, 8. DOI: 10.3389/fimmu.2017.00446.

Pétrilli, V. *et al.* (2007) 'Activation of the NALP3 Inflammasome Is Triggered by Low Intracellular Potassium Concentration'. *Cell Death & Differentiation*, 14(9), pp. 1583–1589. DOI: 10.1038/sj.cdd.4402195.

Phipps, J.C. *et al.* (2010) 'Cigarette Smoke Exposure Impairs Pulmonary Bacterial Clearance and Alveolar Macrophage Complement-Mediated Phagocytosis of

Streptococcus Pneumoniae'. *Infection and Immunity*, 78(3), pp. 1214–1220. DOI: 10.1128/IAI.00963-09.

Pilla, D.M. *et al.* (2014) 'Guanylate Binding Proteins Promote Caspase-11–Dependent Pyroptosis in Response to Cytoplasmic LPS'. *Proceedings of the National Academy of Sciences*, 111(16), pp. 6046–6051. DOI: 10.1073/pnas.1321700111.

Platnich, J.M. and Muruve, D.A. (2019) 'NOD-like Receptors and Inflammasomes: A Review of Their Canonical and Non-Canonical Signaling Pathways'. *Archives of Biochemistry and Biophysics*, 670, pp. 4–14. DOI: 10.1016/j.abb.2019.02.008.

Polosa, R. and Thomson, N.C. (2013) 'Smoking and Asthma: Dangerous Liaisons'. *European Respiratory Journal*, 41(3), pp. 716–726. DOI: 10.1183/09031936.00073312.

Pouwels, S.D. *et al.* (2016) 'Cigarette Smoke-Induced Necroptosis and DAMP Release Trigger Neutrophilic Airway Inflammation in Mice'. *American Journal of Physiology-Lung Cellular and Molecular Physiology*, 310(4), pp. L377–L386. DOI: 10.1152/ajplung.00174.2015.

Pretto, J.J. *et al.* (2014) 'Clinical Use of Pulse Oximetry: Official Guidelines from the Thoracic Society of Australia and New Zealand: TSANZ Guidelines for Pulse Oximetry'. *Respirology*, 19(1), pp. 38–46. DOI: 10.1111/resp.12204.

Price, C.T.D. *et al.* (2011) 'Host Proteasomal Degradation Generates Amino Acids Essential for Intracellular Bacterial Growth'. *Science (New York, N.Y.)*, 334(6062), pp. 1553–1557. DOI: 10.1126/science.1212868.

Prieto, A. *et al.* (2001) 'Defective Natural Killer and Phagocytic Activities in Chronic Obstructive Pulmonary Disease Are Restored by Glycophosphopeptical (Inmunoferón)'. *American Journal of Respiratory and Critical Care Medicine*, 163(7), pp. 1578–1583. DOI: 10.1164/ajrccm.163.7.2002015.

Prina, E., Ranzani, O.T. and Torres, A. (2015) 'Community-Acquired Pneumonia'. *The Lancet*, 386(9998), pp. 1097–1108. DOI: 10.1016/S0140-6736(15)60733-4.

Qiu, S.-L. *et al.* (2017) 'Neutrophil Extracellular Traps Induced by Cigarette Smoke Activate Plasmacytoid Dendritic Cells'. *Thorax*, 72(12), pp. 1084–1093. DOI: 10.1136/thoraxjnl-2016-209887.

Quinton, L.J., Walkey, A.J. and Mizgerd, J.P. (2018) 'Integrative Physiology of Pneumonia'. *Physiological Reviews*, 98(3), pp. 1417–1464. DOI: 10.1152/physrev.00032.2017.

Rahman, I. and Kinnula, V.L. (2012) 'Strategies to Decrease Ongoing Oxidant Burden in Chronic Obstructive Pulmonary Disease'. *Expert Review of Clinical Pharmacology*, 5(3), pp. 293–309. DOI: 10.1586/ecp.12.16.

Rangasamy, T. *et al.* (2004) 'Genetic Ablation of Nrf2 Enhances Susceptibility to Cigarette Smoke-Induced Emphysema in Mice'. *The Journal of Clinical Investigation*, 114(9), pp. 1248–1259. DOI: 10.1172/JCI21146.

Rehwinkel, J. and Gack, M.U. (2020) 'RIG-I-like Receptors: Their Regulation and Roles in RNA Sensing'. *Nature Reviews Immunology*, 20(9), pp. 537–551. DOI: 10.1038/s41577-020-0288-3.

Reitsma, M.B. *et al.* (2021) 'Spatial, Temporal, and Demographic Patterns in Prevalence of Smoking Tobacco Use and Attributable Disease Burden in 204 Countries and Territories, 1990–2019: A Systematic Analysis from the Global Burden of Disease Study 2019'. *The Lancet*, 397(10292), pp. 2337–2360. DOI: 10.1016/S0140-6736(21)01169-7.

Ren, T. *et al.* (2006) 'Flagellin-Deficient Legionella Mutants Evade Caspase-1- and Naip5-Mediated Macrophage Immunity'. *PLoS Pathogens*, 2(3), p. e18. DOI: 10.1371/journal.ppat.0020018.

Richens, T.R. *et al.* (2009) 'Cigarette Smoke Impairs Clearance of Apoptotic Cells through Oxidant-Dependent Activation of RhoA'. *American Journal of Respiratory and Critical Care Medicine*, 179(11), pp. 1011–1021. DOI: 10.1164/rccm.200807-1148OC.

Robbins, C.S. *et al.* (2008) 'Cigarette Smoke Exposure Impairs Dendritic Cell Maturation and T Cell Proliferation in Thoracic Lymph Nodes of Mice'. *Journal of Immunology (Baltimore, Md. : 1950)*, 180(10), pp. 6623–6628.

Robinson, C.G. and Roy, C.R. (2006) 'Attachment and Fusion of Endoplasmic Reticulum with Vacuoles Containing Legionella Pneumophila'. *Cellular Microbiology*, 8(5), pp. 793–805. DOI: 10.1111/j.1462-5822.2005.00666.x.

Rogers, J. *et al.* (1994) 'Influence of Temperature and Plumbing Material Selection on Biofilm Formation and Growth of Legionella Pneumophila in a Model Potable Water System Containing Complex Microbial Flora'. *Applied and Environmental Microbiology*, 60(5), pp. 1585–1592. DOI: 10.1128/aem.60.5.1585-1592.1994.

Rogliani, P. *et al.* (2015) 'Canakinumab for the Treatment of Chronic Obstructive Pulmonary Disease'. *Pulmonary Pharmacology & Therapeutics*, 31, pp. 15–27. DOI: 10.1016/j.pupt.2015.01.005.

Rohmann, K. *et al.* (2011) 'Innate Immunity in the Human Lung: Pathogen Recognition and Lung Disease'. *Cell and Tissue Research*, 343(1), pp. 167–174. DOI: 10.1007/s00441-010-1048-7.

Rossaint, J. and Zarbock, A. (2013) 'Tissue-Specific Neutrophil Recruitment into the Lung, Liver, and Kidney'. *Journal of Innate Immunity*, 5(4), pp. 348–357. DOI: 10.1159/000345943.

Rowbotham, T.J. (1980) 'Preliminary Report on the Pathogenicity of Legionella Pneumophila for Freshwater and Soil Amoebae'. *Journal of Clinical Pathology*, 33(12), pp. 1179–1183.

Ruiz-Moreno, J.S. *et al.* (2018) 'The Common HAQ STING Variant Impairs CGAS-Dependent Antibacterial Responses and Is Associated with Susceptibility to Legionnaires' Disease in Humans' Zamboni, D.S. (ed.). *PLOS Pathogens*, 14(1), p. e1006829. DOI: 10.1371/journal.ppat.1006829.

Saffarzadeh, M. *et al.* (2012) 'Neutrophil Extracellular Traps Directly Induce Epithelial and Endothelial Cell Death: A Predominant Role of Histones' Hartl, D. (ed.). *PLoS ONE*, 7(2), p. e32366. DOI: 10.1371/journal.pone.0032366.

Salwig, I. *et al.* (2021) 'Imaging Lung Regeneration by Light Sheet Microscopy'. *Histochemistry and Cell Biology*, 155(2), pp. 271–277. DOI: 10.1007/s00418-020-01903-8.

Sampath, P. *et al.* (2018) 'Monocyte Subsets: Phenotypes and Function in Tuberculosis Infection'. *Frontiers in Immunology*, 9, p. 1726. DOI: 10.3389/fimmu.2018.01726.

Sauler, M., Bazan, I.S. and Lee, P.J. (2019) 'Cell Death in the Lung: The Apoptosis-Necroptosis Axis'. *Annual Review of Physiology*, 81, pp. 375–402. DOI: 10.1146/annurev-physiol-020518-114320.

Savla, U. *et al.* (2001) 'Prostaglandin E(2) Regulates Wound Closure in Airway Epithelium'. *American Journal of Physiology. Lung Cellular and Molecular Physiology*, 280(3), pp. L421-431. DOI: 10.1152/ajplung.2001.280.3.L421.

Scheller, J. *et al.* (2011) 'The Pro- and Anti-Inflammatory Properties of the Cytokine Interleukin-6'. *Biochimica et Biophysica Acta (BBA) - Molecular Cell Research*, 1813(5), pp. 878–888. DOI: 10.1016/j.bbamcr.2011.01.034.

Schiavoni, G. *et al.* (2004) 'Type I IFN Protects Permissive Macrophages from Legionella Pneumophila Infection through an IFN-Gamma-Independent Pathway'. *Journal of Immunology (Baltimore, Md.: 1950)*, 173(2), pp. 1266–1275. DOI: 10.4049/jimmunol.173.2.1266.

Schmidt, M.E. and Varga, S.M. (2018) 'The CD8 T Cell Response to Respiratory Virus Infections'. *Frontiers in Immunology*, 9, p. 678. DOI: 10.3389/fimmu.2018.00678.

Schneider, C. *et al.* (2014) 'Alveolar Macrophages Are Essential for Protection from Respiratory Failure and Associated Morbidity Following Influenza Virus Infection'. *PLoS Pathogens*, 10(4), p. e1004053. DOI: 10.1371/journal.ppat.1004053.

Schnoor, M., Vadillo, E. and Guerrero-Fonseca, I.M. (2021) 'The Extravasation Cascade Revisited from a Neutrophil Perspective'. *Current Opinion in Physiology*, 19, pp. 119–128. DOI: 10.1016/j.cophys.2020.09.014.

Schroder, K. *et al.* (2004) 'Interferon-γ: An Overview of Signals, Mechanisms and Functions'. *Journal of Leukocyte Biology*, 75(2), pp. 163–189. DOI: 10.1189/jlb.0603252.

Schroder, K. and Tschopp, J. (2010) 'The Inflammasomes'. *Cell*, 140(6), pp. 821–832. DOI: 10.1016/j.cell.2010.01.040.

Schulte, D. *et al.* (2011) 'Stabilizing the VE-Cadherin-Catenin Complex Blocks Leukocyte Extravasation and Vascular Permeability: Necessity of Paracellular Diapedesis *in Vivo*'. *The EMBO Journal*, 30(20), pp. 4157–4170. DOI: 10.1038/emboj.2011.304.

Schulte, H., Mühlfeld, C. and Brandenberger, C. (2019) 'Age-Related Structural and Functional Changes in the Mouse Lung'. *Frontiers in Physiology*, 10, p. 1466. DOI: 10.3389/fphys.2019.01466.

Serbina, N.V. *et al.* (2008) 'Monocyte-Mediated Defense Against Microbial Pathogens'. *Annual Review of Immunology*, 26(1), pp. 421–452. DOI: 10.1146/annurev.immunol.26.021607.090326.

Serbina, N.V. *et al.* (2003) 'TNF/INOS-Producing Dendritic Cells Mediate Innate Immune Defense against Bacterial Infection'. *Immunity*, 19(1), pp. 59–70. DOI: 10.1016/S1074-7613(03)00171-7.

Serhan, C.N. and Levy, B.D. (2018) 'Resolvins in Inflammation: Emergence of the pro-Resolving Superfamily of Mediators'. *The Journal of Clinical Investigation*, 128(7), pp. 2657–2669. DOI: 10.1172/JCI97943.

Shaykhiev, R. *et al.* (2011) 'Cigarette Smoking Reprograms Apical Junctional Complex Molecular Architecture in the Human Airway Epithelium in Vivo'. *Cellular and Molecular Life Sciences: CMLS*, 68(5), pp. 877–892. DOI: 10.1007/s00018-010-0500-x.

Shimbori, C. *et al.* (2016) 'Fibroblast Growth Factor-1 Attenuates TGF-B1-Induced Lung Fibrosis: Effect of Fibroblast Growth Factor-1 on Pulmonary Fibrosis'. *The Journal of Pathology*, 240(2), pp. 197–210. DOI: 10.1002/path.4768.

Shinozawa, Y. *et al.* (2002) 'Role of Interferon-Gamma in Inflammatory Responses in Murine Respiratory Infection with Legionella Pneumophila'. *Journal of Medical Microbiology*, 51(3), pp. 225–230. DOI: 10.1099/0022-1317-51-3-225.

Short, K.R. *et al.* (2016) 'Influenza Virus Damages the Alveolar Barrier by Disrupting Epithelial Cell Tight Junctions'. *European Respiratory Journal*, 47(3), pp. 954–966. DOI: 10.1183/13993003.01282-2015.

Short, K.R. *et al.* (2014) 'Pathogenesis of Influenza-Induced Acute Respiratory Distress Syndrome'. *The Lancet Infectious Diseases*, 14(1), pp. 57–69. DOI: 10.1016/S1473-3099(13)70286-X.

Siegel, S.J. and Weiser, J.N. (2015) 'Mechanisms of Bacterial Colonization of the Respiratory Tract'. *Annual Review of Microbiology*, 69(1), pp. 425–444. DOI: 10.1146/annurev-micro-091014-104209.

da Silva, C.O. *et al.* (2020) 'Alteration of Immunophenotype of Human Macrophages and Monocytes after Exposure to Cigarette Smoke'. *Scientific Reports*, 10(1), p. 12796. DOI: 10.1038/s41598-020-68753-1.

Silveira, T.N. and Zamboni, D.S. (2010) 'Pore Formation Triggered by Legionella Spp. Is an Nlrc4 Inflammasome-Dependent Host Cell Response That Precedes Pyroptosis'. *Infection and Immunity*, 78(3), pp. 1403–1413. DOI: 10.1128/IAI.00905-09.

Sköld, C.M. *et al.* (2003) 'Chronic Smoke Exposure Alters the Phenotype Pattern and the Metabolic Response in Human Alveolar Macrophages'. *Clinical and Experimental Immunology*, 106(1), pp. 108–113. DOI: 10.1046/j.1365-2249.1996.d01-805.x.

So, E.C. *et al.* (2015) 'Creating a Customized Intracellular Niche: Subversion of Host Cell Signaling by Legionella Type IV Secretion System Effectors'. *Canadian Journal of Microbiology*, 61(9), pp. 617–635. DOI: 10.1139/cjm-2015-0166.

Soda, E.A. *et al.* (2017) 'Vital Signs: Health Care-Associated Legionnaires' Disease Surveillance Data From 20 States and a Large Metropolitan Area-United States, 2015'. *American Journal of Transplantation: Official Journal of the American Society of Transplantation and the American Society of Transplant Surgeons*, 17(8), pp. 2215–2220. DOI: 10.1111/ajt.14407.

Soleimani, F. *et al.* (2022) 'Content of Toxic Components of Cigarette, Cigarette Smoke vs Cigarette Butts: A Comprehensive Systematic Review'. *Science of The Total Environment*, 813, p. 152667. DOI: 10.1016/j.scitotenv.2021.152667.

Speir, M. *et al.* (2016) 'Eliminating Legionella by Inhibiting BCL-XL to Induce Macrophage Apoptosis'. *Nature Microbiology*, 1, p. 15034. DOI: 10.1038/nmicrobiol.2015.34.

Spits, H. *et al.* (2013) 'Innate Lymphoid Cells — a Proposal for Uniform Nomenclature'. *Nature Reviews Immunology*, 13(2), pp. 145–149. DOI: 10.1038/nri3365.

Spörri, R. *et al.* (2006a) 'MyD88-Dependent IFN-Gamma Production by NK Cells Is Key for Control of Legionella Pneumophila Infection'. *Journal of Immunology (Baltimore, Md.: 1950)*, 176(10), pp. 6162–6171.

Spörri, R. *et al.* (2006b) 'MyD88-Dependent IFN-γ Production by NK Cells Is Key for Control of *Legionella Pneumophila* Infection'. *The Journal of Immunology*, 176(10), pp. 6162–6171. DOI: 10.4049/jimmunol.176.10.6162.

Stämpfli, M.R. and Anderson, G.P. (2009) 'How Cigarette Smoke Skews Immune Responses to Promote Infection, Lung Disease and Cancer'. *Nature Reviews Immunology*, 9(5), pp. 377–384. DOI: 10.1038/nri2530.

Standiford, T.J. and Ward, P.A. (2016) 'Therapeutic Targeting of Acute Lung Injury and Acute Respiratory Distress Syndrome'. *Translational Research*, 167(1), pp. 183–191. DOI: 10.1016/j.trsl.2015.04.015.

Stanifer, M.L. *et al.* (2020) 'Importance of Type I and III Interferons at Respiratory and Intestinal Barrier Surfaces'. *Frontiers in Immunology*, 11, p. 608645. DOI: 10.3389/fimmu.2020.608645.

Steele, T.W., Lanser, J. and Sangster, N. (1990) 'Isolation of Legionella Longbeachae Serogroup 1 from Potting Mixes'. *Applied and Environmental Microbiology*, 56(1), pp. 49–53.

Steele, T.W. and McLennan, A.M. (1996) 'Infection of Tetrahymena Pyriformis by Legionella Longbeachae and Other Legionella Species Found in Potting Mixes'. *Applied and Environmental Microbiology*, 62(3), pp. 1081–1083. DOI: 10.1128/aem.62.3.1081-1083.1996.

Stehle, C., Hernández, D.C. and Romagnani, C. (2018) 'Innate Lymphoid Cells in Lung Infection and Immunity'. *Immunological Reviews*, 286(1), pp. 102–119. DOI: 10.1111/imr.12712.

Steinert, E.M. *et al.* (2015) 'Quantifying Memory CD8 T Cells Reveals Regionalization of Immunosurveillance'. *Cell*, 161(4), pp. 737–749. DOI: 10.1016/j.cell.2015.03.031.

Stetson, D.B. and Medzhitov, R. (2006) 'Recognition of Cytosolic DNA Activates an IRF3-Dependent Innate Immune Response'. *Immunity*, 24(1), pp. 93–103. DOI: 10.1016/j.immuni.2005.12.003.

Straus, W.L. *et al.* (1996) 'Risk Factors for Domestic Acquisition of Legionnaires Disease. Ohio Legionnaires Disease Group'. *Archives of Internal Medicine*, 156(15), pp. 1685–1692.

Stringer, K.A. *et al.* (2007) 'Cigarette Smoke Extract-Induced Suppression of Caspase-3-like Activity Impairs Human Neutrophil Phagocytosis'. *American Journal of Physiology. Lung Cellular and Molecular Physiology*, 292(6), pp. L1572-1579. DOI: 10.1152/ajplung.00325.2006.

Strzelak, A. *et al.* (2018) 'Tobacco Smoke Induces and Alters Immune Responses in the Lung Triggering Inflammation, Allergy, Asthma and Other Lung Diseases: A Mechanistic Review'. *International Journal of Environmental Research and Public Health*, 15(5). DOI: 10.3390/ijerph15051033.

Sun, L. *et al.* (2013) 'Cyclic GMP-AMP Synthase Is a Cytosolic DNA Sensor That Activates the Type I Interferon Pathway'. *Science*, 339(6121), pp. 786–791. DOI: 10.1126/science.1232458.

Sussan, T.E. *et al.* (2009) 'Targeting Nrf2 with the Triterpenoid CDDO-Imidazolide Attenuates Cigarette Smoke-Induced Emphysema and Cardiac Dysfunction in Mice'. *Proceedings of the National Academy of Sciences of the United States of America*, 106(1), pp. 250–255. DOI: 10.1073/pnas.0804333106.

Sutterwala, F.S. *et al.* (2006) 'Critical Role for NALP3/CIAS1/Cryopyrin in Innate and Adaptive Immunity through Its Regulation of Caspase-1'. *Immunity*, 24(3), pp. 317–327. DOI: 10.1016/j.immuni.2006.02.004.

Swanson, K.V., Deng, M. and Ting, J.P.-Y. (2019) 'The NLRP3 Inflammasome: Molecular Activation and Regulation to Therapeutics'. *Nature Reviews Immunology*, 19(8), pp. 477–489. DOI: 10.1038/s41577-019-0165-0.

Szulc-Dąbrowska, L. *et al.* (2020) 'Cathepsins in Bacteria-Macrophage Interaction: Defenders or Victims of Circumstance?' *Frontiers in Cellular and Infection Microbiology*, 10, p. 601072. DOI: 10.3389/fcimb.2020.601072.

Takeuchi, O. and Akira, S. (2010) 'Pattern Recognition Receptors and Inflammation'. *Cell*, 140(6), pp. 805–820. DOI: 10.1016/j.cell.2010.01.022.

Talhout, R. *et al.* (2011) 'Hazardous Compounds in Tobacco Smoke'. *International Journal of Environmental Research and Public Health*, 8(2), pp. 613–628. DOI: 10.3390/ijerph8020613.

Tamashiro, E. *et al.* (2009) 'Cigarette Smoke Exposure Impairs Respiratory Epithelial Ciliogenesis , Cigarette Smoke Exposure Impairs Respiratory Epithelial Ciliogenesis'. *American Journal of Rhinology & Allergy*, 23(2), pp. 117–122. DOI: 10.2500/ajra.2009.23.3280.

Tate, M.D. *et al.* (2016) 'Reassessing the Role of the NLRP3 Inflammasome during Pathogenic Influenza A Virus Infection via Temporal Inhibition'. *Scientific Reports*, 6(1), p. 27912. DOI: 10.1038/srep27912.

Tateda, K., Moore, T.A., Newstead, M.W., *et al.* (2001) 'Chemokine-Dependent Neutrophil Recruitment in a Murine Model of Legionella Pneumonia: Potential Role of Neutrophils as Immunoregulatory Cells'. *Infection and Immunity*, 69(4), pp. 2017–2024. DOI: 10.1128/IAI.69.4.2017-2024.2001.

Tateda, K., Moore, T.A., Deng, J.C., *et al.* (2001) 'Early Recruitment of Neutrophils Determines Subsequent T1/T2 Host Responses in a Murine Model of Legionella Pneumophila Pneumonia'. *Journal of Immunology (Baltimore, Md.: 1950)*, 166(5), pp. 3355–3361.

Tateda, K. *et al.* (1998) 'Serum Cytokines in Patients with Legionella Pneumonia: Relative Predominance of Th1-Type Cytokines'. *Clinical and Diagnostic Laboratory Immunology*, 5(3), pp. 401–403.

Taylor, A.E. *et al.* (2010) 'Defective Macrophage Phagocytosis of Bacteria in COPD'. *European Respiratory Journal*, 35(5), pp. 1039–1047. DOI: 10.1183/09031936.00036709.

Taylor, M., Ross, K. and Bentham, R. (2009) 'Legionella, Protozoa, and Biofilms: Interactions within Complex Microbial Systems'. *Microbial Ecology*, 58(3), pp. 538–547. DOI: 10.1007/s00248-009-9514-z.

Tecchio, C., Micheletti, A. and Cassatella, M.A. (2014) 'Neutrophil-Derived Cytokines: Facts Beyond Expression'. *Frontiers in Immunology*, 5. DOI: 10.3389/fimmu.2014.00508.

Thimmulappa, R.K. *et al.* (2012) 'Oxidized Phospholipids Impair Pulmonary Antibacterial Defenses: Evidence in Mice Exposed to Cigarette Smoke'. *Biochemical and Biophysical Research Communications*, 426(2), pp. 253–259. DOI: 10.1016/j.bbrc.2012.08.076.

Todt, J.C. *et al.* (2013) 'Smoking Decreases the Response of Human Lung Macrophages to Double-Stranded RNA by Reducing TLR3 Expression'. *Respiratory Research*, 14(1), p. 33. DOI: 10.1186/1465-9921-14-33.

Torres, A. *et al.* (2021) 'Pneumonia'. *Nature Reviews Disease Primers*, 7(1), p. 25. DOI: 10.1038/s41572-021-00259-0.

Torres, A. *et al.* (2013) 'Risk Factors for Community-Acquired Pneumonia in Adults in Europe: A Literature Review'. *Thorax*, 68(11), pp. 1057–1065. DOI: 10.1136/thoraxjnl-2013-204282.

Trinchieri, G. (2003) 'Interleukin-12 and the Regulation of Innate Resistance and Adaptive Immunity'. *Nature Reviews Immunology*, 3(2), pp. 133–146. DOI: 10.1038/nri1001.

Troeger, C. *et al.* (2018) 'Estimates of the Global, Regional, and National Morbidity, Mortality, and Aetiologies of Lower Respiratory Infections in 195 Countries, 1990–2016: A Systematic Analysis for the Global Burden of Disease Study 2016'. *The Lancet Infectious Diseases*, 18(11), pp. 1191–1210. DOI: 10.1016/S1473-3099(18)30310-4.

Tschernig, T. *et al.* (2015) 'Chronic Inhalation of Cigarette Smoke Reduces Phagocytosis in Peripheral Blood Leukocytes'. *BMC Research Notes*, 8(1), p. 705. DOI: 10.1186/s13104-015-1706-7.

Uribe-Querol, E. and Rosales, C. (2017) 'Control of Phagocytosis by Microbial Pathogens'. *Frontiers in Immunology*, 8. DOI: 10.3389/fimmu.2017.01368.

Van Deusen, A. *et al.* (2009) 'Secondhand Smoke and Particulate Matter Exposure in the Home'. *Nicotine & Tobacco Research*, 11(6), pp. 635–641. DOI: 10.1093/ntr/ntp018.

van de Laar, L. *et al.* (2016) 'Yolk Sac Macrophages, Fetal Liver, and Adult Monocytes Can Colonize an Empty Niche and Develop into Functional Tissue-Resident Macrophages'. *Immunity*, 44(4), pp. 755–768. DOI: 10.1016/j.immuni.2016.02.017.

Varet, J. *et al.* (2010) 'VEGF in the Lung: A Role for Novel Isoforms'. *American Journal of Physiology. Lung Cellular and Molecular Physiology*, 298(6), pp. L768-774. DOI: 10.1152/ajplung.00353.2009.

Vasilescu, D.M. *et al.* (2020) 'Comprehensive Stereological Assessment of the Human Lung Using Multiresolution Computed Tomography'. *Journal of Applied Physiology*, 128(6), pp. 1604–1616. DOI: 10.1152/japplphysiol.00803.2019.

Vasilescu, D.M. *et al.* (2013) 'Stereological Assessment of Mouse Lung Parenchyma via Nondestructive, Multiscale Micro-CT Imaging Validated by Light Microscopic Histology'. *Journal of Applied Physiology*, 114(6), pp. 716–724. DOI: 10.1152/japplphysiol.00855.2012.

Vaughan, A.E. *et al.* (2015) 'Lineage-Negative Progenitors Mobilize to Regenerate Lung Epithelium after Major Injury'. *Nature*, 517(7536), pp. 621–625. DOI: 10.1038/nature14112.

Vivier, E. *et al.* (2008) 'Functions of Natural Killer Cells'. *Nature Immunology*, 9(5), pp. 503–510. DOI: 10.1038/ni1582.

Vlahos, R. *et al.* (2006) 'Differential Protease, Innate Immunity, and NF-KappaB Induction Profiles during Lung Inflammation Induced by Subchronic Cigarette Smoke Exposure in Mice'. *American Journal of Physiology. Lung Cellular and Molecular Physiology*, 290(5), pp. L931-945. DOI: 10.1152/ajplung.00201.2005.

Vomund, S. *et al.* (2017) 'Nrf2, the Master Regulator of Anti-Oxidative Responses'. *International Journal of Molecular Sciences*, 18(12). DOI: 10.3390/ijms18122772.

Vos, T. *et al.* (2020) 'Global Burden of 369 Diseases and Injuries in 204 Countries and Territories, 1990–2019: A Systematic Analysis for the Global Burden of Disease Study 2019'. *The Lancet*, 396(10258), pp. 1204–1222. DOI: 10.1016/S0140-6736(20)30925-9.

Wang, H. *et al.* (2018) 'MAIT Cells Protect against Pulmonary Legionella Longbeachae Infection'. *Nature Communications*, 9(1), p. 3350. DOI: 10.1038/s41467-018-05202-8.

Wang, L. *et al.* (2021) 'MCC950, a NLRP3 Inhibitor, Ameliorates Lipopolysaccharide-Induced Lung Inflammation in Mice'. *Bioorganic & Medicinal Chemistry*, 30, p. 115954. DOI: 10.1016/j.bmc.2020.115954.

Wang, X. *et al.* (2019) 'Melatonin Alleviates Cigarette Smoke-Induced Endothelial Cell Pyroptosis through Inhibiting ROS/NLRP3 Axis'. *Biochemical and Biophysical Research Communications*, 519(2), pp. 402–408. DOI: 10.1016/j.bbrc.2019.09.005.

Wang, Yong. *et al.* (2020) 'Necroptosis Mediates Cigarette Smoke-Induced Inflammatory Responses in Macrophages'. *International Journal of Chronic Obstructive Pulmonary Disease*, 15, pp. 1093–1101. DOI: 10.2147/COPD.S233506.

Whiley, H. and Bentham, R. (2011) 'Legionella Longbeachae and Legionellosis'. *Emerging Infectious Diseases*, 17(4), pp. 579–583. DOI: 10.3201/eid1704.100446.

White, P.C. *et al.* (2018) 'Cigarette Smoke Modifies Neutrophil Chemotaxis, Neutrophil Extracellular Trap Formation and Inflammatory Response-Related Gene Expression'. *Journal of Periodontal Research*, 53(4), pp. 525–535. DOI: 10.1111/jre.12542.

White, R.C. and Cianciotto, N.P. (2019) 'Assessing the Impact, Genomics and Evolution of Type II Secretion across a Large, Medically Important Genus: The Legionella Type II Secretion Paradigm'. *Microbial Genomics*, 5(6). DOI: 10.1099/mgen.0.000273.

Wood, R.E. *et al.* (2015) 'Dot/Icm Effector Translocation by Legionella Longbeachae Creates a Replicative Vacuole Similar to That of Legionella Pneumophila despite Translocation of Distinct Effector Repertoires'. *Infection and Immunity*, 83(10), pp. 4081–4092. DOI: 10.1128/IAI.00461-15.

Wright, J.R. (2005) 'Immunoregulatory Functions of Surfactant Proteins'. *Nature Reviews Immunology*, 5(1), pp. 58–68. DOI: 10.1038/nri1528.

Wynn, T.A. and Vannella, K.M. (2016) 'Macrophages in Tissue Repair, Regeneration, and Fibrosis'. *Immunity*, 44(3), pp. 450–462. DOI: 10.1016/j.immuni.2016.02.015.

Xavier, R.F. *et al.* (2013) 'Effects of Cigarette Smoking Intensity on the Mucociliary Clearance of Active Smokers'. *Respiration*, 86(6), pp. 479–485. DOI: 10.1159/000348398.

Xiong, J. *et al.* (2019) 'Functions of Group 2 Innate Lymphoid Cells in Tumor Microenvironment'. *Frontiers in Immunology*, 10, p. 1615. DOI: 10.3389/fimmu.2019.01615.

Xu, L. *et al.* (2010) 'Inhibition of Host Vacuolar H+-ATPase Activity by a Legionella Pneumophila Effector'. *PLoS Pathogens*, 6(3), p. e1000822. DOI: 10.1371/journal.ppat.1000822.

Xu, M. *et al.* (2008) 'The Influence of Nicotine on Granulocytic Differentiation - Inhibition of the Oxidative Burst and Bacterial Killing and Increased Matrix Metalloproteinase-9 Release'. *BMC Cell Biology*, 9, p. 19. DOI: 10.1186/1471-2121-9-19.

Yang, Y. *et al.* (2019) 'Recent Advances in the Mechanisms of NLRP3 Inflammasome Activation and Its Inhibitors'. *Cell Death & Disease*, 10(2), p. 128. DOI: 10.1038/s41419-019-1413-8.

Yoshida, M. *et al.* (2019) 'Involvement of Cigarette Smoke-Induced Epithelial Cell Ferroptosis in COPD Pathogenesis'. *Nature Communications*, 10(1), p. 3145. DOI: 10.1038/s41467-019-10991-7.

Yu, V.L. *et al.* (2002) 'Distribution of Legionella Species and Serogroups Isolated by Culture in Patients with Sporadic Community-Acquired Legionellosis: An International Collaborative Survey'. *The Journal of Infectious Diseases*, 186(1), pp. 127–128. DOI: 10.1086/341087.

Zaiss, D.M.W. *et al.* (2015) 'Emerging Functions of Amphiregulin in Orchestrating Immunity, Inflammation, and Tissue Repair'. *Immunity*, 42(2), pp. 216–226. DOI: 10.1016/j.immuni.2015.01.020.

Zamboni, D.S. *et al.* (2006) 'The Birc1e Cytosolic Pattern-Recognition Receptor Contributes to the Detection and Control of Legionella Pneumophila Infection'. *Nature Immunology*, 7(3), pp. 318–325. DOI: 10.1038/ni1305.

Zemans, R.L. *et al.* (2011) 'Neutrophil Transmigration Triggers Repair of the Lung Epithelium via β-Catenin Signaling'. *Proceedings of the National Academy of Sciences*, 108(38), pp. 15990–15995. DOI: 10.1073/pnas.1110144108.

Zemans, R.L., Colgan, S.P. and Downey, G.P. (2009) 'Transepithelial Migration of Neutrophils: Mechanisms and Implications for Acute Lung Injury'. *American Journal of Respiratory Cell and Molecular Biology*, 40(5), pp. 519–535. DOI: 10.1165/rcmb.2008-0348TR.

Zepp, J.A. and Morrisey, E.E. (2019) 'Cellular Crosstalk in the Development and Regeneration of the Respiratory System'. *Nature Reviews Molecular Cell Biology*, 20(9), pp. 551–566. DOI: 10.1038/s41580-019-0141-3.

Zhang, L. *et al.* (2018) 'SOCS-1 Suppresses Inflammation Through Inhibition of NALP3 Inflammasome Formation in Smoke Inhalation-Induced Acute Lung Injury'. *Inflammation*, 41(4), pp. 1557–1567. DOI: 10.1007/s10753-018-0802-y.

Zhang, M.-Y. *et al.* (2021) 'Cigarette Smoke Extract Induces Pyroptosis in Human Bronchial Epithelial Cells through the ROS/NLRP3/Caspase-1 Pathway'. *Life Sciences*, 269, p. 119090. DOI: 10.1016/j.lfs.2021.119090.

Zhang, W. *et al.* (2011) 'Cigarette Smoke Modulates PGE2 and Host Defence against Moraxella Catarrhalis Infection in Human Airway Epithelial Cells'. *Respirology*, 16(3), pp. 508–516. DOI: 10.1111/j.1440-1843.2010.01920.x.

Zhang, Y. *et al.* (2018) 'Suppression of Neutrophil Antimicrobial Functions by Total Particulate Matter From Cigarette Smoke'. *Frontiers in Immunology*, 9, p. 2274. DOI: 10.3389/fimmu.2018.02274.

Zheng, D., Liwinski, T. and Elinav, E. (2020) 'Inflammasome Activation and Regulation: Toward a Better Understanding of Complex Mechanisms'. *Cell Discovery*, 6(1), p. 36. DOI: 10.1038/s41421-020-0167-x.

Zheng, S. *et al.* (2016) 'Lipoxin A4 Promotes Lung Epithelial Repair Whilst Inhibiting Fibroblast Proliferation'. *ERJ Open Research*, 2(3). DOI: 10.1183/23120541.00079-2015.

Ziltener, P., Reinheckel, T. and Oxenius, A. (2016) 'Neutrophil and Alveolar Macrophage-Mediated Innate Immune Control of Legionella Pneumophila Lung Infection

via TNF and ROS'. *PLoS Pathogens*, 12(4), p. e1005591. DOI: 10.1371/journal.ppat.1005591.

Zuo, L. *et al.* (2014) 'Interrelated Role of Cigarette Smoking, Oxidative Stress, and Immune Response in COPD and Corresponding Treatments'. *American Journal of Physiology. Lung Cellular and Molecular Physiology*, 307(3), pp. L205-218. DOI: 10.1152/ajplung.00330.2013.

Zuo, W. *et al.* (2015) 'P63(+)Krt5(+) Distal Airway Stem Cells Are Essential for Lung Regeneration'. *Nature*, 517(7536), pp. 616–620. DOI: 10.1038/nature13903.